DESIGN AND SYNTHESES OF POTENTIALLY CPL EXHIBITING CHIRAL COUMARIN DERIVATIVES

A THESIS SUBMITTED TO
THE GRADUATE SCHOOL OF NATURAL AND APPLIED SCIENCES
OF
MIDDLE EAST TECHNICAL UNIVERSITY

BY

BERÇİN VERDA ASYA

IN PARTIAL FULFILLMENT OF THE REQUIREMENTS
FOR
THE DEGREE OF MASTER OF SCIENCE
IN
CHEMISTRY

FEBRUARY 2022

Approval of the thesis:

DESIGN AND SYNTHESES OF POTENTIALLY CPL EXHIBITING CHIRAL COUMARIN DERIVATIVES

submitted by **BERÇİN VERDA ASYA** in partial fulfillment of the requirements for the degree of **Master of Science** i**n Chemistry, Middle East Technical University** by,

Prof. Dr. Halil Kalıpçılar
Dean, Graduate School of **Natural and Applied Sciences** _____

Prof. Dr. Özdemir Doğan
Head of the Department, **Chemistry** _____

Prof. Akın Akdağ
Supervisor, **Chemistry, METU** _____

Examining Committee Members:

Prof. Dr. Metin Zora
Chemistry Department, METU _____

Prof. Dr. Akın Akdağ
Chemistry Department, METU _____

Prof. Dr. Özdemir Doğan
Chemistry Department, METU _____

Assoc. Prof. Dr. Serhan Türkyılmaz
Chemistry Department, METU _____

Assoc. Prof. Dr. Yunus Emre Türkmen
Chemistry Department, İ.D. Bilkent University _____

Date: 04.02.2022

I hereby declare that all information in this document has been obtained and presented in accordance with academic rules and ethical conduct. I also declare that, as required by these rules and conduct, I have fully cited and referenced all material and results that are not original to this work.

Name Last Name : Berçin Verda Asya

Signature :

ABSTRACT

DESIGN AND SYNTHESES OF POTENTIALLY CPL EXHIBITING CHIRAL COUMARIN DERIVATIVES

Asya, Berçin Verda
Master of Science, Chemistry
Supervisor: Prof. Dr. Akın Akdağ

February 2022, 115 pages

Interaction of chiral organic compounds with polarized light is an emerging concept that has the potential of widespread application areas. Thus, CPL exhibiting compounds are in high demand. Specifically, the synthesis of circularly polarized light exhibiting organic compounds is a challenging yet promising task. In this study, chiral fluorescent organic compounds with coumarin derivatives as chromophore groups have been synthesized. Enantiomers of tartaric acid derivatives have been utilized as the chiral core unit. Besides their characterization analyses, photophysical and chiroptical studies of the compounds have been accomplished through UV-Vis, fluorescence and CD spectroscopy in methanol, chloroform, acetonitrile, and tetrahydrofuran. CPL studies of these compounds were conducted with the home-made CPL instrument. The CPL results are assuring but still need enhancement.

Keywords: circularly polarized light, circularly polarized luminescence, circular dichroism, coumarin, tartaric acid

ÖZ

DAİRESEL POLARİZE IŞIK YAYMA POTANSİYELİNE SAHİP KİRAL KUMARİN TÜREVLERİNİN TASARIM VE SENTEZİ

Asya, Berçin Verda
Yüksek Lisans, Kimya
Tez Yöneticisi: Prof. Dr. Akın Akdağ

Şubat 2022, 115 sayfa

Son zamanlarda yüksek ilgi gören kiral organik moleküllerin polarize ışık ile etkileşimi, yaygın uygulama alanları potansiyeline sahiptir. Bu nedenle dairesel polarize ışık yayma potansiyeline sahip bileşikler yüksek talep görmektedir. Özellikle, dairesel polarize ışık yayma potansiyeline sahip organik bileşiklerin sentezi zorlu ama umut verici çalışmalardır. Bu çalışmada, kromofor grupları olarak kumarin türevleri olan kiral floresan organik bileşikler sentezlenmiştir. Tartarik asit türevlerinin enantiyomerleri, kiral birim olarak kullanılmıştır. Sentezlenen yeni bileşiklerin karakterizasyon analizlerinin yanı sıra UV-Vis, Floresan ve CD spektroskopisi ölçümleri ile fotofiziksel özellikleri de incelenmiştir. Bu bileşiklerin CPL analizleri ev yapımı CPL cihazı ile gerçekleştirilmiştir. CPL sonuçları umut verici olmakla birlikte geliştirilmeye muhtaçtır.

Anahtar Kelimeler: dairesel polarize ışık, dairesel polarize lüminesans, dairesel dikroizm, kumarin, tartarik asit

To the loving memory of my uncle, big eagle, Enis Gürhan Ateşağaoğlu…

ACKNOWLEDGMENTS

Writing this thesis was a journey that enlightened my life from many perspectives. I still have a long way to go, but I am already so far from where I used to be, and I am proud of that. There were many people in this journey who played important roles in every piece of this thesis and guided me during this path.

First and foremost, one person made this research possible and meaningful, Prof. Dr. Akın Akdağ. He started believing in me when I was a fresh undergraduate student, he saw my potential back then and guided me patiently till the end. Thus, I would like to express my deepest gratefulness and thanks to him for giving me the chance to work with him.

I kindly offer my gratitude to the rest of the committee members: Prof. Dr. Metin Zora, Prof. Dr. Özdemir Doğan, Assoc. Prof. Dr. Serhan Türkyılmaz and Assoc. Prof. Dr. Yunus Emre Türkmen for assisting me with their valuable comments, thoughts, and criticisms in shaping the final draft of this study.

I also would like to thank Assoc. Prof. Dr. İrem Erel Göktepe and Dilara Gündoğdu for DLS measurements.

I would like to thank TUBITAK for the scholarship. The work for the project (118Z710) is partially included in this thesis.

There are two special people who are the hidden heroes of this thesis, Gizem Çalışgan Ünay and Perihan Öztürk Düzenli. I cannot imagine what I would do without their guidance not just in academic but also in personal life. They were and always be like elderly sisters to me with their endless love, support, and guidance. There were many times that they lightened my darkness. I will always feel so lucky to have those powerful women by myside. There are no such words that I can express my gratefulness to them. Thank you for being there!

I would like to extend my sincere thanks to my group member: Ece Ayça Erdoğan, Bengi Şentürk, Bulem Çakmak, Ege Hoşgör, Doruk Baykal, Oğuzhan Albayrak and all other current and former AARG members for making me feel so lucky to work with them. Each day was so informative yet so joyful with those people. They supported me with their endless patience, guided me with their valuable opinions but most importantly they were always there when I needed them. Thank you for being my second family!

Besides those valuable people from the academic circle, I would like to thank my friends: Taha Yücel, Çağlayan Kızıleniş, Umut Aydemir, Gizem Damla Ateşağaoğlu and Cağrı Alan for always believing in me when even I don't believe in myself. Thank you for not letting me fall!

Some special gratitude goes to my uncle Mustafa Erhan Ateşağaoğlu who has always been my biggest motivational support.

Last but not least, I would like to offer my deepest gratitude to my mother, Enim Ateşağaoğlu, for always believing and supporting me but most importantly making me the person I am right now. I am a strong woman because a strong woman raised me.

I love you so much mom!

TABLE OF CONTENTS

LIST OF FIGURES

FIGURES

LIST OF SCHEMES

SCHEMES

LIST OF ABBREVIATIONS

ABBREVIATIONS

CD	Circular Dichroism
CPL	Circularly Polarized Luminescent
DIEA	*N, N*-Diisopropiletilamin
DMP	2,2-Dimethoxypropane
EDC	1-Ethyl-3-(3-dimethylaminopropyl) carbodiimide
HOBt	Hydroxybenzotriazole

CHAPTER 1

INTRODUCTION

1.1 Light

Throughout the history, the definition and properties of light were a question of debate and there were four theoretical descriptions of light being corpuscular theory, wave theory, electromagnetic theory and quantum theory.[1]

Isaac Newton published *"Opticks"*, in 1704, and revealed his theory called *"corpuscular theory of light"* which claims that light is the combination of small different particles called *corpuscles* and move through space.[2] However later, Newton's theory failed to explain diffraction, interference and polarization of light. With Huygens' postulations about wave nature of light in *"Traite de la Lumiere",* which can be translated as *"Treatise on Light",* Thomas Young and Robert Hooke supported wave theory so that the diffraction, interference and polarization properties of light is enlightened.[3,4,5,6] Subsequently, Maxwell defined light as a wave that is the combination of an oscillating electromagnetic field with charged particles and his definition is referred to as "classical paradigm of light as electromagnetic waves".[7] With that, scientists worked to understand the properties of light. There were many difficulties to describe it in classical concepts of "particle" or "wave". Our understanding of light today was concluded by Albert Einstein, as he stated it was not possible to explain the phenomena of light considering particle and wave properties separately, it is only logical when they are both considered exclusively.[8] Having both "particle" and "wave" features; light has various properties. With these inherently different properties of light, it just not causes the sensation of sight to the human eye but also helps to investigate the nature of the

universe. Both the intensity, propagation direction, frequency, and polarization properties are very important for that manner.

1.1.1 Absorption and Emission of Light

Planck postulated that, in the 1800s, light is composed of energetic particles called *photons*.[5] After the postulation of Planck, Einstein explained further that light travels in bundles of energy, confirming photons having both particle-like and wave-like properties. Each photon has an energy that is related to the frequency of vibration given by Planck's famous equation (Equation 1).

$$\mathbf{E = h\upsilon} \qquad \text{Equation 1}$$

Where h and υ correspond to Planck's constant (6.63×10^{-34} J.s) and frequency, respectively.

When light interacts with matter, it is observed that light is absorbed. This absorption was later on found to affect the electronic states of the matter that electrons from lower energy state move to the upper state. The energy difference between the lower and the upper state should match the incoming photons energy as can be inferred from Planck's equation. Measurement of this is called the electronic spectrum of that matter. Light with lower energy causes differences in the vibrational level of the matter. High energy light (x-ray and gamma rays) can ionize matter. Although these last two events are extremely important, we will concentrate on the electronic spectrum of matter which mainly deals with the UV-Vis region (200-800 nm) of the electromagnetic spectrum.

Early on light interaction with matter was found to be an intriguing concept. With Planck's equation in hand and the photoelectric effect it could be concluded that transfer of energy as photons results in absorption and emission of light.[7, 9] For absorption of light, photons having the same energy as the difference of two

electronic states, ground and excited states, use their energy to move one electron from ground to excited state as shown in Figure 1.[9]

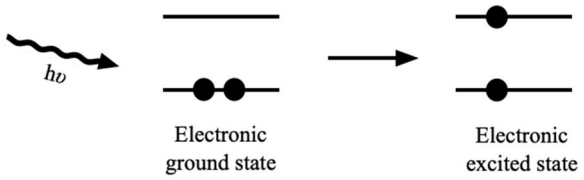

Figure 1. Pictorial representation of absorption process.

There are fundamental principles for the experimental measurement of absorption spectra. According to Beer-Lambert's Law, (equation 2) the absorption of radiation is dependent upon, concentration, path length, the intensity of the incident beam, and extinction coefficient.[10]

$$\mathbf{A = \varepsilon bC} \qquad \text{Equation 2}$$

Where ε: extinction coefficient (L x mol^{-1} x cm^{-1}), b: path length (cm) and C: concentration (mol x L^{-1})

Quantity of absorption is reported as optical density (OD) and absorption spectra are generally plotted as OD versus wavelength (λ, in nm). The equation for optical density is shown in equation 3 whereas I_0 is the intensity of light and I_T is the intensity of transmitted light.

$$\mathbf{OD = \log (I_0/I_T)} \qquad \text{Equation 3}$$

The process is called emission when an excited atom or molecule emits a photon of energy having the same as the difference between two electronic states shown in Figure 2. Emission can be taught as the reverse process of absorption.[9]

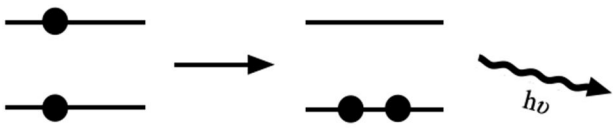

Figure 2. Pictorial representation of emission process.

Experimental measurement of emission spectra is obtained by the collection of data at a fixed excitation wavelength and constant intensity for the incident light (I_0). Like absorption spectra, emission spectra are plotted as emission intensity (I_e) versus wavelength (λ, in nm) and the relation can be shown as Equation 4.[7,9]

$$I_e = 2.3lCI_0\varepsilon\Phi \qquad \text{Equation 4}$$

Where l: path length (cm), C: concentration (mol x L^{-1}), ε: extinction coefficient (L x mol^{-1} x cm^{-1}), Φ: quantum yield.

1.1.1.1 UV-Vis Absorption and Fluorescence Spectroscopy

The Ultraviolet (UV) region of the electromagnetic spectrum approximately comprises between 100-380 nm range whereas the visible (Vis) region comprises between 380-750 nm. With UV-Vis spectroscopy transmittance, reflectance and photoluminescence studies are done and it is related to the outermost electrons and their excitation.[11] Absorption of light occurs typically in 10^{-15} s whereas emission from an excited molecule after absorption of light occurs longer than 10^{-9} s.[12]

1.1.1.1.1 UV-Vis Absorption Spectroscopy

Absorption bands in the UV-Vis region are determined by the transitions between electronic energy states that are related to the transitions between molecular orbitals.[13]

The general bonding molecular orbitals have σ and π MOs. According to the pairing theorem σ^* and π^* orbitals also arise as antibonding orbitals. In some molecules, non-bonding orbitals are located in between bonding and antibonding orbitals. Thus, the absorption phenomena possibilities are $\sigma \rightarrow \sigma^*$, $\sigma \rightarrow \pi^*$, $\pi \rightarrow \pi^*$, $n \rightarrow \sigma^*$, $n \rightarrow \pi^*$.

Although in a molecule having all the molecular orbitals mentioned above can have the transition stated, not all transitions occur due to the selection rule. [14]

Energetically, the transitions fall into the UV-Vis region. To measure this, one has to device an instrument called UV-Vis spectrometer whose block diagram is given below in Figure 3.

Figure 3. Block Diagram of UV-Vis Instrument.

1.1.1.1.2 Photoluminescence Spectroscopy

Emission spectrum of a compound can constitute two events: fluorescence and phosphorescence. Where fluorescence is the emission from singlet excited state (S_1) and phosphorescence is from triplet excited state (T_1) (Kasha's Rule) and the fluorescence energy is higher than phosphorescence energy. There are several molecules that do not obey Kasha's rule, these molecules and the events are not in the scope of this thesis. Fluorescence and phosphorescence spectroscopies are referred to as photoluminescence spectroscopy. The graphical representation of these phenomena is shown in Figure 4. The process of transition between singlet to triplet state is called intersystem crossing (ISC).[11,15]

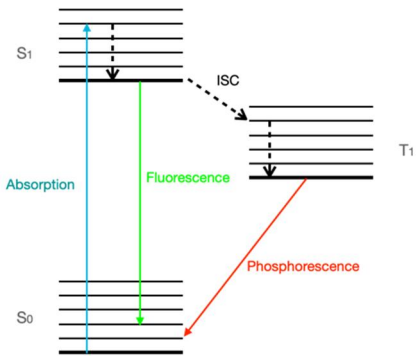

Figure 4. Pictorial representation of absorption, fluorescence, and phosphorescence.

The energy of emitted photon is usually lower than the absorbed photon. This is due to the different deactivation pathways occurring in a molecule, i.e vibrational relaxations.

Chromophores do not necessarily fluoresce due to other deactivation pathways such as Conical intersections but the ones that emit a photon are called fluorophores and each has its own fluorescence properties that are intrinsic and can be modified with the environment.[16] Fluorescence and phosphorescence events can be measured with an instrument called fluorometer in which the light source is 90° to the detector. The plot of fluorescence intensity versus wavelength is called fluorescence spectrum.[17] A simple block diagram of a fluorescence spectrophotometer can be shown as in Figure 5.

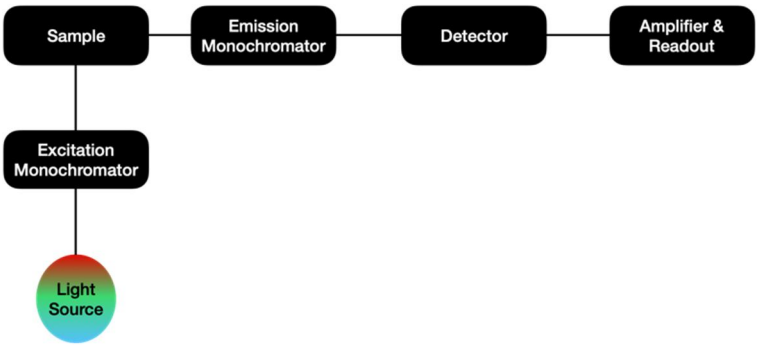

Figure 5. Block diagram of Fluorescence Spectrophotometer.

1.1.2 Polarization Of Light

Polarization of light is an important phenomenon for the understanding of electromagnetic radiation among the entire spectral range. Malus, in 1808, identified that the originally unpolarized light converted to partially polarized light with a dielectric surface. Later in 1816-1817, Fresnel and Young carried out the interference experiments, independently, and concluded a very meaningful result that orthogonally polarized beams do not interfere since vertical and horizontal

polarization, as well as left- and right- circular polarization, generates a binary set of orthogonal modes.[18]

As mentioned before, light is electromagnetic radiation. Perpendicular oscillation of magnetic and electric fields forms an electromagnetic wave, as shown in Figure 6. Three mutually perpendicular cartesian axes, x, y, and, z, represents a wave.

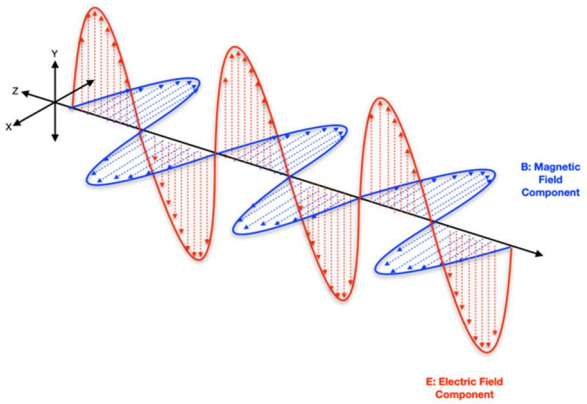

Figure 6. Pictorial representation of electric (red) and magnetic (blue) field components of light.

Polarization can simply be referred to as the asymmetry between the propagation and vibration direction of the light wave.[19] According to different characteristics of polarization, polarized light can be divided into linearly, circularly, and elliptically polarized light. Basically, refining one of the electric fields and eliminating the others is considered as linearly polarized light as shown in Figure 7a. Further, linearly polarized light could be turned into circularly polarized light with a delay of $\lambda/4$ by a quarter wavelength retarder that results in two planes, having the same amplitude, propagating with a 90° phase delay as shown in Figure 7b.[20] In order to form the desired polarization, optical devices are known as electro-optic light modulators are used.

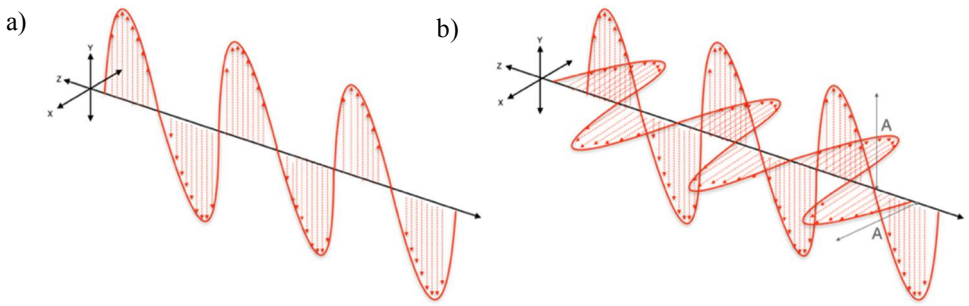

Figure 7. Pictorial representation of a) linearly polarized and b) circularly polarized light

1.1.2.1 Linearly Polarized Light

Polarization of a light wave is, determined by the way its electric field vector, $\vec{E}(\vec{r},\vec{t})$, oscillates. As it can be seen in figure x, when the oscillation of electric field $\vec{E}(\vec{r},\vec{t})$ is in one fixed plane, linearly polarized light is generated. When light has its electric field oscillating in xz plane while propagating along z-axis then it is said to be x-polarized or linearly polarized light.[19,21] Linearly polarized light can be produced by an unpolarized light beam through linear polarizers, which selects only one wave of light as shown in Figure 8.[22]

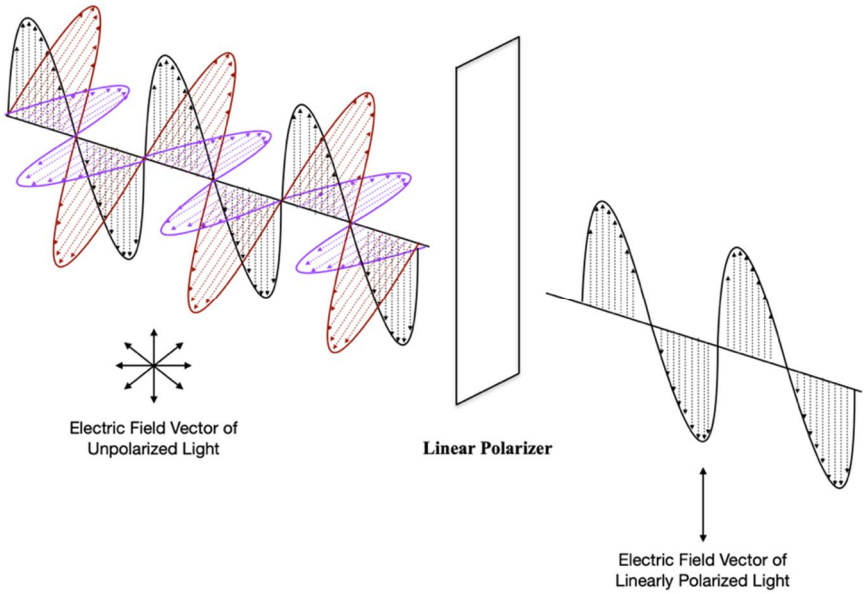

Figure 8. Pictorial representation of generation linearly polarized light from unpolarized light using a linear polarizer and their electric field vectors.

1.1.2.2 Circularly Polarized Light

When linearly polarized light also has a circular motion, circular polarization occurs thus, light becomes circularly polarized when the magnitude remains the same while the direction of the $\vec{E}(\vec{r},t)$ rotates along propagation axes with the propagation time. Left or right circularly polarized light is generated depending upon the rotational direction. In other words, circular polarization will occur when the horizontal and vertical components of the electric field have equal amplitudes but one of them having a phase delay of $\pi/2$ ($-\pi/2$) with respect to the other.[18]

Circularly polarized light is first discovered by Augustin Fresnel in 1822. Using Fresnel triprism, left and right circularly polarized components of a plane-polarized beam are resolved. Fresnel tripism, shown in Figure 9, can be made by placing a right-handed quartz between two quartz left-handed half prisms. During the experiment of Fresnel, light propagated parallel to the optic axes thus not allowing it to be affected by double refraction however Fresnel still observed, at the exit facet,

two beams with small angular separation. In order to understand whether these emerging beams are linearly polarized or not Fresnel used double refraction calcite and concluded that each beam is orthogonal to the other.[23]

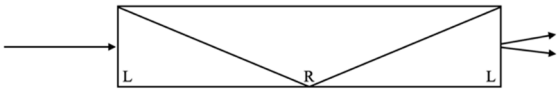

Figure 9. Fresnel Tripism.

Circularly polarized light can be formed from linearly polarized light, shown in Figure 10, via an optical device called quarter-wave plate in which one axis of linearly polarized light is delayed ¼ wavelength relative to the orthogonal axis and according to the delayed wave, left or right-handed helices occur.[22,24]

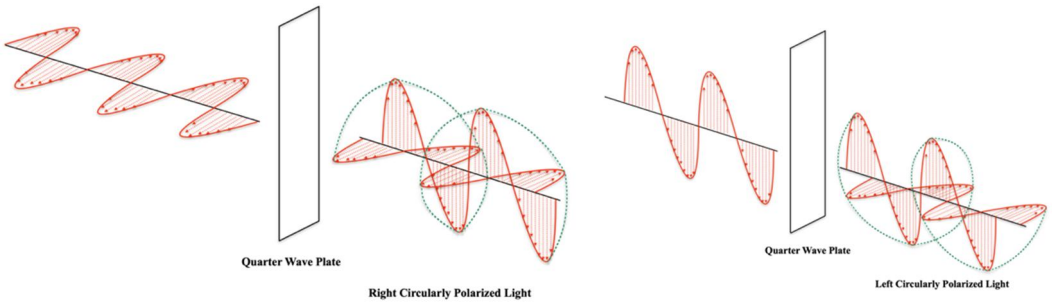

Figure 10. Pictorial representation of right- and left- circularly polarized light generation with a quarter-wave plate.

Since Pasteur, it is known that chiral molecules interact with polarized light differently. That is chiral molecules are capable of rotating the plane-polarized light in different angles. This is measured with polarimeters. This, in fact, implies that chiral molecules act like polarizers. This observation led to the development of several spectroscopic techniques to study chirality.

1.2 Chirality

Derived from Greek Word χειρ (hand), *chirality* is a geometric property of rigid objects that devoid of improper rotation axes (S_n). The concept was first coined in 1893 by Lord Kelvin.[25] Molecules that are non-superimposable on their mirror image are called chiral molecules and they have two specular forms which are called enantiomers or optical isomers. Chemical properties of enantiomers are different in an unsymmetrical environment but the same in a symmetrical one.[26]

There are different types of chirality, shown in Figure 11, chiral objects either can have a chiral center (Figure 11 a.), chiral axis (Figure 11 b.), chiral plane (Figure 11 c.), or have helical chirality (Figure 11 d.).

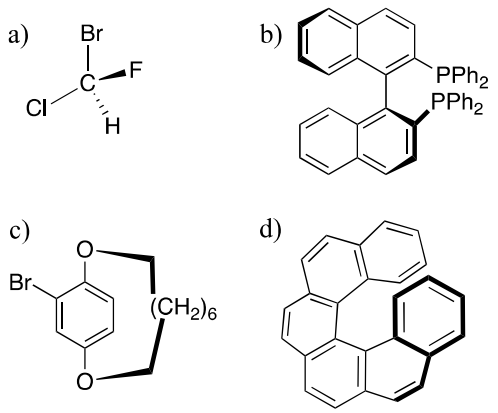

Figure 11. Chiral molecules having a) center of chirality, b) chiral axis, c) chiral plane and d) helical chirality.

For molecules having a center of chirality, there is a central C atom which is surrounded by four different atoms (Figure 11 a.). In other types of chirality, there is not any chiral center but lacks S_n. When the source of chirality possesses from a restriction around an axis it is called axial chirality (Figure 11 b). Unlike axial chirality, in helical chirality molecules have a curved skeleton with terminal rings in opposite directions (Figure 11 d). When a molecule has two dissymmetric non-coplanar rings it possesses planar chirality (Figure 11 c).[19]

Chirality is omnipresent in nature, it can be seen in the helices followed out by the arms of galaxies and even in the first forms of life in dinosaurs.[13,14] Even during the molecular evolution of Earth, according to the biomolecules homochirality phenomenon, only single handedness is selected by the nature resulting in the availability of many enantiopure biomolecules. While RNA, DNA, and polypeptides are all right-handed (*D*), amino acid molecules are designated as left-handed (*L*).[29] However, it is important to emphasize that the less common enantiomers may also be present in some systems, such as the presence of *D*-alanine and *D*-glutamate in the cell wall of bacteria.[26]

Chiral compounds become very important due to their applications in various areas mainly, in drug development. This led to the development of asymmetric synthesis, chiral recognition, enantioseparation, and chiral luminescent materials.[30]

One of the main techniques to identify molecular chirality is using the chirality of light, circularly polarized light in particular, *vide supra*. Circularly polarized light has a helical structure allowing it to be used as a chiral reagent for the identification of chiral molecules.[31] Among many other electromagnetic interactions, forceful chiral light-matter interactions encompass optical rotation, circular dichroism, and circular luminescence.

1.3 Chiroptical Spectroscopy

Spectroscopic techniques based on the interaction between chiral matter with circularly polarized light are called chiroptical spectroscopies. According to the handedness of polarization, chiral molecules interact differently with circularly polarized light. Stereochemical information about chiral molecules can be obtained via chiroptical spectroscopy. Depending upon the polarizability left- and right-circularly polarized components of light travels at different velocities after interaction with a chiral object causing the rotation of the polarized light toward left or right. In the case of achiral molecules, even though they rotate the polarization

vector, there is always an oppositely oriented molecule that cancels the rotation effect and consequently, the polarization angle of the light will not change at the end. In other words, the interaction difference between left- and right- circularly polarized light with the sample is what chiroptical spectroscopy is based on.[32] Chiroptical signal is the differential interaction between the energy of the electromagnetic radiation and the energy gap of a transition that results in absorption or emission band.[26] Circular dichroism (CD) and Circularly Polarized Luminescence (CPL) are types of chiroptical spectroscopy. While CD spectroscopy originates with the molecules in their electronic ground state, CPL originates from the electronically excited state.[18]

1.3.1 Circular Dichroism (CD) Spectroscopy

When a medium containing a chiral molecule interacts with a circularly polarized light, the intensity of emerging and entering lights are different due to the absorption of light. The intensity of right- and left- absorbed light by chiral molecules is different and this differential absorption is called circular dichroism (CD). [19] When right- and left-handed light passes through a chiral molecule, it results in spectral features involving negative or positive peaks.[34] The characteristic change in circular dichroism around the absorption band of a substance is called the "Cotton Effect", discovered by Aimé Cotton in 1895 using potassium chromium (III) tartrate. Magnitude crosses zero at absorption maxima with a rapid change in opposite directions before and after. As shown in Figure 12, the positive Cotton effect is observed when optical rotation first increases with decreasing wavelength and the negative Cotton effect when optical rotation first decreases with decreasing wavelength. The sign of the signal depends upon the chromophore and the properties of the electronic transition.[35,36]

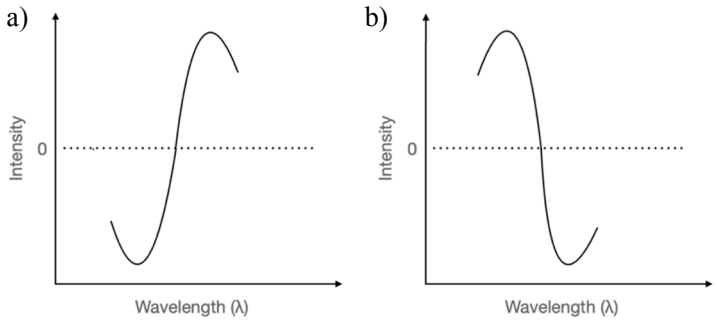

Figure 12. Positive (a) and negative (b) cotton effect curves

The magnitude of the signal is the absorbance difference in right and left circularly polarized light as a function of wavelength as shown in equation 5.[34]

$$\Delta A_{CD}(\lambda) = A_L(\lambda) - A_R(\lambda) \qquad \text{Equation 5}$$

A simple block diagram of CD spectroscopy can be shown as in figure 13:

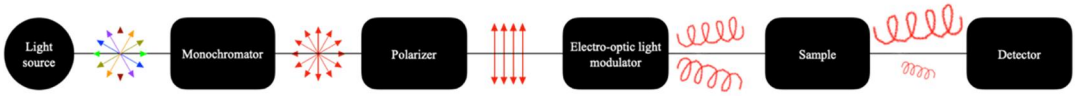

Figure 13. Simple Block Diagram of CD spectroscopy.

Light arising from the light source first passes through a monochromator resulting in light with a single wavelength which then linearly polarized through a polarizer. In order to obtain a circularly polarized light, it then passes through a quarter-wave plate, in a commercial instrument electro-optic light modulator. Sample absorbs the circularly polarized light, and the difference between left- and right-handed circularly polarized light is detected by the detector after being transmitted.

With the works of Biot, Pasteur, and Cotton starting 1960s, techniques that underlie the CD instrumentation for the illumination of equilibrium structures of chiral molecules become popular.[18,38,39] Well-known applications of CD spectroscopy are based upon the study of the helicity of biopolymers and the absolute stereochemistry

of organic molecules. Major information about both the conformation and electronic state of the chromophore-containing molecule can be provided by CD spectroscopy.

1.3.2 Circularly Polarized Luminescence (CPL) Spectroscopy

As mentioned before chiral molecules can act as polarizing mediums. With that in mind, chiral molecules can emit light which can be polarized. If a chiral molecule is emitting circularly polarized light, this can be measured with CPL spectroscopy.

Both information about molecules' conformation and structure in their photoexcited state can be obtained using CPL spectroscopy. Circularly Polarized Luminescence spectroscopy is the emission analogue of CD spectroscopy. Thus the differential emission of left- and right- circularly polarized light by chiral non-racemic luminescent systems is classified as CPL.[40] The spectroscopy is based on the spontaneous difference in luminescence intensities between left and right circularly polarized light. This difference can be defined with the equation 6.[33]

$$\Delta I(\lambda) = I_L(\lambda) - I_R(\lambda) \qquad \text{Equation 6}$$

It is more common to report the degree of CPL in terms of the luminescence dissymmetry factor g_{lum}, equation 7, due to the difficulties in the measurement of absolute emission intensities.

$$g_{lum} = \frac{\Delta I}{0.5\, I} = \frac{I_L - I_r}{\frac{1}{2}(I_L + I_r)} \qquad \text{Equation 7}$$

One can expect that the larger $|g_{lum}|$ values mean larger CPL activity refers to the good polarization degree of the emitted light. Various variables can change the g_{lum} value some of them can be listed as; orientation of molecules, temperature, and solvent polarity.[24]

1.3.2.1 Circularly Polarized Luminescent Materials

CPL exhibiting molecules are very promising candidates for various areas including, optical quantum information, optical data storage, molecular photoswitches, medical imaging techniques, and chirality sensing.[41] The combination of a luminophore and chiral environment results in the CPL-active material. Even though the lanthanide complexes are mainly focused on early research of CPL materials with high g_{lum} values (0.05-0.5) their applications are limited because of their low photoluminescence quantum yield.[30] Transition-metal complexes exhibited both high g_{lum} and photoluminescence quantum yield however due to the cost, toxicity, and rareness of these transition-metals encountered difficulty to be used.[42] Simple organic molecules are found more promising for CPL activity owing to their fine photophysical properties, tunable chiral centers, easy synthesis, low cost, and toxicity. Various organic materials have been reported as CPL-active material over the past years such as transition metal complexes, conjugated polymers, and small organic polymers.[20] The first example of CPL-active simple organic molecule (+)-(S,S)-trans-β-hydrindanone, shown in Figure 14, is reported in 1967 by Oosterhoff and Emeis with a g_{lum} value as $+3.5x10^{-2}$ at 361 nm.[43]

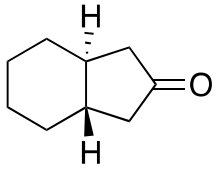

Figure 14. Structure of (+)- (S, S)-trans-β-hydrindanone.

(+)- (S,S)-trans-β-hydrindanone, which is a bicyclic ketone, has an inherently achiral carbonyl chromophore however due to the chiral structure that it is embedded in, its electronic transitions are chirally perturbed. By exciting the carbonyl chromophore at 313 nm in isooctane solution it shows a CPL.[40] This first example inspired the synthesis of many other chiral ketones, shown in Figure 15, that exhibits CPL in UV region by carbonyl fluorescence.[44,45]

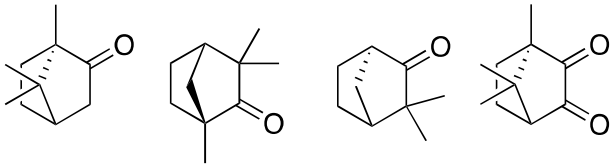

Figure 15. Left to right; (1R)-camphor, (1R)-fenchone, (1R)-camphenilone, and (1R)-camphorquinone.

For both above-mentioned molecules, g_{lum} values were typically within the range of 10^{-3} to 10^{-2}. These relatively low g_{lum} values are due to the low fluorescence quantum yields of the involved carbonyl centered transitions which are under the classification of $n \rightarrow \pi^*$ transitions.[40] In 1979 Barnett, Drake and Mason reported the first chiral aromatic simple organic molecule calycanthine, shown in Figure 16, with a g_{lum} value up to +8 x 10^{-3} upon UV excitation in ethanol.[46]

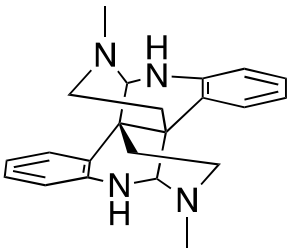

Figure 16. Structure of Calycanthine.

Aniline chromophore involved in the calycanthine is not chiral however, as in the case of chiral ketones, it is chirally perturbed by the chiral structure. In this case, the transitions are $\pi \rightarrow \pi^*$ transitions with higher fluorescent efficiencies.[40]

These small organic molecules generally have good solubility in organic solvents that reduces the fluorescence quenching by aggregation and also having small size and lacking a transition metal in their structure increases their usage in specific manufacturing areas where toxicity and stability are problematic.[40]

Higher g_{lum} values are observed for organic systems in their aggregated states.[47,48] This is due to the strong orbital angular momentum of chiral helical molecular assemblies that will allow to turn the spin polarization.[49] Thus, a strong CPL signal can be generated upon electro-excitation by a helically organized luminophore. A popular strategy to achieve that is to cooperate chiral moieties with planar conjugated luminophores to form helical assemblies.[50] The long-range ordering of molecules in their helical aggregated states results in this strong CPL effect.

1.3.2.2 CPL Instrumentation

There are both home-built and commercial instruments reported in the literature over past decades. The home-built instrument's design is based on a fluorescence spectrometer.[24] The simple block diagram of a home-made Circularly Polarized Luminescence instrument is shown in figure 17.

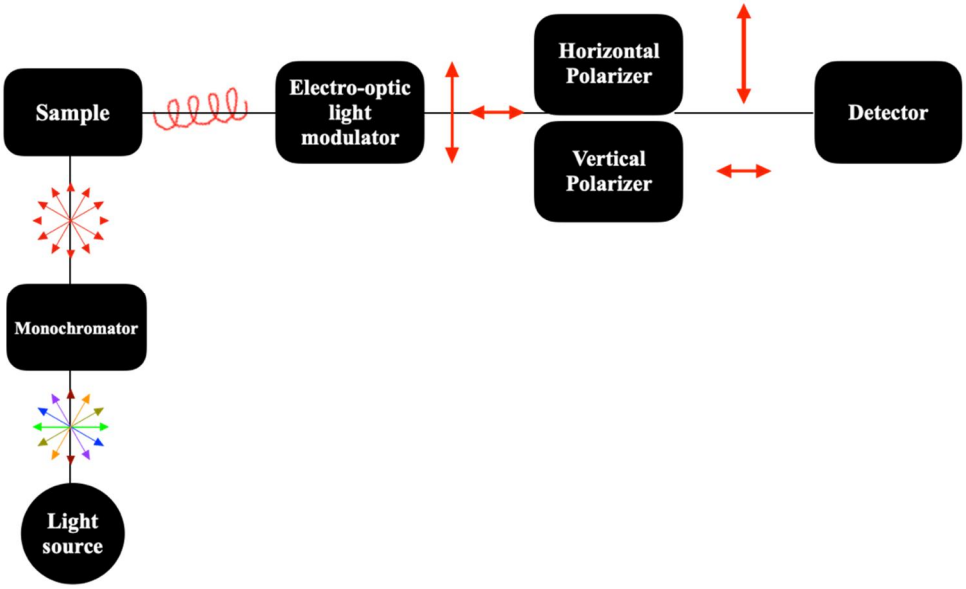

Figure 17. Simple Block Diagram of a home-made CPL instrument.

Light arising from the light modulator is fixed at a picked frequency with a monochromator then the intensity of luminescence light's circularly polarized

component is selectively modulated whereas it is converted into its horizontal and vertical components and both are separately passes through a linear polarizers and detector first measures the intensity difference between horizontal and vertical component for both left and right handed circularly polarized light and with that the intensity difference between left and right circularly polarized light can be detected.

In order to minimize the depolarization sources, there should be no extra component between the sample and modulator. The use of a quarter-wave plate, as the modulator, behind the optical element to modulate the light intensity is essential because circularly polarized light will emerge elliptically polarized thus the difference in optical path length will be a quarter of a wavelength of the light at a certain level of stimulation.[40,51]

The search for CPL emitting materials is in high demand. With that in mind, the fluorophores in chiral environment are taught to be good candidates for this purpose. For example, coumarin and coumarin derivatives could serve this purpose.

1.4 Coumarin

Coumarin (2H-1-Benzopyran-2-one), shown in Figure 18, is an aromatic compound having the C_9H_6O formula bearing benzene nucleus with pyrone ring and carbonyl moiety is in the second position. Coumarins are colorless crystalline solids with a vanilla-like smell and they are naturally found in various plants, mostly in fruit parts.[52,53]

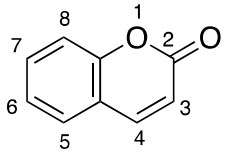

Figure 18. Structure of coumarin (2H-1-Benzopyran-2-one) and assigned numbers.

William Henry Perkin was the first one to synthesize, shown in Scheme 1, and introduce coumarin in 1868 even though it was first isolated in 1820 by A. Vogel from tonka beans but he misinterpreted it as benzoic acid.[54]

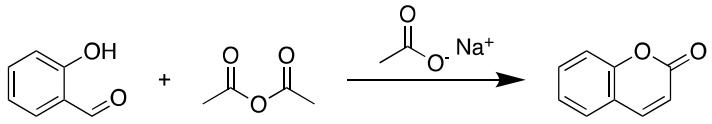

Scheme 1. Synthesis of coumarin via Perkin Reaction

Coumarin containing molecules are highly used in therapeutic areas in the drug industry. Due to applications of coumarin and its derivatives in both physical, biological and chemical fields they are broadly investigated throughout the years.[55] Owing to their short synthetic routes and photostability, coumarins are widely used as photonic materials. Even though coumarin itself has a week fluorescent activity many fluorescent tags and probes are based on coumarin dyes since its photophysical activities can be easily improved with structural modifications. Electron donating groups in 7-position and electron-withdrawing groups in 3-position improve the spectral features owing to inductive and mesomeric effects. Generally, coumarin derivatives have an absorption maxima around 300-350 nm whereas an emission maxima around 400-450 nm.[56]

1.4.1 Benzocoumarin

Benzocoumarins, also known as benzochromenones, are a family of π-extended coumarin derivatives with promising properties as a photonic material.[56] There are four different benzocoumarin derivatives being benzo[*h*]coumarin, benzo[*g*]coumarin, benzo[*f*]coumarin and benzo[*c*]coumarin depending upon the fused position of an additional aromatic ring to the coumarin core as shown in Figure 19.[57] Among those derivatives, benzo[*c*]coumarin exhibits diverse photophysical properties compared to others since it has "crossed" conjugation resulting in less contribution to the efficiency of absorption and emission wavelengths. Owing to

their “linear” conjugation benzo[*h*]coumarin, benzo[*g*]coumarin, benzo[*f*]coumarin derivatives exhibit larger wavelength emission and absorption spectra with an increased quantum yield. Benzo[*g*]coumarins are predicted have longer wavelength absorption and emission owing to their larger transition dipole moments. Since benzo[*h*]coumarin and benzo[*f*]coumarin have bent shape structures they have shorter conjugation lengths with decreased transition dipole moments.[58]

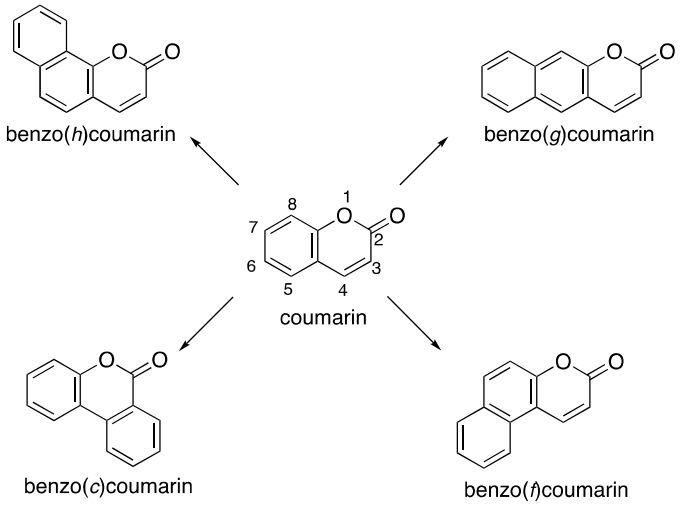

Figure 19. Chemical structures of benzocoumarin derivatives.

With the advanced photophysical properties of benzocoumarin derivatives, they provide some auspicious features over coumarin itself. Like coumarin, it is also possible to enhance these photophysical properties with increasing intramolecular charge transfer (ICT) via substitution of electron-withdrawing or donating groups to appropriate positions of benzocoumarin derivatives. With these enhanced photophysical properties of benzocoumarin derivatives, drawbacks arousing from shorter-wavelength absorption and emission of coumarin derivatives can be alleviated.[45–47]

There should also be a chiral unit in the molecule for it to be a cpl active, *vide supra,* and tartaric acid is an auspicious candidate for cooperation with the coumarin derivatives.

1.5 Tartaric Acid

Tartaric acid (TA), 2,3-dihydroxybutanedioic acid, is an eminent organic acid and one of the most well-known naturally occurring chiral compounds. Jean Baptiste Biot is the one that identified its chirality in 1832. TA has two asymmetric carbons and depending upon their orientation three stereoisomeric forms of TA exists being, *L*(+)-tartaric acid, *D*(+)-tartaric acid and *meso*-tartaric acid, shown in Figure 20. Among two enantiomers of tartaric acid *L*(+)-tartaric acid is the most abundant form of it in nature and it commonly used in many industries e.g., pharmaceutical, food and polyester. Both *L*(+), and *D*(-) enantiomers are also highly important for scientific applications.[59–61]

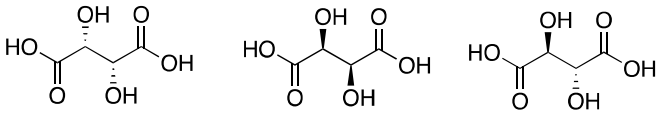

Figure 20. Stereoisomeric forms of tartaric acid.

Tartaric acid is a good chiral scaffold since both enantiomers are easily available and low-priced. It can be derivatize into many fine-tuned molecules with two unambiguous stereocenters.[59] One of the prominent derivatives of tartaric acid is TADDOLs, tetraaryl-2,2-dimethyl-1,3-dioxolan-4,5-dimethanols, (Figure 21). They are multifaceted chiral auxiliaries and can be used as for many purposes in enantioselective synthesis e.g., stoichiometric chiral reagents, catalytic hydrogenation, stereoregular metathesis polymerization.[60,62]

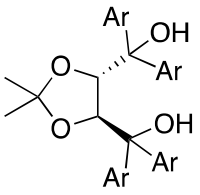

Figure 21. Structure of Taddol

Amato and co-workers reported two TADDOL derivatives (Figure 22), 2,2-dimethyl-trans-4,5-bis(di(1-naphthyl)hydroxymethyl)- 1,3-dioxolane and 2,2-dimethyl-trans-4,5-bis(di(2-naphthyl)-hydroxymethyl)-1,3-dioxolane, that can lead to oppositely signed CD and CPL signals on solution with a g_{lum} value of approximately 9.4 x 10^{-3} at 410 nm and 3.9 x10^{-3} at 375 nm.[63]

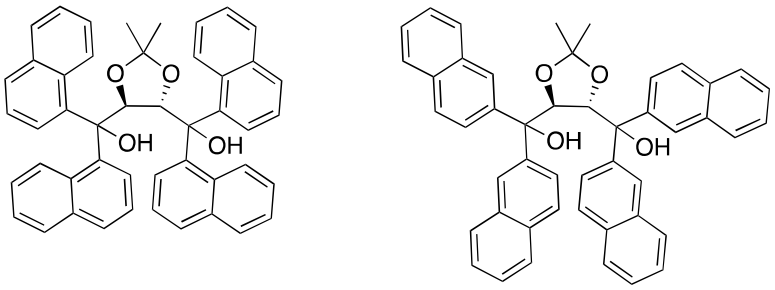

Figure 22. Structure of 2,2-dimethyl-trans-4,5-bis(di(1-naphthyl) hydroxymethyl)-1,3-dioxolane (left) and 2,2- dimethyl-trans-4,5-bis(di(2-naphthyl)-hydroxymethyl)-1,3-dioxolane(right).

Also in this thesis, tartaric acid is used as a chiral scaffold for target products.

CHAPTER 2

AIM OF THE STUDY

Circularly polarized light exhibiting compounds is an emerging concept that has the potential of widespread application areas. Small organic compounds are remarkable and promising candidates for CPL exhibiting materials. Compounds which are exhibiting CPL are chiral and besides their point chirality, these compounds also have helical chirality as well. Previous studies in our laboratories proposed that such phenomena can be induced with tartaric acid derivatives. [64] With this in mind, this study aims to synthesize coumarin conjugates of tartaric acid derivatives. Coumarin derivatives are known to be stable fluorophores affected by chiral units attached to them. In this context, both *L* and *D* enantiomers of **C1**, **C2**, **BC1**, and **BC2** will be synthesized and subsequently, their spectroscopic and chiroptic studies will be carried out.

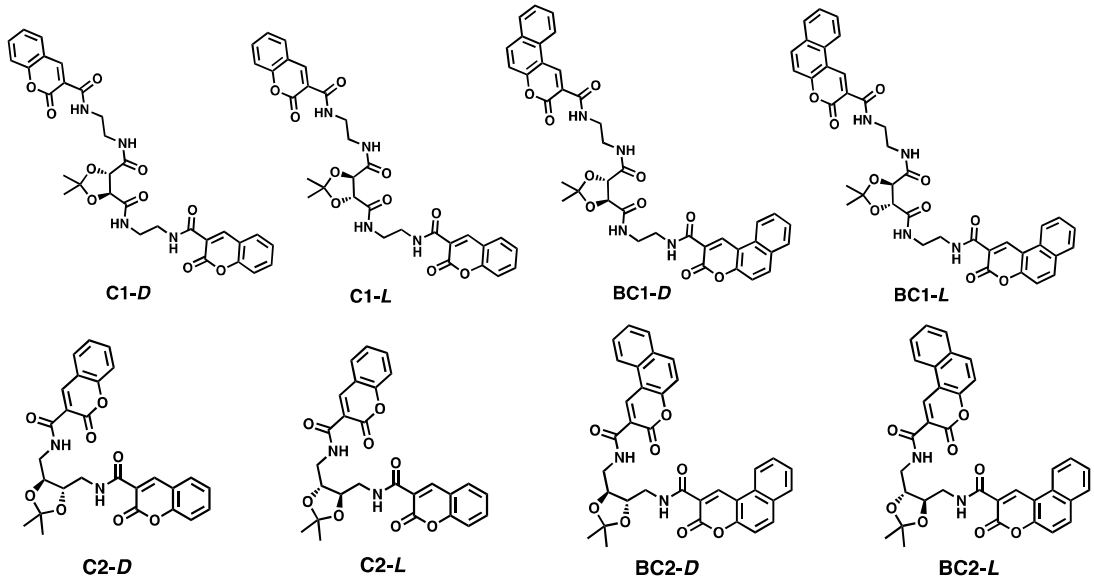

CHAPTER 3

RESULTS AND DISCUSSION

3.1 Synthesis of Coumarin and Benzo[*f*]coumarin Derivatives

In the literature, it is known that the treatment of salicylaldehyde with diethyl malonate furnishes ethyl coumarin-3-carboxylate.[65] Our synthesis toward coumarin derivatives also started with treating salicylaldehyde with diethyl malonate in the presence of piperidine in ethanol under reflux conditions. This reaction yielded ethyl coumarin-3-carboxylate with a 94 % yield (Scheme 2,a). With this successful reaction in hand, 2-hydroxy-1-naphthaldehyde was treated with diethyl malonate in the presence of piperidine in ethanol under reflux conditions to yield ethyl benzo[*f*]coumarin-3-carboxylate, 88% (Scheme 2,a)

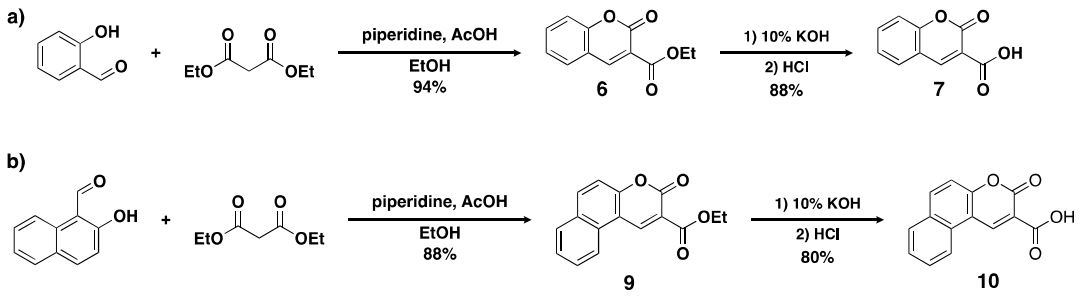

Scheme 2. Syntheses of **a)** coumarin-3-carboxylic acid, **b)** benzo[f]coumarin-3-carboxylix acid.

Coumarin derivatives were subjected to saponification at 3 positions with 10% KOH in water. The carboxylates were then acidified to get 3-carboxylic acid derivatives of coumarins (Scheme 2).

3.2 Synthesis of Tartaric Acid Derivatives

Syntheses of all tartaric acid derivatives were started from esterification of both *D* and *L* tartaric acids in ethanol with $SOCl_2$ (Scheme 3). With this reaction, diethyl tartrate was obtained in a 98% yield. Subsequently, the diol units on diethyl tartrates were protected as acetonide by treating with 2,2-dimethoxypropane (DMP) in acetone in the presence of pTSA (Scheme 3).

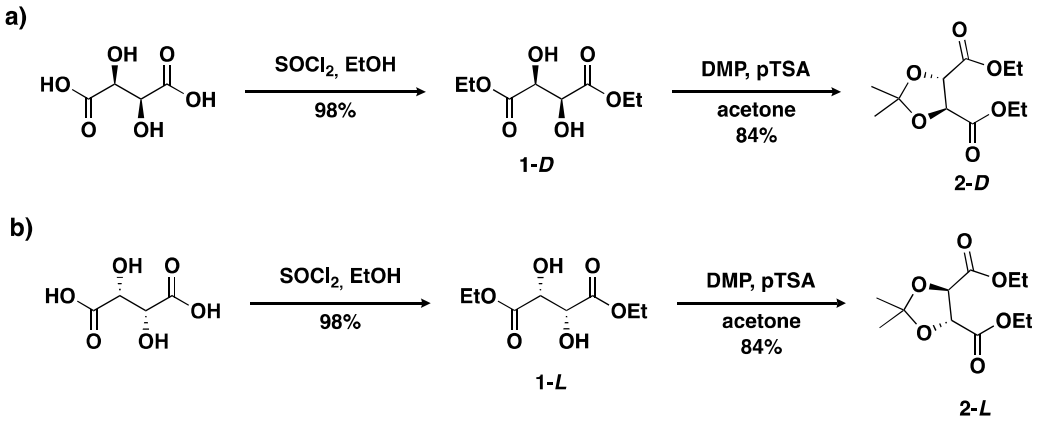

Scheme 3. Synthesis of **a)** *D*, **b)** *L* protected diethyl tartrates starting from tartaric acid

3.2.1 Synthesis of compound 3

Fully protected tartaric acid was then treated with excess 1,2-ethylenediamine to get compound **3**. The work-up for this reaction was cumbersome due to difficulty in removal of excess 1,2-ethylenediamine from the reaction medium which is achieved by suspending the crude reaction mixture in methanol then adding toluene onto it. This process resulted in the formation of a glue-like yellowish-brown product after removing the solvents. (Scheme 4).

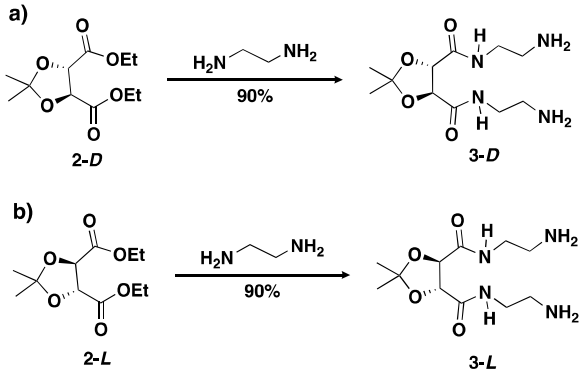

Scheme 4. Synthesis of **a)** compound **3-*D***, **b)** compound **3-*L*** from corresponding protected diethyl tartrate.

3.2.2 Synthesis of compound 5

Fully protected tartaric acid was treated with ammonia gas in a high-pressure vessel at 55°C yielded the amide form, 91.59% (Scheme 5). Subsequently, treatment of the amide with $LiAlH_4$ in a one-pot reaction did not yield satisfactory results [64]. With this in mind, the following reduction was performed in a Soxhlet apparatus in THF. Due to the limited solubility of the amide in THF, it is loaded in the porous thimble and $LiAlH_4$ was suspended with THF in the flask. The reaction furnished target compound **5** in a 51% yield.

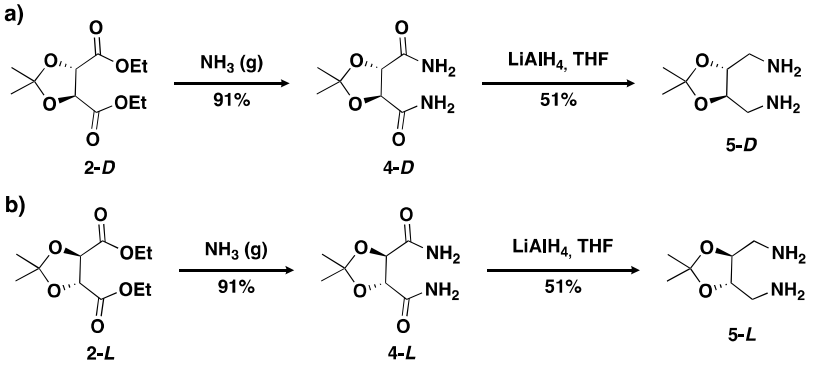

Scheme 5. Syntheses of **a)** compound **5-*D***, **b)** compound **5-*L*** starting from protected diethyl tartrate.

3.3 Coupling of Diamines with Coumarin Derivatives

With compounds **3-*D***, **3-*L***, **5-*D***, and **5-*L*** in hand, they were coupled with compounds **7** and **10** separately.

Compound **7** was refluxed in $SOCl_2$ to obtain the corresponding acyl chloride, compound **8** which was then treated with **3-*D*** and **3-*L*** separately in DCM in the presence of pyridine. The reaction mixture was then subjected to column chromatography and after purification desired compounds, **C1-*D*** and **C1-*L***, were obtained in less than 5% yield (Scheme 6). The limited solubility of **3-*D*** and **3-*L*** in DCM could be the reasoning behind this low yield.

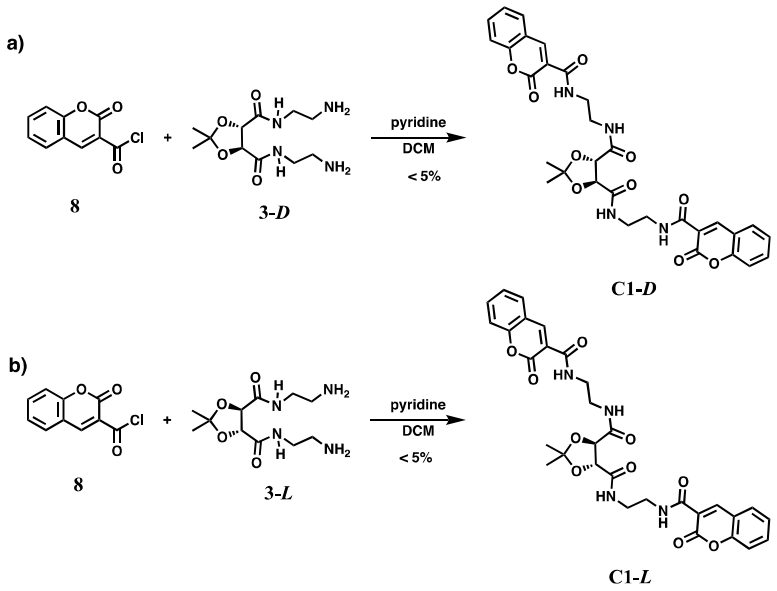

Scheme 6. Syntheses of **a) C1-*D* b) C2-*L*** from acyl chloride.

To overcome the low yield problem a 1-ethyl-3-carbodiimide (EDC) coupling procedure was followed. Due to the lack of solubility in DCM, the solvent was changed to DMF. The coupling reaction was executed by dissolving compound **7** in DMF followed by the addition of EDC.HCl, HOBt, and Hunig's base. Subsequent addition of compound **3** after 2 hours and stirring overnight under Ar atmosphere yielded the crude product. The residue was further purified with column

chromatography to get the desired compound with a 10% yield. From this experience was concluded that the coupling reaction works better than the acyl chloride procedure. Therefore, the other compounds were synthesized following this EDC coupling procedure (Scheme 7).

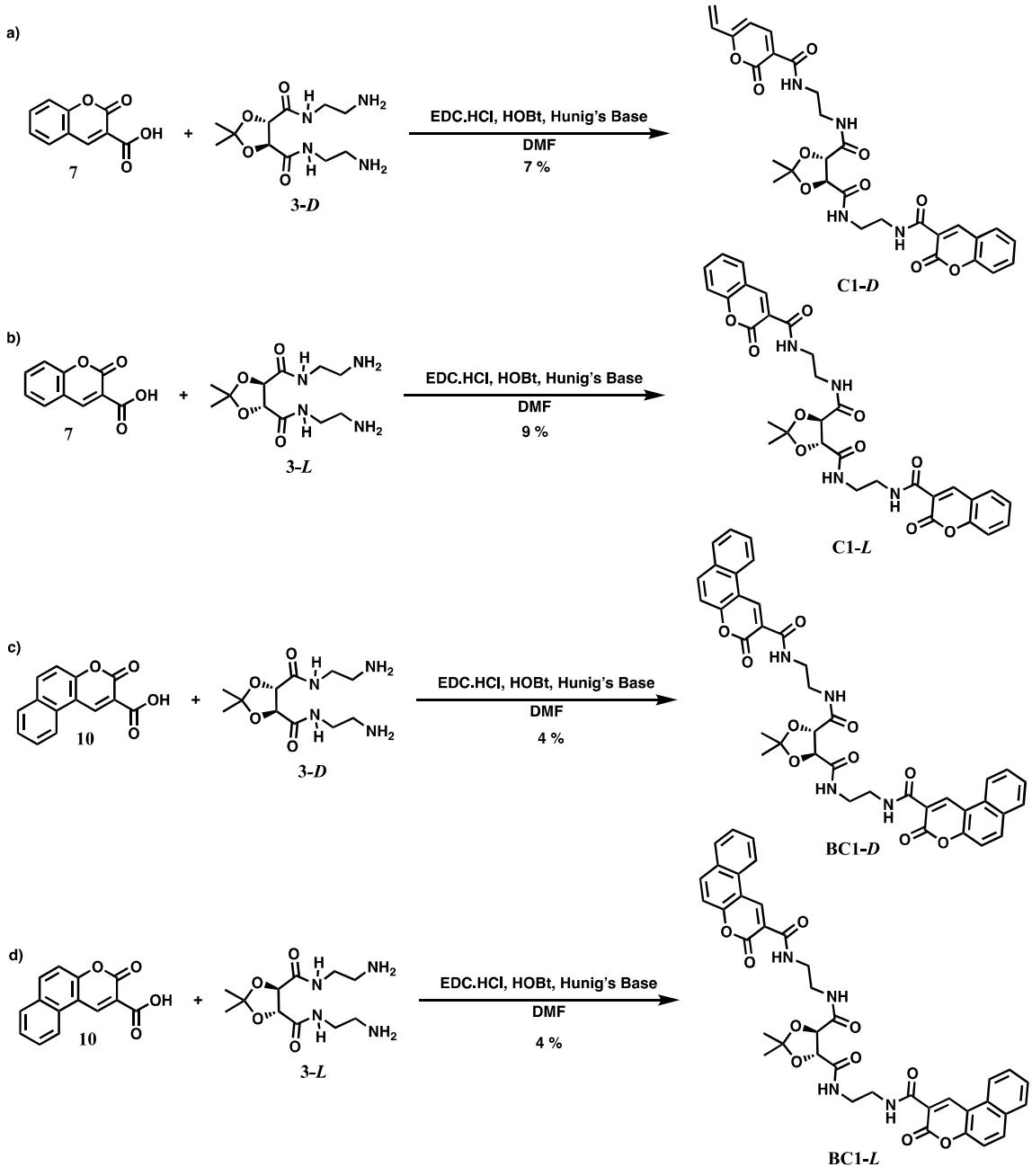

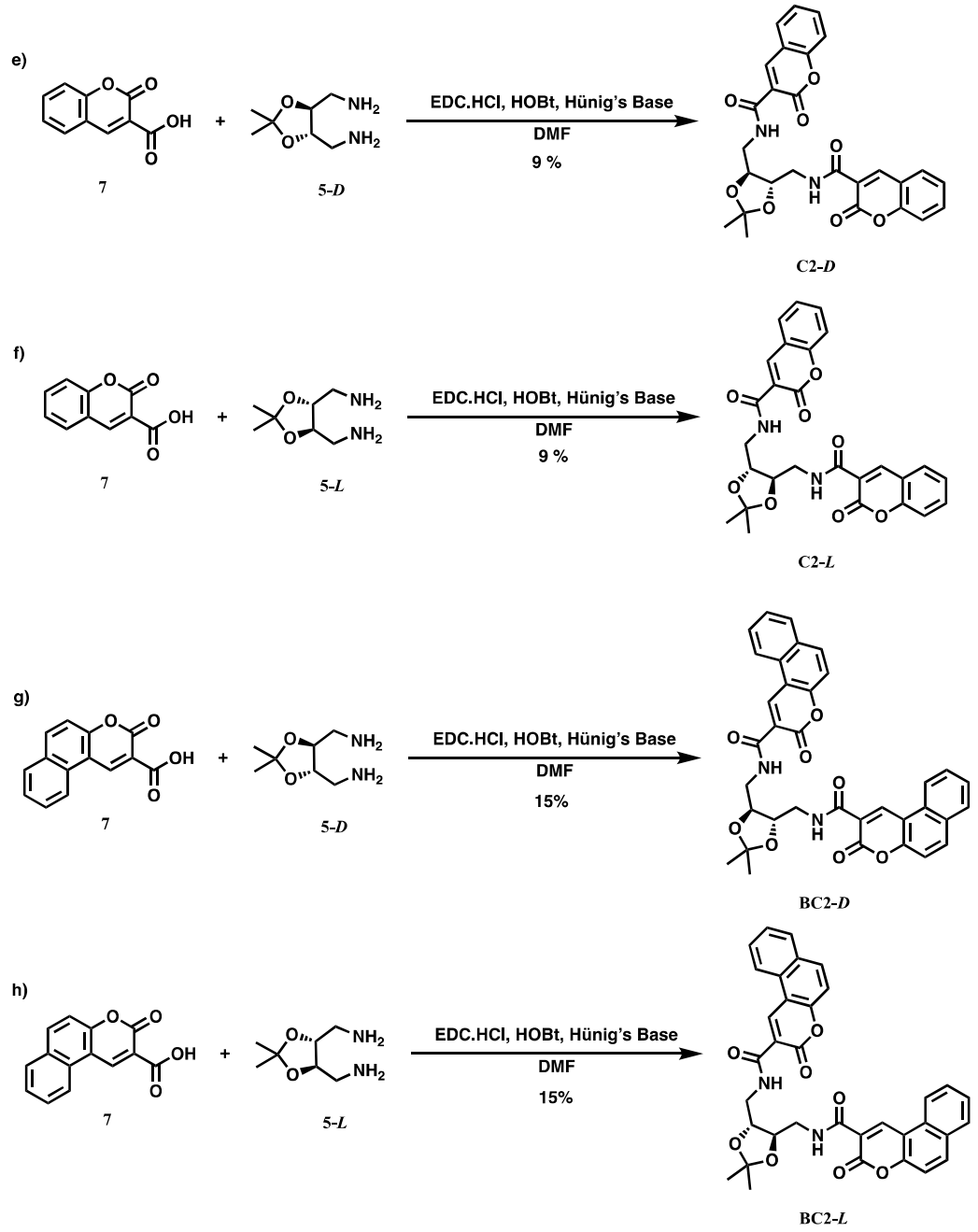

Scheme 7. Syntheses of **a) C1-*D*, b) C1-*L*, c) BC1-*D*, d) BC1-*L*, e) C2-*D*, f) C2-*L*, g) BC2-*D*, h) BC2-*L*** with EDC coupling method.

3.4 Spectroscopic Studies

In this section of the thesis, we considered UV-Vis, Fluorescence and Circular Dichroism (CD) studies of the synthesized compounds. Moreover, the aggregation studies of these compounds were also performed and investigated with the same instrumental techniques. Since the compounds are chiral, the aggregated molecules would form chiral assemblies. These aggregated assemblies are further studied with our home-made CPL instrument which is a basic modification of fluorometer with in-built polarizers.

3.4.1 Spectroscopic Studies of Tartaric Acid Derivatives Bearing 3-carboxy-Coumarin

The syntheses of compounds **C1-*D***, **C1-*L***, **C2-*D***, and **C2-*L*** were discussed above. Initially, UV-Vis spectra of **C1-*L*** and **C2-*L*** were recorded in four different solvents; acetonitrile (ACN), chloroform ($CHCl_3$), methanol (MeOH), and tetrahydrofuran (THF) (Figure 23). For **C1**, a slight red-shift (5 nm) was observed for $CHCl_3$ and MeOH compared to the ones in THF and ACN (Figure 23a). For **C2**, a slight redshift (3 nm) was observed only in $CHCl_3$ between all solvents in the UV-Vis spectra (Figure 23b).

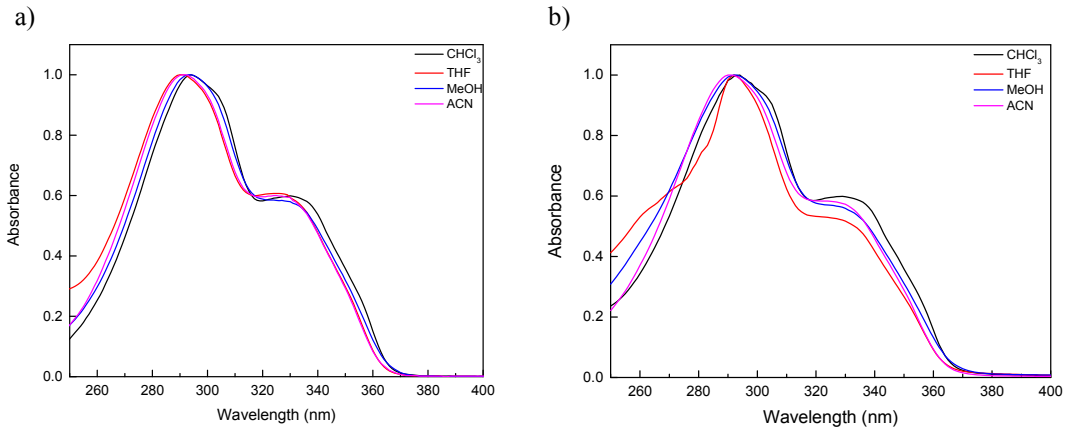

Figure 23. Normalized UV-Vis spectra of **a) C1-*L*** (10^{-5}M) **b) C2-*L*** (10^{-5}M) in CHCl3 (black), THF (red), MeOH (blue) and ACN (pink)

In our aggregation studies, two solvents were necessary; one solvent to completely dissolve the compound and the other one to not dissolve. With this in mind and UV-Vis results in hand, MeOH was chosen as the solvent for further spectroscopic investigations due to its good miscibility with water, which is used as a non-dissolving solvent.

Similar excitation and emission spectra are observed for both **C1** and **C2** in fluorescence studies (Figure 24). It is seen that the UV-Vis and fluorescence spectra are not affected by the groups bonded to coumarin-3-carboxylates.

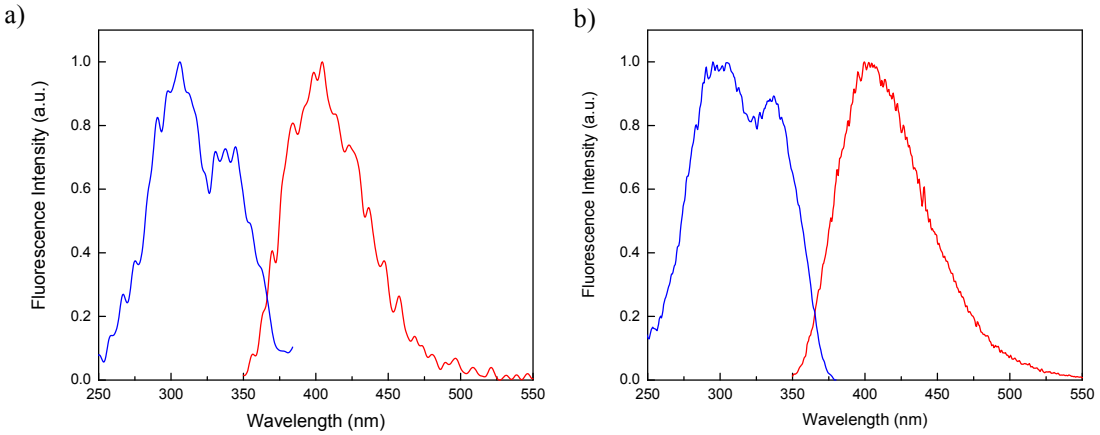

Figure 24 Excitation (blue) and Emission (red) Spectra of compound **a) C1-*L*** (10^{-8} M) **b) C2-*L*** (10^{-8}M) in MeOH

So far, *L* forms of **C1** and **C2** were studied. When measuring CD spectra both enantiomeric forms of **C1** and **C2** were recorded in MeOH. As seen in figure 23, CD spectra of *L* and *D* forms were displaying opposite CD activities in the absorption region of the chromophore group that are symmetric with respect to origin (Figure 25). Wolf et al previously reported that incorporating chiral moiety at the 4 position of coumarin would give rise to chiroptical sensing.[66] Congruently, in our studies we observed that installing a chiral group to 3-carboxylate coumarins would also exhibit chiroptical sensing.

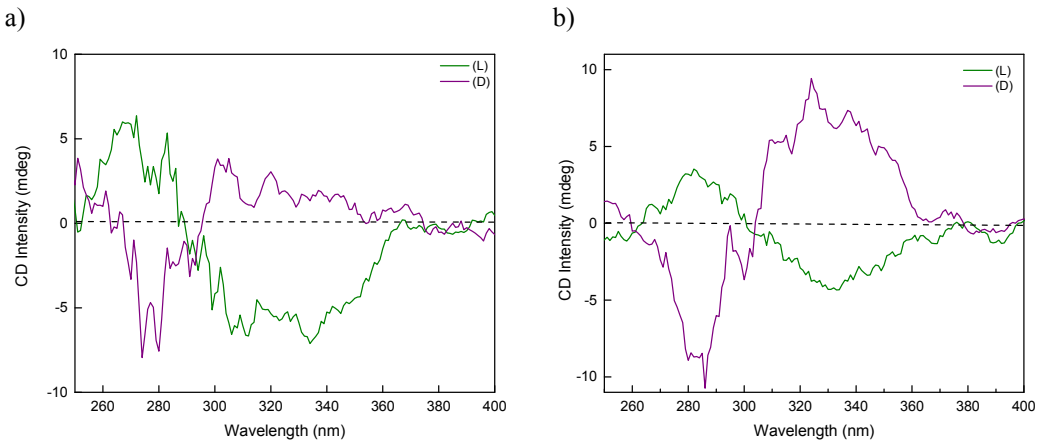

Figure 25. CD spectra of a) **C1-*L*** and **C1-*D*** (10^{-5}M) b) **C2-*L*** and **C2-*D*** (10^{-5}M) in MeOH

3.4.1.1 Aggregation Studies of Tartaric Acid Derivatives Bearing 3-carboxy-Coumarin

Aggregation studies were performed by adding water in different ratios to the MeOH solutions of **C1** and **C2** which are well-dissolved in MeOH whereas non-dissolved in water. Therefore, increasing water content should lead to aggregation whereby coumarin units will stack on top of each other through π - π interactions, which was our initial hypothesis. Such interactions would rise a red-shift (J-aggregate) or blue-shift (H-aggregate) in the UV-Vis spectrum.[67]

When DLS measurements were performed, it was found that solutions of **C1-*D*, C1-*L*, C2-*L*,** and **C2-*D*** containing 80% water have appreciable hydrodynamic sizes, 127 ± 1.82 nm, 127 ± 11.3 nm, 494.1 ± 39.5 nm, 354.2 ±26.9 nm respectively. (Appendix G)

UV-Vis spectrum of **C1-*L*** with varied water content from 20% to 80% showed that the significant red-shift (8 nm) after 60% (Figure 26a). For the case of **C2,** there is also a slight red-shift (3 nm) as the water content increases from 20% to 80% (Figure 26b).

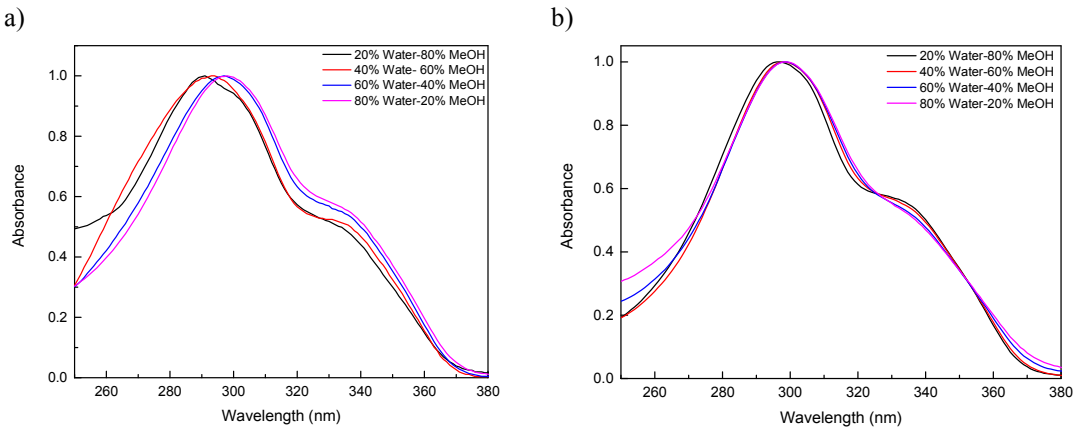

Figure 26. Normalized UV-Vis spectra of a) **C1-*L*** (10^{-6}M) b) **C2-*L***(10^{-6}M) in 20% water-80% MeOH (black), 40% water-60% MeOH (red), 60% water-40% MeOH (blue), 80% water-20% MeOH (pink) solutions.

With the UV-Vis results in hand for aggregation, fluorescence studies of these were also studied. For **C1** a significant red-shift (27 nm) was observed as the water content increases in fluorescence emission was observed (Figure 27a). In the case of **C2**, a red-shift (10 nm) was observed while not that prominent as **C1** (Figure 27b).

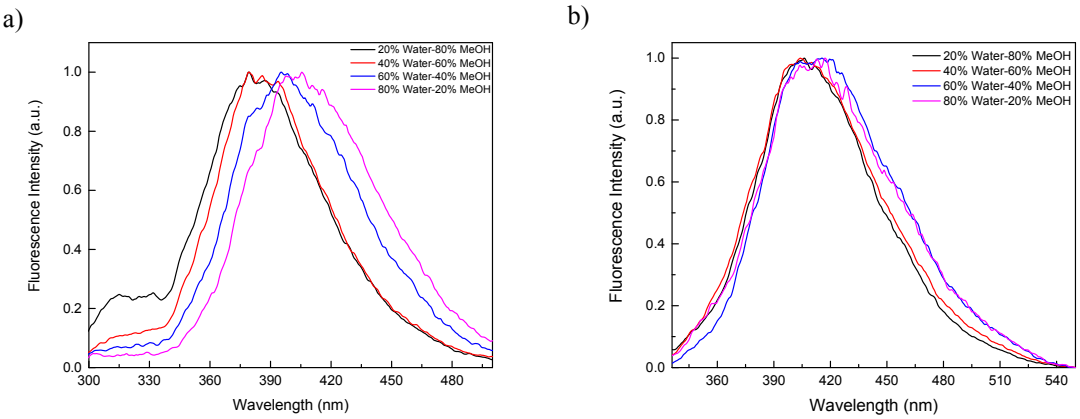

Figure 27. Normalized Fluorescence emission spectra of a) **C1-*L*** (10^{-8}M) b) **C2-*L*** (10^{-8}M) in 20% water-80% MeOH (black), 40% water-60% MeOH (red), 60% water-40% MeOH (blue), 80% water-20% MeOH (pink) solutions.

Aggregation studies for **C1** and **C2** were carried on with CD spectra which were recorded for both *L* and *D* forms with varying water content in MeOH. Opposite CD activities have remained same for two enantiomers (Figure 28). CD intensity increased with increasing water content indicating that the formed aggregates are ordered.

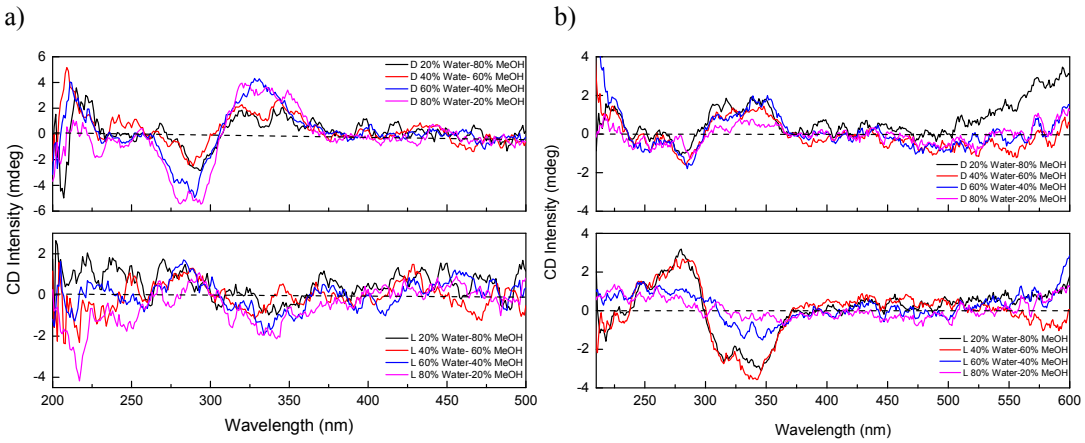

Figure 28. CD spectra of **a) C1-*L*** and **C1-*D*** (10^{-6}M) **b) C2-*L*** and **C2-*D*** (10^{-6}M) in 20% water-80% MeOH (black), 40% water-60% MeOH (red), 60% water-40% MeOH (blue), 80% water-20% MeOH (pink) solutions

For CPL studies of aggregates, the fluorometer with in-built polarizers is used. A Fresnel Rhomb was placed at 45° to the middle of the sample and linear emission polarizers. Hereby, circularly polarized light luminescing from the sample will be converted into linearly polarized light after passing through Fresnel Rhomb. CPL results were obtained from the difference between horizontal and vertical light intensities that were measured with the detector. Picture from our home-made instrument is shown in Figure 29. Compared CPL measurements of $Eu(facam)_3$ complex is given in Appendix F.

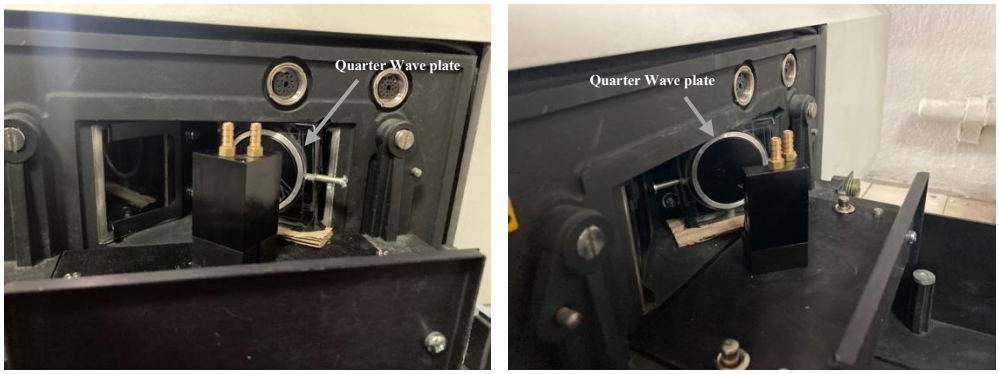

Figure 29. Home-made CPL Instrument.

CPL activity was seen for both **C1** and **C2**. For **C2**, however, up to 60% water content both *L* and *D* forms exhibited CPL signals on the same side (Appendix F, Figure 65). For 80% water content we have seen reversed CPL signals for L and D which are still not the same intensity in both directions (Figure 30).

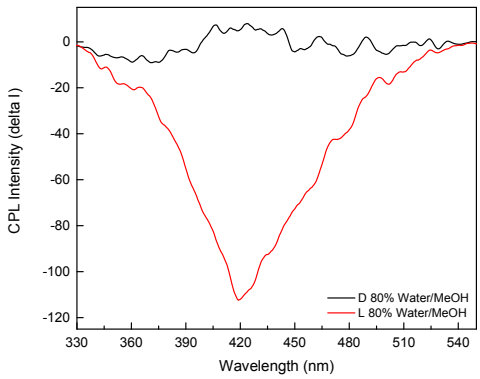

Figure 30. CPL spectra of **C1-*L*** and **C1-*D*** (10^{-6}M) in 80% Water-20% MeOH

For **C2** CPL analyses of these aggregates were measured at different times. It was observed that the CPL signals change from solution to solution with the same solvent content. For example, 60% water-40% MeOH solution were prepared two times, each time the CPL signals were different. Measurement of the same solution on different days resulted in the same CPL spectra qualitatively. This suggests that observed aggregates have different aggregation states. Moreover, the ambient temperature varied drastically in our labs, this could also be a factor for observing different CPL results. Furthermore such a trend was observed also in CD Spectra. Similar results were observed for 80% and 90% water solutions. (Figure 31)

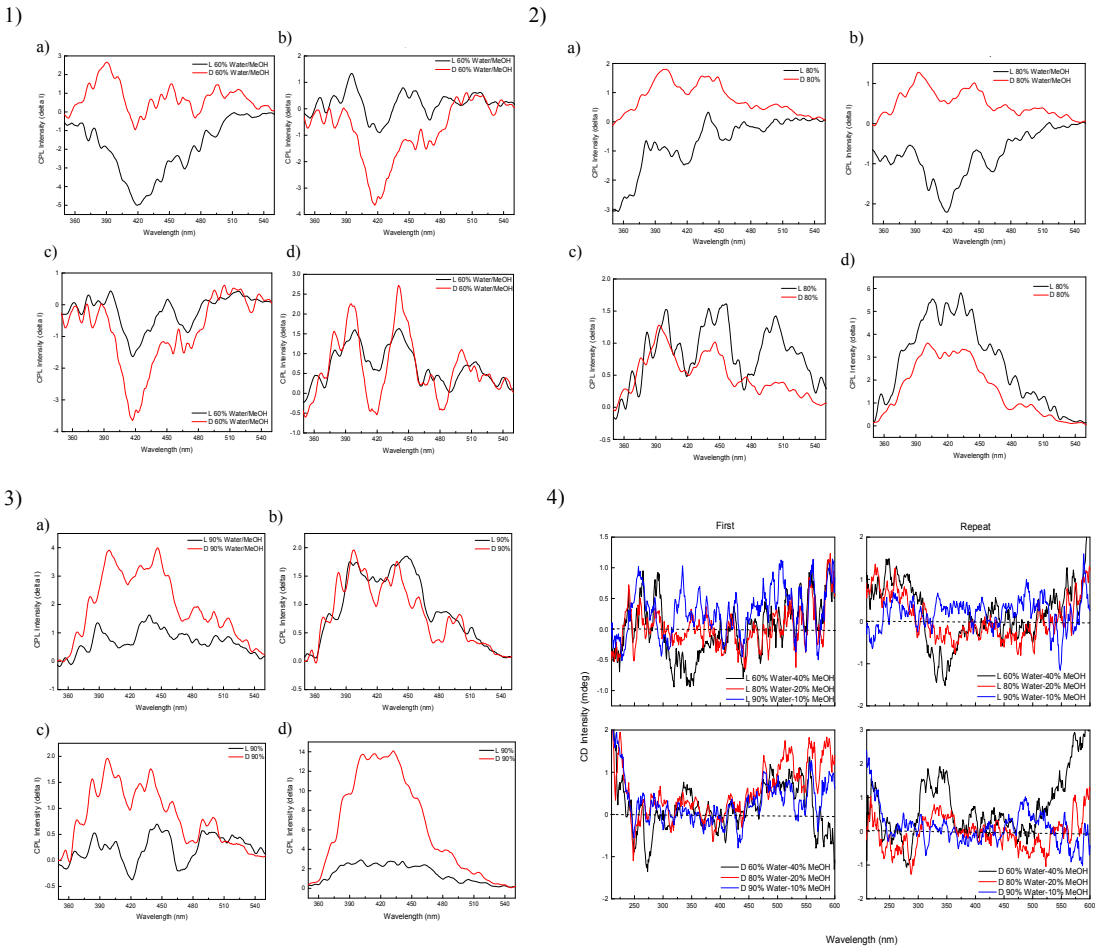

Figure 31. 1) CPL spectra of **C2-*L*** and **C2-*D*** at 60% water-40%MeOH solution, **2)** CPL spectra of **C2-*L*** and **C2-*D*** at 80% water-20%MeOH solution, **3)** CPL spectra of **C2-*L*** and **C2-*D*** at 90% water-10%MeOH solution **a)** first solution **b)** first solution rested at ambient conditions for 24 hours, **c)** second solution, **d)** second solution rested at ambient conditions for 24 hours **3)** CD spectra of **C2-*L*** and **C2-*D*** at 60% water-40%MeOH solution (black), 80% water-20%MeOH solution (red), 90% water-10%MeOH solution (blue).

3.4.2 Spectroscopic Studies of Tartaric Acid Derivatives Bearing 3-carboxy-benzo[*f*]coumarin

The syntheses of compounds **BC1-*D***, **BC1-*L***, **BC2-*D***, and **BC2-*L*** were discussed above, *vide supra*. Like coumarin derivates, mentioned above, spectroscopic studies of **BC1** and **BC2** were initialized with recording in UV-Vis spectra in $CHCl_3$, MeOH, ACN and THF. As can be seen in Figure 32, a prominent red shift (4 and 7 nm respectively) was observed in $CHCl_3$ for both **BC1** and **BC2**.

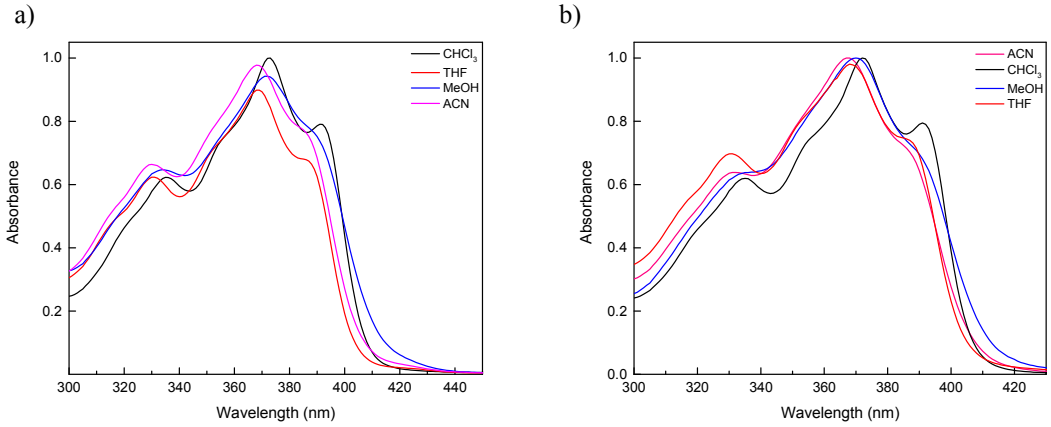

Figure 32. Normalized UV-Vis spectra of **a) BC1-*L*** (10^{-5}M) **b) BC2-*L*** (10^{-5}M) in $CHCl_3$ (black), THF (red), MeOH (blue) and ACN (pink).

In order to choose a suitable solvent for further studies solvent screening on CD spectra was also carried out with the same solvents. For **BC1** highest CD intensity was observed with acetonitrile (Figure 33a) and for **BC2** even though the highest intensity was observed with THF (Figure 33b), second highest one, ACN, was the solvent of choice to be consistent with **BC1**.

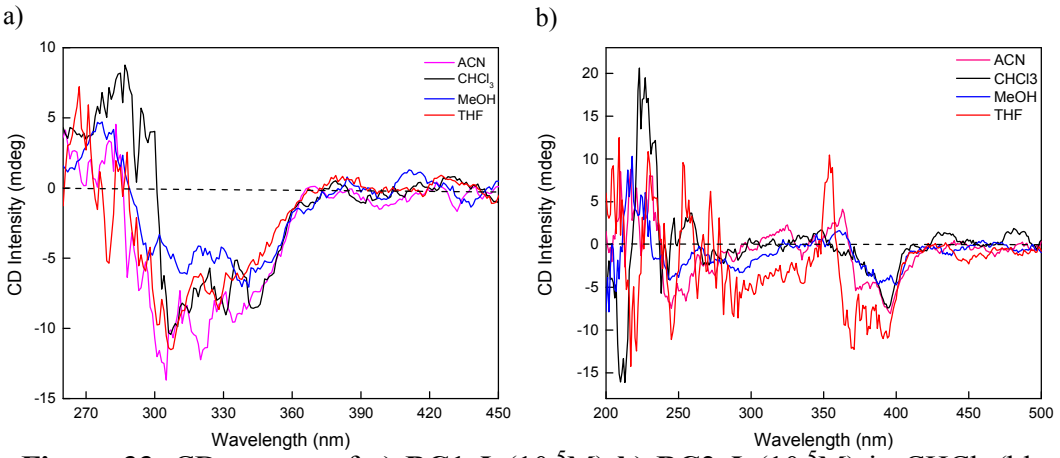

Figure 33. CD spectra of **a) BC1-*L*** (10^{-5}M) **b) BC2-*L*** (10^{-5}M) in $CHCl_3$ (black), THF (red), MeOH (blue) and ACN (pink).

As can be seen from Figure 34, CD spectra of *L* and *D* forms were displaying opposite CD activities in the absorption region of the chromophore group, that are symmetric with respect to origin.

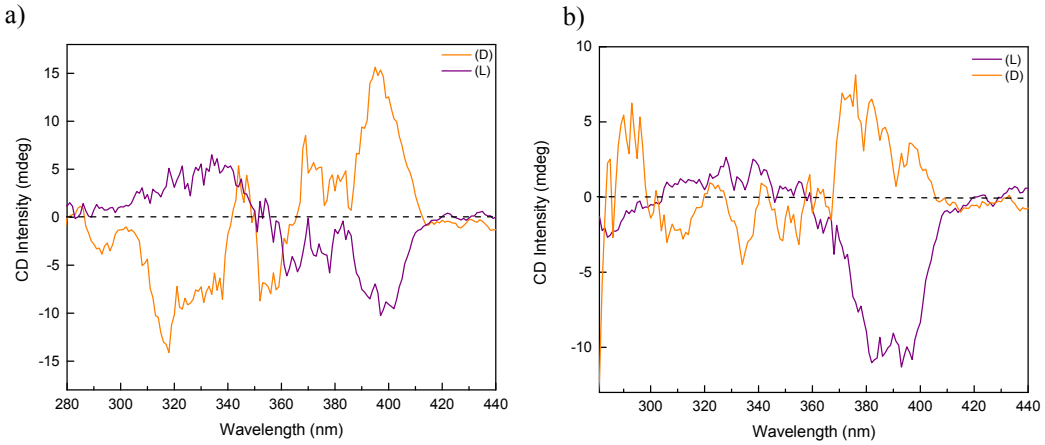

Figure 34. CD spectra of **a) C1-*L*** and **C1-*D*** (10^{-5}M) **b) C2-*L*** and **C2-*D*** (10^{-5}M) in ACN

Similar excitation and emission spectra are observed for both **BC1** and **BC2** in fluorescence studies (Figure 35).

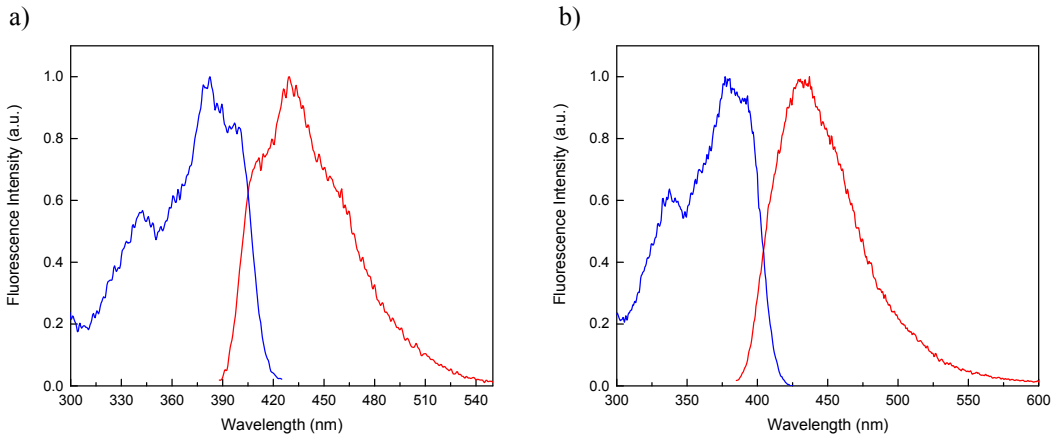

Figure 35. Excitation (blue) and Emission (red) Spectra of compound **a) BC1-*L*** (10^{-8}M) **b) BC2-*L*** (10^{-8}M) in ACN

As in coumarin derivatives (**C1** and **C2**), *vide supra*, it is seen that the UV-Vis and fluorescence spectra are not affected by the groups bonded to benzo[*f*]coumarin-3-carboxylates.

3.4.2.1 Aggregation Studies of Tartaric Acid Derivatives bearing 3-carboxy-benzo[*f*]coumarin

ACN, as dissolving, and water, as non-dissolving, were the solvents of choice for the aggregation studies of **BC1** and **BC2**. Solutions are prepared by increasing water content in the medium.

When DLS measurements were performed, it was found that 80% water content solutions of **BC1-*D*, BC1-*L*, BC2-*L*,** and B**C2-*D*** have appreciable hydrodynamic sizes, 130 ± 4.21 nm, 469 ± 38.1 nm, 864 ± 374 nm, 426 ±290 nm respectively.

UV-Vis spectrum of **BC1-*L*** with varied water content from 20% to 80% showed that increasing water content results in prominent red-shift (8 nm) (Figure 36a). For **BC2-*L*** despite observing a red-shift (7 nm) with increasing water content in the medium,

broadening on the absorption band was also observed after 70% water content (Figure 36b).

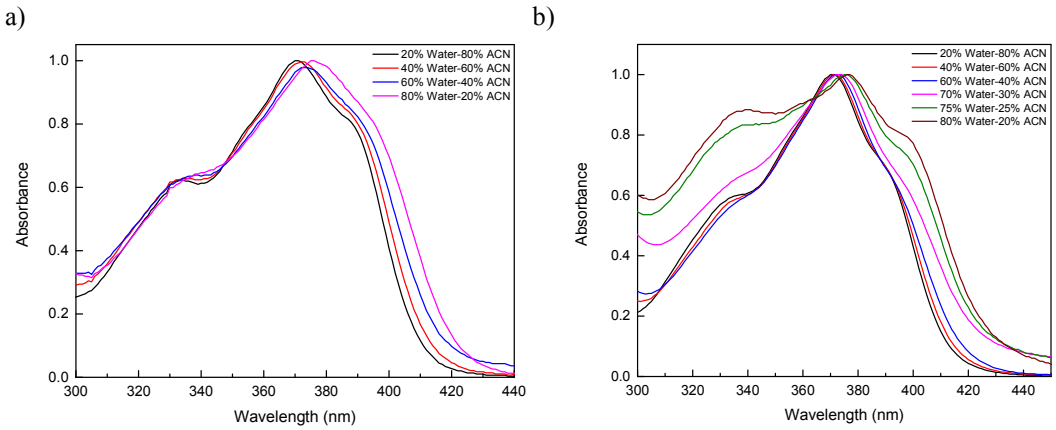

Figure 36. Normalized UV-Vis spectra of **a) BC1-*L*** (10^{-6}M) **b) BC2-*L*** in various Water/ACN solutions

With the UV-Vis results in hand for aggregation, fluorescence studies of these were also studied. For both **BC1** and **BC2**. Like their absorption, increasing water content in the medium resulted in a red-shift on their emission band. Gradual shift (13 nm) was observed for **BC2** (Figure 37b) whereas a prominent red shift (37 nm) was observed for **BC1** in 80% Water/ACN solution (Figure 37a).

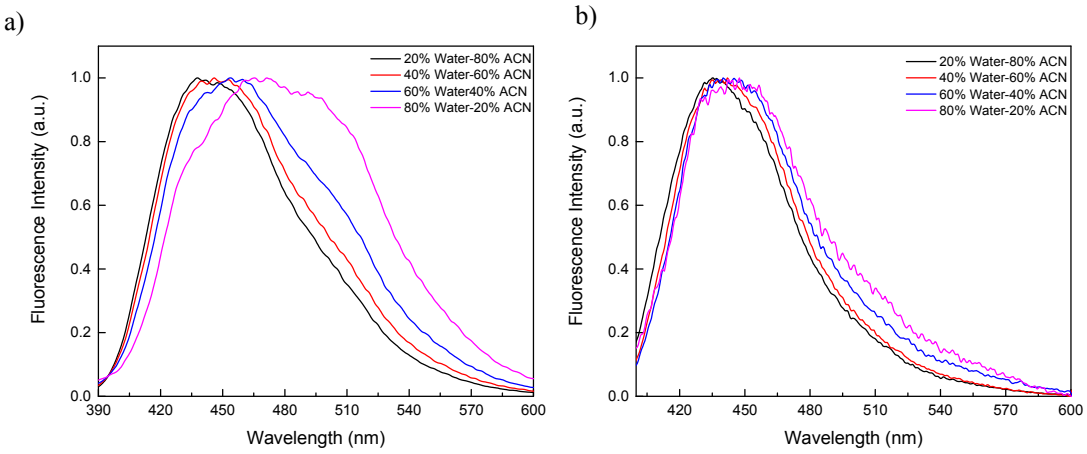

Figure 37. Normalized Fluorescence emission spectra of **a) BC1-*L*** (10^{-8}M) **b) BC2-*L*** (10^{-8}M) in 20% water-80% ACN (black), 40% water-60% ACN (red), 60% water-40% ACN (blue), 80% water-20% ACN (pink) solutions

As can be seen from Figure 38, prominent shift in the emission of **BC1** could also be seen with human-eye, it is obvious that the color is changing from blue to green as water content increases in the medium.

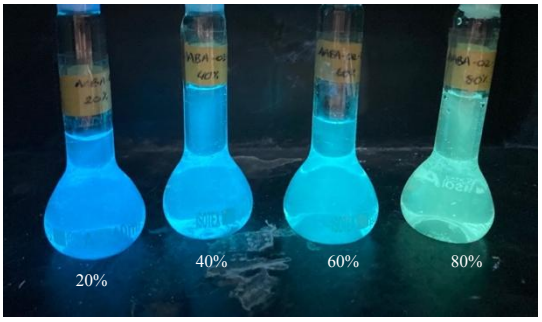

Figure 38. BC1-*L* aggregation solutions (left to right water content 20%, 40%, 60%, and 80%) under 365 nm light.

Aggregation studies for **BC1** and **BC2** were carried on with CD spectra which were recorded for both *L* and *D* forms with varying water content in ACN. Opposite CD activities have remained the same for two enantiomers. For **BC1** highest CD intensity was observed for 60% and 80% water/ACN solutions (Figure 39).

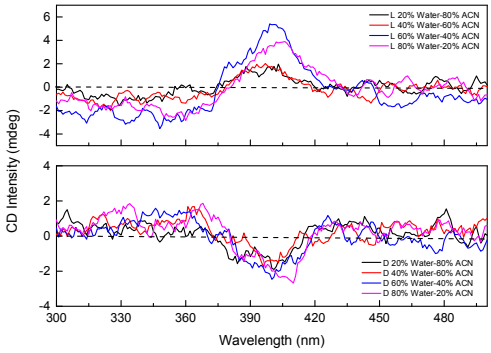

Figure 39. CD spectra of **BC1-*L*** and **BC1-*D*** (10^{-5}M) in 20% water-80% ACN (black), 40% water-60% ACN (red), 60% water-40% ACN (blue), 80% water-20% ACN (pink).

For **BC2**, the increase in CD intensity was also observed with increasing water content (Figure 40a). For 80% water/ACN solution an excessive increase was

observed (Figure 40b). This is probably due to formed aggregates have a CD activity in addition to inherent CD activity arising from the point chirality.

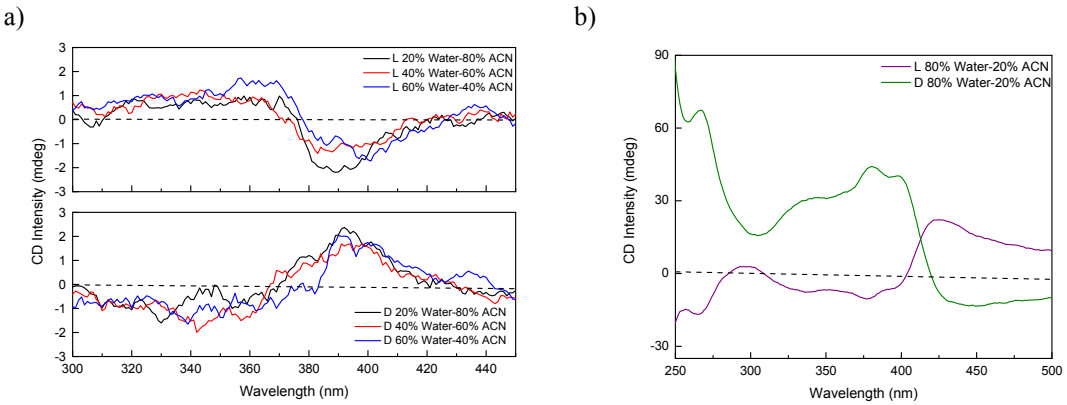

Figure 40. CD spectra of **a) BC2-*L*** and **BC2-*D*** (10^{-6}M) in 20% water-80% ACN (black), 40% water-60% ACN (red), 60% water-40% ACN (blue) solutions **b**) **BC2-*L*** and **BC2-*D*** (10^{-6}M) in 80% water/ACN solution

For benzo[*f*]coumarin derived compounds (**BC1**& **BC2**) CPL measurements were run in similar manner that was run for the coumarin derivatives. Even though they were expected to form better aggregates due to larger surface area of benzo[*f*]coumarin than the coumarin, as observed in UV-Vis and fluorescence studies, CPL studies revealed that for enantiomeric forms reversed CPL intensities were not observed. Furthermore, the CPL signals were on the same size for both enantiomeric forms (Appendix F).

CHAPTER 4

CONCLUSION

The syntheses of 8 new compounds were accomplished. Even though the last step installing coumarin units on tartaric acid derivatives was low in yield, the final compounds were purified and characterized. Spectroscopic properties of these compounds were investigated using UV-Vis, fluorescence, CD and CPL. It is seen that, coumarins and benzo[*f*]coumarins modified at 3 position with carboxylate shows chiroptical properties. The aggregation studies for coumarin bearing compounds were run in MeOH-water while benzo[*f*]coumarin bearing compounds were studied in ACN-water. UV-Vis, fluorescence and CD studies showed the formation of ordered aggregates. It is manifestly seen that better aggregates are formed for compounds bearing compound **3** (**C1** & **BC1**) rather than compound **5** (**C2** & **BC2**) as tartaric acid derivative. The CPL studies with a home-made CPL instrument showed varied CPL intensities.

CHAPTER 5

EXPERIMENTAL

5.1 Methods and Materials

All starting materials and solvents except ethyl acetate and hexane were purchased from Sigma Aldrich and were used without further purifications. Solvents used for Flash Chromatography were distilled prior to use (EtOAc and Hexane over $CaCl_2$). The reactions were monitored by thin layer chromatography (TLC) (Merck Silica Gel 60 F254) and visualized by UV light at 254 nm.

Structural evaluation of the synthesized compounds was accomplished with the instruments stated below.

^{1}H and ^{13}C nuclear magnetic resonance spectra of the compounds were recorded in deuterated solvents with Bruker Avance III Ultrashield 400 Hz NMR spectrometer. The chemical shifts were stated in parts per million (ppm) with tetramethylsilane (TMS) as internal reference. Spin multiplicities were indicated as s (singlet), d (doublet), dd (doublet of doublet), t (triplet), tt (triplet of triplet), m (multiplet) and coupling constants (J) were reported as in Hz (Hertz). ^{1}H NMR, ^{13}C NMR, and other NMR techniques spectra of compounds were given in Appendix A. NMR spectra were processed with MestReNova program.

Infrared (IR) Spectra were recorded with Thermo Scientific Nicolet iS10 ATR-IR spectrometer. Signal locations were reported in reciprocal centimeter (cm^{-1}). The IR spectra of the compounds synthesized are given in Appendix B.

UV-Vis measurements were recorded with Shimadzu UV-2450 spectrophotometer. Spectroscopic measurements were carried out in methanol, acetonitrile, tetrahydrofuran, and chloroform. UV absorption spectra were processed with

OriginPro 2019. The UV-Vis spectra of the compounds synthesized are given in Appendix E.

High Resolution Mass Spectra (HRMS) were processed in positive mode on (ESI) using Time of Flight mass analyzer. The high-resolution mass spectra of compounds synthesized are given in Appendix C.

Fluorescence measurements were recorded with Perkin Elmer LS55 spectrofluorometer. Spectroscopic measurements were carried out in methanol, acetonitrile, tetrahydrofuran, and chloroform of spectroscopic grade. The fluorescence spectra of the compounds synthesized are given in Appendix D. Fluorescence spectra were processed with OriginPro 2019 program.

CD measurements were recorded with Jasco J-1500 CD Spectrometer. Spectroscopic measurements were carried out in methanol, acetonitrile, tetrahydrofuran, and chloroform of spectroscopic grade. CD spectra were processed with OriginPro 2019.

CPL measurements were recorded with home-made CPL instrument. Spectroscopic measurements were carried out in methanol and acetonitrile of spectroscopic grade and water. CPL spectra were processed with OriginPro 2019. The CPL spectra of the compounds synthesized are given in Appendix F.

5.2 Synthesis of Tartaric Acid Derivatives

5.2.1 Synthesis of **diethyl 2,3-dihydroxybutanedioate**

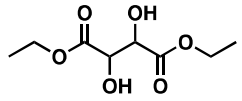

(1)

To a tartaric acid (5.0 g, 33.31 mmol, 1.0 eq) solution in EtOH (20 mL), $SOCl_2$ (12.60 mL, 174.3 mmol, 5.2 eq) was added via dropping funnel at 0°C. After 1 hour of stirring at room temperature, the mixture was heated to reflux for 3 hours. Solvent and excess $SOCl_2$ were removed *in vacuo* to yield the white-yellow oily product (6.8 g, 98 %). ^{1}H NMR (400 MHz, $CDCl_3$) δ 4.55 (s, 2H), 4.33 (t, 3H), 3.10 (s, 2H), 1.35 (t, 6H).

5.2.2 Synthesis of **diethyl 2,2-dimethyl-1,3-dioxolane-4,5-dicarboxylate**[68]

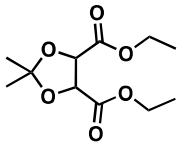

(2)

To a solution of compound **(1)** (6.2 g, 30.4 mmol, 1 eq) in acetone (100 mL), 2,2-dimethoxy propane (12.6 mL, 103.3 mmol, 3.4 eq) and p-toluenesulfonic acid (2.1 g, 12.16 mmol, 0.4 eq) are added. The resulting mixture was stirred overnight at room temperature. Afterwards, ammonium hydroxide was added, and white precipitates were filtered off. Acetone was removed under *vacuo*. The mixture was extracted with DCM and water. Combined organic layers were dried over Na_2SO_4 and DCM was removed *in vacuo* to yield orange liquid as the product (6.35g, 85 %).[1] 1H NMR (400 MHz, $CDCl_3$) δ 4.78 (s, 2H), 4.29 (q, J = 7.1, 2.0 Hz, 4H), 1,51 (s, 6H) 1.32 (q, J = 7.2, 2.0 Hz, 6H).

5.2.3 Synthesis of N^4,N^5-bis(2-aminoethyl)-2,2-dimethyl-1,3-dioxolane-4,5-dicarboxamide[69]

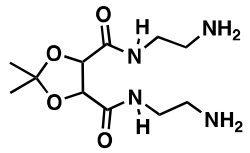

(3)

Compound **(2)** (1.0 g, 4.1 mmol, 1 eq) and ethylenediamine (5 mL, 74.9 mmol, 18.3 eq) were mixed at room temperature and the resulting mixture was stirred 2 days at room temperature. Excess ethylenediamine was co-evaporated with methanol and toluene several times *in vacuo* and vacuum-dried for 1 day (1.0 g, 89 %). ^{1}H NMR (400 MHz, MeOD) δ δ 4.60 (s, 2H), 3.44 – 3.35 (m, 2H), 3.34 – 3.25 (m, 2H), 2.82 – 2.74 (m, 4H), 1.50 (s, 6H).

5.2.4 Synthesis of 2,2-dimethyl-1,3-dioxolane-4,5-dicarboxamide[70]

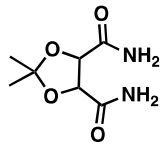

(4)

Solution of diethyl 2,2-dimethyl-1,3-dioxolane-4,5-dicarboxylate **(2)** (3.1 g, 12.59 mmol) in EtOH (30 mL) was cooled with liquid nitrogen to -40°C and ammonia gas was bubbled through the solution until it was saturated. The resulting solution is directly placed in the high-pressure reactor and heated overnight to 55^{o}C. After cooling the resulting medium to room temperature, excess ammonia and ethanol were removed *in vacuo* to yield brown solids (2.17 g, 92 %). ^{1}H NMR (400 MHz, DMSO-d_6) δ 7.49 (s, 2H), 7.42 (s, 2H), 4.43 (s, 2H), 1.39 (s, 6H).

5.2.5 Synthesis of **(2,2-dimethyl-1,3-dioxolane-4,5-diyl)dimethanamine**[70]

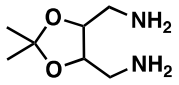

(5)

To a solution of $LiAlH_4$ (1.30 g, 33.2 mmol, 2.50 eq) in THF, compound **(4)** (2.5 g, 13.29 mmol, 1 eq) was extracted with a Soxhlet thimble. The resulting mixture was refluxed for 6 hours followed by stirring at room temperature for 16 hours. Afterwards, the reaction was quenched by a minimum amount of water and 15% NaOH solution. The mixture was filtered, and precipitates were washed several times with THF. THF was removed *in vacuo* from combined filtrates to yield corresponding diamine (1.1 g, 52 %). ^{1}H NMR (400 MHz, $CDCl_3$) δ 3.81 - 3.76 (m, 2H), 2.90 - 2.80 (m, 4H), 1.41 (s, 6H)

5.3 Synthesis of Coumarin Derivatives

5.3.1 Synthesis of **ethyl 2-oxo-2*H*-chromene-3-carboxylate**[65]

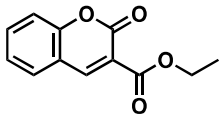

(6)

Salicylaldehyde (1.7 mL, 16.4 mmol, 1 eq), diethyl malonate (5.0 mL, 32.8 mmol, 2 eq), piperidine (0.9 mL, 9.2 mmol, 0.56 eq) and few drops of acetic acid are mixed in EtOH (50 mL). The resulting mixture was refluxed overnight. After removing some of the EtOH *in vacuo*, the solution is poured into a beaker containing ice-water. The generated white precipitates are filtered and further dried in *vacuo* (3.37 g, 94 %). ^{1}H NMR (400 MHz, $CDCl_3$) δ 8.56 (s, 1H), 7.72 – 7.61 (m, 2H), 7.43 – 7.32 (m, 2H), 4.44 (q, J = 7.1 Hz, 2H), 1.43 (t, J = 7.1 Hz, 3H).

5.3.2 Synthesis of **coumarin-3-carboxylic acid**[65]

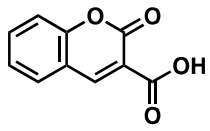

(7)

Compound **(6)** (2 g, 9.16 mmol) was added to 10% KOH solution in water and resulting mixture was refluxed for 2 hours. Afterwards the solution was cooled to room temperature and transferred into a beaker followed by acidization with conc. HCl. The generated white solids are filtered and dried in vacuum (1.3g, 75 %) ^{1}H NMR (400 MHz, $CDCl_3$) δ 12.31 (bs, 1H), 8.99 (s, 1H), 7.85 – 7.77 (m, 2H), 7.56 – 7.48 (m, 2H).

5.3.3 Synthesis of **coumarin-3-acyl chloride**

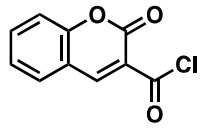

(8)

Compound **(7)** (0.7 g, 3.68 mmol, 1 eq) was added to $SOCl_2$ (16 mL) followed by the addition of a few drops of DMF and the resulting mixture is refluxed for 4 hours. Excess $SOCl_2$ was removed in vacuo to yield yellow solids (0.70 g, 91 %) and used directly in the next step without any further purification.

5.3.4 Synthesis of **ethyl 3-oxo-3*H*-benzo[*f*]chromene-2-carboxylate**[71]

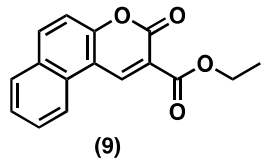

(9)

2-hydroxy-1-naphtahldehyde (1.5 g, 8.7 mmol, 1 eq), diethyl malonate (1.5 mL, 9.8 mmol, 1.12 eq), piperidine (0.8 mL, 8.18 mmol, 0.9 eq) and 10 drops of acetic acid

are mixed in EtOH (50 mL). Resulting mixture was refluxed overnight. After removing some of the EtOH *in vacuo*, solution is poured into a beaker containing ice-water. The generated white precipitates are filtered (2.1g, 88 %) ^{1}H NMR (400 MHz, $CDCl_3$) δ 9.37 (s, 1H), 8.40 – 8.32 (m, 1H), 8.16 – 8.10 (m, 1H), 8.00 – 7.93 (m, 1H), 7.82 – 7.74 (m, 1H), 7.67 – 7.60 (m, 1H), 7.53 – 7.46 (m, 1H), 4.50 (q, 2H), 1.48 (t, 3H).

5.3.5 Synthesis of **3-oxo-3*H*-benzo[*f*]chromene-2-carboxylic acid**[71]

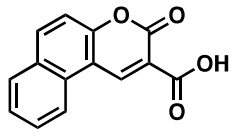

(10)

Compound **(9)** (1.5 g, 5.59 mmol) was added to 10% KOH solution in water and the resulting mixture was refluxed for 2 hours. Afterwards, the solution was cooled to room temperature and transferred into a beaker followed by acidization with conc. HCl. The generated white solids are filtered and dried in vacuum (1.07 g, 80 %) ^{1}H NMR (400 MHz, DMSO-d_6) δ 9.38 (s, 1H), 8.60 (d, J = 8.5 Hz, 1H), 8.32 (d, J = 9.1 Hz, 1H), 8.09 (d, J = 8.1 Hz, 1H), 7.78 (t, J = 7.6 Hz, 1H), 7.66 (t, J = 7.5 Hz, 1H), 7.60 (d, J = 9.0 Hz, 1H).

5.4 Synthesis of Final Products

5.4.1 Synthesis of **C1**

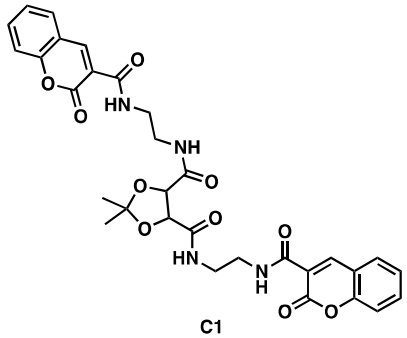

C1

To a solution of compound **(3)** (0.17 g, 0.63 mmol, 1 eq) in DCM (15 mL), pyridine (0.13 mL, 1.58 mmol, 2.5 eq) was added followed by addition of compound **(8)** (0.3 g, 1.58 mmol, 2,5 eq) was added slowly. The resulting mixture was stirred overnight at room temperature. Afterwards, the residue was extracted with 1M HCl solution (50 mL). Combined organic layers were dried over Na_2SO_4 and DCM was removed *in vacuo*. The residue was purified with column chromatography using thin silica as stationary phase. The product was obtained as white solid (0.01 g, 3 %)

To a stirred solution of compound **(7)** (0.50 g, 2.63 mmol, 2.2 eq) in DMF (15 mL), EDC.HCl (0.50 g, 2.63 mmol, 2.2 eq), HOBt (0.35 g, 2.63 mmol, 2.2 eq) and DIEA (1.24 mL, 7.2 mmol, 6 eq) are added and the resulting mixture is stirred for 1 hour at room temperature under Ar atmosphere. Afterwards, compound **(5)** was added and the resulting solution was stirred overnight at room temperature. The mixture was extracted with EtOAc and aq $NaHCO_3$ solution. Combined organic layers were dried over Na_2SO_4 and EtOAc was removed *in vacuo*. The residue was purified with column chromatography using thin silica as stationary phase followed by washing with diethyl ether. The product was obtained as yellow solid (59 mg, 10 %) m.p:178°C ^{1}H NMR (400 MHz, $CDCl_3$) δ 9.03 (t, 1H), 8.90 (s, 1H), 7.73 – 7.68 (m, 2H), 7.54 (t, J = 6.0 Hz, 1H), 7.44 – 7.39 (m, 2H), 4.60 (s, 1H), 3.69 – 3.64 (m, 2H), 3.60 – 3.53 (m, 2H), 1,52 (s, 6H). ^{13}C NMR (75 MHz, $CDCl_3$) δ 170.13, 162.32, 161.33, 154.44, 154.41, 148.50, 134.23, 129.85, 125.36, 118.56, 118.53, 118.21,

116.66, 112.38, 77.37, 39.41, 39.33, 26.12. IR: 3345, 3042, 1697, 1524 HRMS: (ESI-MS) m/z: $[M+H]^+$ Calcd for $C_{31}H_{31}N_4O_{10}^+$ 619.2040, found 619.2035 (for ***L*** enantiomer), 619.2042 (for ***D*** enantiomer).

5.4.2 Synthesis of **BC1**

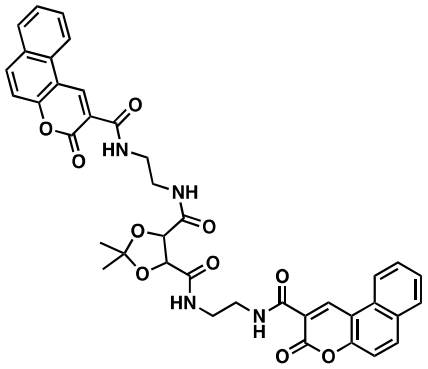

BC1

To a stirred solution of compound **(10)** (0.50 g, 2.08 mmol, 2.6 eq) in DMF (15 mL), EDC.HCl (0.39 g, 2.08 mmol, 2.6 eq), HOBt (0.28 g, 2.08 mmol, 2.6 eq) and DIEA (2.15 mL, 12.48 mmol, 6 eq) are added and resulting mixture is stirred for 1 hour at room temperature under Ar atmosphere. Afterwards compound **(3)** was added and resulting solution stirred overnight at room temperature. Mixture was extracted with EtOAc and aq $NaHCO_3$ solution. Combined organic layers were dried over Na_2SO_4 and EtOAc was removed *in vacuo*. The residue purified with column chromatography using thin silica as stationary phase. The product was obtained as yellow solid (32 mg, 4 %) m.p: 162°C ^{1}H NMR (400 MHz, $CDCl_3$) δ 9.62 (s, 2H), 9.09 (t, 2H), 8.41 – 8.36 (m, 2H), 8.10 – 8.06 (m, 2H), 7.92 – 7.86 (m, 2H), 7.78 – 7.71 (m, 3H), 7.63 – 7.54 (m, 5H), 4.63 (s, 2H), 3.74 – 3.67 (m, 4H), 3.65 – 3.58 (m, 4H), 1.54 (s, 6H). ^{13}C NMR (75 MHz, $CDCl_3$) δ 170.15, 162.69, 161.37, 154.89, 130.31, 129.42, 129.20, 129.10, 121.89, 116.69, 116.29, 113.21, 112.44, 77.24, 39.51, 29.73, 26.17. IR: 3323, 2923, 1702, 1529 HRMS: (ESI-MS) m/z: $[M+H]^+$ Calcd for $C_{39}H_{35}N_4O_{10}^+$ 719.2353, found 719.2352 (for both ***L*** & ***D*** enantiomer).

5.4.3 Synthesis of **C2**

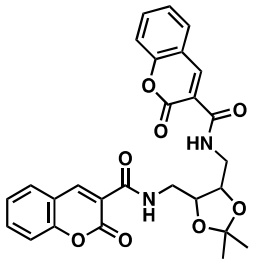

C2

To a stirred solution of compound **(7)** (0.50 g, 2.63 mmol, 2.2 eq) in DMF (15 mL), EDC.HCl (0.50 g, 2.63 mmol, 2.2 eq), HOBt (0.35 g, 2.63 mmol, 2.2 eq) and DIEA (1.24 mL, 7.2 mmol, 6 eq) are added and resulting mixture is stirred for 1 hour at room temperature under Ar atmosphere. Afterwards, compound **(5)** was added and the resulting solution was stirred overnight at room temperature. Mixture was extracted with EtOAc and aq $NaHCO_3$ solution. Combined organic layers were dried over Na_2SO_4 and EtOAc was removed *in vacuo*. The residue was purified with column chromatography using thin silica as stationary phase followed by washing with diethyl ether. The product was obtained as yellow solid (59 mg, 10 %) m.p: 182 °C ^{1}H NMR (400 MHz, $CDCl_3$) δ 9.12 (t, 2H), 8.91 (s, 2H), 7.72 – 7.63 (m, 4H), 7.43 – 7.34 (m,45H), 4.04 (s, 2H), 3.90 – 3.82 (m, 2H), 3.74 – 3.67 (m, 3H), 1,50 (s, 6H). ^{13}C NMR (75 MHz, $CDCl_3$) δ 161.94, 161.28, 154.47, 148.60, 134.14, 129.85, 125.29, 118.59, 118.22, 116.66, 109.62, 76.56, 40.23, 27.17. IR: 3342, 2985, 1710, 1530 HRMS: (ESI-MS) m/z: $[M+H]^+$ Calcd for $C_{27}H_{25}N_2O_8^+$ 505.16.11, found 505.1611 (for ***L*** enantiomer), 505.1613 (for ***D*** enantiomer).

5.4.4 Synthesis of **BC2**

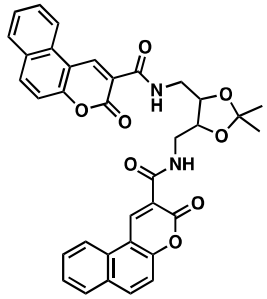

BC2

To a stirred solution of compound **(10)** (1.6 g, 6.5 mmol, 2.6 eq) in DMF (15 mL), EDC.HCl (1.24 g, 6.5 mmol, 2.6 eq), HOBt (0.88 g, 6.5 mmol, 2.6 eq) and DIEA (2.5 mL, 15 mmol, 6 eq) are added and resulting mixture is stirred for 1 hour at room temperature under Ar atmosphere. Afterwards compound **(5)** was added and resulting solution stirred overnight at room temperature. Mixture was extracted with EtOAc and aq $NaHCO_3$ solution. Combined organic layers were dried over Na_2SO_4 and EtOAc was removed *in vacuo*. The residue purified with column chromatography using thin silica as stationary phase followed by washing with diethyl ether. The product was obtained as yellow solid (24 mg, 15 %) m.p: 174°C ^{1}H NMR (400 MHz, $CDCl_3$ δ 9.69 (s, 2H), 9.22 (t, *J* = 5.8 Hz, 2H), 8.42 (d, *J* = 8.4 Hz, 2H), 8.10 (d, *J* = 9.1 Hz, 2H), 7.94 (d, *J* = 8.0 Hz, 2H), 7.74 (t, *J* = 7.8 Hz, 2H), 7.63 (t, *J* = 7.5 Hz, 2H), 7.48 (d, *J* = 9.1 Hz, 2H), 4.12 (s, 2H), 3.92 (d, *J* = 6.6 Hz, 2H), 3.76 (d, *J* = 14.1 Hz, 2H), 1.51 (s, 6H). ^{13}C NMR (75 MHz, $CDCl_3$) δ 162.40, 155.00, 144.21, 135.91, 130.38, 129.57, 129.18, 126.78, 122.05, 116.73, 116.36, 113.31, 77.24, 40.41, 27.21. IR: 3323, 2892, 1710, 1563 HRMS: (ESI-MS) m/z: $[M+H]^+$ Calcd for $C_{35}H_{29}N_2O_8^+$ 605.1924, found 605.1922 (for ***L*** enantiomer)

REFERENCES

(1) International Electrotechnical Commission, *International electrotechnical vocabulary*, Genéve, 1987. ISBN: 978-2-8273-0006-8

(2) *Newton's Optics*; Shapiro, A. E., Buchwald, J. Z., Fox, R., Eds.; Oxford University Press, 2017 DOI: 10.1093/oxfordhb/9780199696253.013.7

(3) *National Association of Broadcasters Engineering Handbook*, 11th edition.; Cavell, G. C., National Association of Broadcasters, Eds.; Routledge: New York, NY, 2018. ISBN: 978-1-138-93051-3

(4) Al-Azzawi, A. *Light and Optics: Principles and Practices*; Eds.; CRC PRESS, 2019. ISBN: 978-0-367-38956-7

(5) Wayne, R. P. *Photochemistry*; Butterworths: London, 1970. ISBN: 978-0-408-70065-8

(6) Huygens, C. *Treatise on Light*; 1678. ISBN: 978-3-7481-1712-4

(7) Turro, N. J.; Ramamurthy, V.; Scaiano, J. C. *Principles of Molecular Photochemistry: An Introduction*; University Science Books: Sausalito, Calif, 2009. ISBN: 978-1-891389-57-3

(8) Einstein, A.; Infeld, L.; Isaacson, W. *The Evolution of Physics: From Early Concepts to Relativity and Quanta*; 2007. ISBN: 978-0-671-20156-2

(9) Wardle, B. *Principles and Applications of Photochemistry*; Wiley: Chichester, U.K, 2009. ISBN: 978-0-470-01493-6

(10) Mechanisms of UV Stabilization. In Handbook of UV Degradation and Stabilization; Elsevier, 2015; 37–65. ISBN: 978-1-895198-86-7

(11) Picollo, M.; Aceto, M.; Vitorino, T. UV-Vis Spectroscopy. *Physical Sciences Reviews* **2019**, *4,* 5-9. DOI: 10.1515/psr-2018-0008

(12) Chow, W. S. Photosynthesis: From Natural Towards Artificial. *Journal of Biological Physics* **2003**, *29*, 447–459. DOI: 10.1023/A:1027371022781

(13) Karge, H. G.; Weitkamp, J. *Characterization I: UV/Vis Spectroscopy*; 2004. ISBN: 978-3-540-69751-0

(14) Byers, L. R. A Teaching Aid for the Conceptualization of the Franck-Condon Principle. *Journal of Chemical Education* **1975**, *52*, 790. DOI: 10.1021/ed052p790

(15) Aoki, T. *Photoluminescence Spectroscopy In Characterization of Materials*; Eds.; Kaufmann, E. N., Ed.; John Wiley & Sons, Inc.: Hoboken, NJ, USA, 2012. ISBN: 978-0-471-26696-9

(16) Huix-Rotllant, M.; Nikiforov, A.; Thiel, W.; Filatov, M. *Description of Conical Intersections with Density Functional Methods. In Density-Functional Methods for Excited States*; Eds.; Ferré, N., Filatov, M., Huix-Rotllant, M., Eds.; Topics in Current Chemistry; Springer International Publishing: Cham, 2015; 445–476. ISBN: 978-3-319-22080-2

(17) Albani, J. R. *Principles and Applications of Fluorescence Spectroscopy*, 1st ed.; Wiley, 2007, 88-113. DOI: 10.1002/9780470692059

(18) Chekhova, M.; Banzer, P. *Polarization of Light: In Classical, Quantum, and Nonlinear Optics*; De Gruyter, 2021, 10-22. DOI: 10.1515/9783110668025

(19) Polavarapu, P. L. *Chiroptical Spectroscopy: Fundamentals and Applications*; Eds.; Taylor & Francis, 2017. ISBN: 978-1-4200-9246-2

(20) Deng, Y.; Wang, M.; Zhuang, Y.; Liu, S.; Huang, W.; Zhao, Q. Circularly Polarized Luminescence from Organic Micro-/Nano-Structures. *Light: Science & Applications* **2021**, *10*, 1–18. DOI: 10.1038/s41377-021-00516-7

(21) Shan, J.; Dadap, J. I.; Heinz, T. F. Circularly Polarized Light in the Single-Cycle Limit : The Nature of Highly Polychromatic Radiation of Defined Polarization. *Optics Express* **2009**, *17*, 7431–7439. DOI: 10.1364/OE.17.007431

(22) Cronin, T. W. A Different View: Sensory Drive in the Polarized-Light Realm. *Current Zoology* **2018**, *64,* 513–523. DOI: 10.1093/cz/zoy040

(23) Oriol, A.; Enric, G.; Razvigor, O. The Fresnel Triprism and the Circular Polarization of Light. *Photonic Techniques and Technologies* **1822**, *3*, 44-45. DOI: 10.1051/photon/2019S444

(24) Han, J.; Guo, S.; Lu, H.; Liu, S.; Zhao, Q.; Huang, W. Recent Progress on Circularly Polarized Luminescent Materials for Organic Optoelectronic Devices. *Advanced Optical Materials* **2018**, *6*, 1-32. DOI: 10.1002/adom.201800538

(25) Kelvin, B. W. T. *Molecular Tactics of a Crystal*.; Hardpress Publishing, 1894.

(26) Albano, G.; Pescitelli, G.; Di Bari, L. Chiroptical Properties in Thin Films of π-Conjugated Systems. *Chemical Reviews* **2020**, *120*, 10145–10243. ISBN: 978-1-290-24614-9

(27) Cameron, R. P.; Götte, J. B.; Barnett, S. M.; Yao, A. M. Chirality and the Angular Momentum of Light. *Philosophical Transactions of the Royal Society A* **2017**, *375*, 3-5. DOI: 10.1098/rsta.2015.0433

(28) Cameron, R. P.; Cameron, J. A.; Barnett, S. M. *Stegosaurus Chirality*, Cornell University **2016**. DOI: arXiv: 1611.08760

(29) Blackmond, D. G. The Origin of Biological Homochirality. *Cold Spring Harb Perspectives in Biology* **2019**, *11,* 1-10. DOI: 10.1101/cshperspect.a032540

(30) Li, X.; Xie, Y.; Li, Z. The Progress of Circularly Polarized Luminescence in Chiral Purely Organic Materials. *Advanced Photonics Research* **2021**, *2* ,1–21. DOI: 10.1002/adpr.202000136

(31) Ayuso, D.; Neufeld, O.; Ordonez, A. F.; Decleva, P.; Lerner, G.; Cohen, O.; Ivanov, M.; Smirnova, O. Synthetic Chiral Light for Efficient Control of Chiral Light – Matter Interaction. *Nature Photonics* **2019**, *13*, 866-871. DOI: 10.1038/s41566-019-0531-2

(32) Sachs, J.; Günther, J.-P.; Mark, A. G.; Fischer, P. Chiroptical Spectroscopy of a Freely Diffusing Single Nanoparticle. *Nature Communications* **2020**, *11*, 4513. DOI: 10.1038/s41467-020-18166-5

(33) Richardson, F. S. Circularly Polarized Luminescence Spectroscopy. *Chemical Reviews* **1986**, *86* 1-9. DOI: 10.1021/cr00071a001

(34) Nitto, J. M. D. I.; Kenney, J. M. Noise Characterization in Circular Dichroism Spectroscopy. *Applied Spectroscopy*. **2012**, *66*, 180–187. DOI: 10.1366/11-06417

(35) Eliel, E. L.; Wilen, S. H.; Mander, L. N. *Stereochemistry of Organic Compounds*; Wiley: New York, 1994. ISBN: 978-0-471-01670-0

(36) Laur, P. *The First Decades after the Discovery of CD and ORD by Aimé Cotton in 1895*. Eds.; John Wiley & Sons, Inc.: Hoboken, NJ, USA, 2012; pp 1–35. DOI: 10.1002/9781118120392.ch1

(37) Goldbeck, R. A.; Kim-shapiro, D. B.; Kliger, D. S. Fast Natural And Magnetic Circular Dichroism Spectroscopy. *Annual Review of Physical Chemistry* **1997**, *48*, 453–479. DOI:10.1146/annurev.physchem.48.1.453

(38) Superfibers, N. Polarisation Modulation - the Measurement of Linear and Circular Dichroism. *Journal of Physics E: Scientific Instruments* **1986**, *19*, 170-173. DOI:10.1088/0022-3735/19/3/002

(39) Fukazawa, T.; Fujita, Y. Polarization Modulated Transmission Spectroellipsometry. *Review of Scientific Instruments* **1996**, *67*, 1951-1955. DOI: 10.1063/1.1146949

(40) Sμnchez-carnerero, E. M.; Agarrabeitia, A. R.; Moreno, F.; Maroto, B. L.; Muller, G.; Ortiz, M. J.; De, S. Circularly Polarized Luminescence from Simple Organic Molecules. *Chemistry Europe* **2015**, *21*, 13488–13500. DOI: 10.1002/chem.201501178

(41) Zhang, M.; Li, K.; Zang, S. Progress in Atomically Precise Coinage Metal Clusters with Aggregation-Induced Emission and Circularly Polarized Luminescence. *Advanced Optical Materials* **2020**, *8*, 1–26. DOI: 10.1002/adom.201902152

(42) Emeis, C. A.; Oosterhoff, L. J. Emission Of Circularly Polarised Radiation by Optically Active Compounds. **1967**, *1*, 129–132. DOI: 10.1016/0009-2614(67)85007-3

(43) Ploeg, D.; Chemistry, T. O.; Laboratories, G. Circular Polarization in the Fluorescence of ß , -Enones : Distortion in the ^{1}n* State. *Journal of the American Chemical Society* **1983**, *105*, 285–290. DOI: 10.1021/ja00339a015

(44) Steinberg, N.; Gafni, A.; Steinberg, I. Z. Measurement of the Optical Activity of Triplet-Singlet Transitions. The Circular Polarization of Phosphorescence of

Camphorquinone and Benzophenone. *Journal of the American Chemical Society* **1981**, *102*, 1636–1640. DOI: 10.1021/ja00397a006

(45) Barnett, C. J.; Drake, A. F.; Mason, S. F. The Polarized Luminescence And Vibrational Optical Activity Of Calycanthine. *Bulletin des Sociétés Chimiques Belges* **1979**, *11*, 853–862. DOI: 10.1002/bscb.19790881104

(46) Zinna, F.; Giovanella, U.; Bari, L. D. Highly Circularly Polarized Electroluminescence from a Chiral Europium Complex. *Advanced Materials* **2015**, *27*, 1791–1795. DOI: 10.1002/adma.201404891

(47) Sang, Y.; Han, J.; Zhao, T.; Duan, P.; Liu, M. Circularly Polarized Luminescence in Nanoassemblies: Generation, Amplification, and Application. *Advanced Materials* **2020**, *32*, 1-33. DOI: 10.1002/adma.201900110

(48) Roose, J.; Tang, B. Z.; Wong, K. S. Circularly-Polarized Luminescence (CPL) from Chiral AIE Molecules and Macrostructures. *Small* **2016**, *12*, 6495–6512. DOI: 10.1002/smll.201601455.

(49) Song, F.; Zhao, Z.; Liu, Z.; Lam, J. W. Y.; Tang, B. Z. Circularly Polarized Luminescence from AIEgens. *Journal of Materials Chemistry C* **2020**, *8*, 3284–3301. DOI: 10.1039/C9TC07022B.

(50) Liu, J.; Su, H.; Meng, L.; Zhao, Y.; Deng, C.; Ng, J. C. Y.; Lu, P.; Faisal, M.; Lam, J. W. Y.; Huang, X.; Wu, H.; Wong, K. S.; Tang, B. Z. What Makes Efficient Circularly Polarised Luminescence in the Condensed Phase: Aggregation-Induced Circular Dichroism and Light Emission. *Chemical Science* **2012**, *3*, 2737-2738. DOI: 10.1039/c2sc20382k.

(51) Steinberg, I. Z.; Gafni, A. Sensitive Instrument for the Study of Circular Polarization of Luminescence. *Review of Scientific Instruments* **1972**, *43*, 409–413. DOI: 10.1063/1.1685648

(52) Mukhtar, A.; Mansha, A.; Asim, S.; Shahzad, A.; Bibi, S. Excited State Complexes of Coumarin Derivatives. *Journal of Fluorescence* **2021**, *32*, 1-17. DOI: 10.1007/s10895-021-02807-z

(53) Fatima, S.; Mansha, A.; Asim, S.; Shahzad, A. Absorption Spectra of Coumarin and Its Derivatives. *Chemical Papers* **2021**, *76*, 627-638. DOI: 10.1007/s11696-021-01902-6

(54) P. K. Jain; Himanshu, J. Coumarin: Chemical and Pharmacological Profile. *Journal of Applied Pharmaceutical Science* **2012**, *2*, 236-240 DOI: 10.7324/JAPS.2012.2643

(55) Yu, T.; Yang, S.; Zhao, Y.; Zhang, P.; Lv, Z.; Fan, D.; Geng, Z. Synthesis and Fluorescence Properties of 7-Hydroxy-3-(2-Pyridyl)Coumarin Derivatives. *Research on Chemical Intermediates* **2012**, *38*, 215–222. DOI: 10.1007/s11164-011-0339-2

(56) Kim, D.; Xuan, Q. P.; Moon, H.; Jun, Y. W.; Ahn, K. H. Synthesis of Benzocoumarins and Characterization of Their Photophysical Properties. *Asian Journal of Organic Chemistry* **2014**, *3*, 1089–1096. DOI: 10.1002/ajoc.201402107

(57) Jung, Y.; Jung, J.; Huh, Y.; Kim, D. Benzo[g]Coumarin-Based Fluorescent Probes for Bioimaging Applications. *Journal of Analytical Methods in Chemistry* **2018**, *3,* 1–11. DOI: 10.1002/ajoc.201402107

(58) Tasior, M.; Kim, D.; Singha, S.; Krzeszewski, M.; Ahn, K. H.; Gryko, D. T. π-Expanded Coumarins: Synthesis, Optical Properties and Applications. *Journal of Materials Chemistry C* **2015**, *3*, 1421–1446. DOI: 10.1039/C4TC02665A

(59) Ghosh, A. K.; Koltun, E. S.; Bilcer, G. Tartaric Acid and Tartrates in the Synthesis of Bioactive Molecules. *Synthesis* **2001**, *9*, 1281–1301. DOI: 10.1055/s-2001-15217

(60) Gratzer, K.; Gururaja, G. N.; Waser, M. Towards Tartaric-Acid-Derived Asymmetric Organocatalysts: Towards Tartaric-Acid-Derived Asymmetric Organocatalysts. *European Journal of Organic Chemistry* **2013**, *21*, 4471–4482. DOI: 10.1002/ejoc.201201675

(61) Kodama, S.; Yamamoto, A.; Matsunaga, A.; Hayakawa, K. Direct Chiral Resolution of Tartaric Acid in Food Products by Ligand Exchange Capillary Electrophoresis Using Copper(II)–d-Quinic Acid as a Chiral Selector. *Journal*

of Chromatography A **2001**, *932*, 139–143. DOI: 10.1016/S0021-9673(01)01228-6

(62) Seebach, D.; Beck, A. K.; Heckel, A. TADDOLs, Their Derivatives, and TADDOL Analogues: Versatile Chiral Auxiliaries. *Angewandte Chemie International Edition* **2001**, *40*, 92–138. DOI: 10.1002/1521-3773(20010105)40:1<92::AID-ANIE92>3.0.CO;2-K

(63) Amako, T.; Nakabayashi, K.; Mori, T.; Inoue, Y.; Fujiki, M.; Imai, Y. Sign Inversion of Circularly Polarized Luminescence by Geometry Manipulation of Four Naphthalene Units Introduced into a Tartaric Acid Scaffold. *Chemical Communications* **2014**, *50*, 12836–12839. DOI: 10.1039/C4CC04228J.

(64) Çalışgan, G. Studies Towards Synthesis Of Urea Containing Helical Polymers, Middle East Technical University, 2016.

(65) Luo, X.; He, X.-D.; Zhao, Y.-C.; Chen, C.; Chen, B.; Wu, Z.-B.; Wang, P.-Y. FRET-Based Fluorescent and Colorimetric Probe for Selective Detection of Hg(II) and Cu(II) with Dual-Mode: FRET-Based Fluorescent and Colorimetric Probe for Selective Detection of Hg(II) and Cu(II) with Dual-Mode. *Journal of Heterocyclic Chemistry* **2017**, *54*, 2650–2655. DOI: 10.1002/jhet.2863

(66) Thanzeel, F. Y.; Balaraman, K.; Wolf, C. Click Chemistry Enables Quantitative Chiroptical Sensing of Chiral Compounds in Protic Media and Complex Mixtures. *Nature Communications* **2018**, *9*, 5323. DOI: 10.1038/s41467-018-07695-9

(67) Kistler, K. A.; Pochas, C. M.; Yamagata, H.; Matsika, S.; Spano, F. C. Absorption, Circular Dichroism, and Photoluminescence in Perylene Diimide Bichromophores: Polarization-Dependent H- and J-Aggregate Behavior. *Journal of Physical Chemistry B* **2012**, *116*, 77–86. DOI: 10.1021/jp208794t.

(68) Kim, B. M.; Bae, S. J.; So, S. M.; Yoo, H. T.; Chang, S. K.; Lee, J. H.; Kang, J. Synthesis of a Chiral Aziridine Derivative as a Versatile Intermediate for HIV Protease Inhibitors. *Organic Letters* **2001**, *3*, 2349–2351. DOI: 10.1021/ol016147s

(69) Maurer, A.; Zeyher, C.; Amin, B.; Kalbacher, H. A Periodate-Cleavable Linker for Functional Proteomics under Slightly Acidic Conditions: Application for the Analysis of Intracellular Aspartic Proteases. *Journal of Proteome Research* **2013**, *12*, 199–207. DOI: 10.1021/pr300758c

(70) Shainyan, B. A.; Nindakova, L. O.; Ustinov, M. V.; Chipanina, N. N.; Sherstyannikova, L. V. New Chiral Diamines of the Dioxolane Series: (+)-(4S,5S)-2,2-Dimethyl-4,5-Bis(Diphenylaminomethyl)- 1,3-Dioxolane and (+)-(4S,5S)-2,2-Dimethyl-4,5-Bis(Methyl- Aminomethyl)-1,3-Dioxolane. Russian *Journal of Organic Chemistry* **2002**, *38*, 1802–1805. DOI: 10.1023/A:1022528016140

(71) Zhang, H.; Yu, T.; Zhao, Y.; Fan, D.; Qian, L.; Yang, C.; Zhang, K. Syntheses, Characterization and Fluorescent Properties of Two Triethylene-Glycol Dicoumarin-3-Carboxylates. *Spectrochimica Acta Part A: Molecular and Biomolecular Spectroscopy* **2007**, *68*, 725–727. DOI: 10.1016/j.saa.2006.12.052

APPENDICES

A. NMR Spectra

NMR spectra were recorded at Bruket Avance III Ultrashield 400 Hz $CDCl_3$, MeOH, and DMSO were used as solvents in all records.

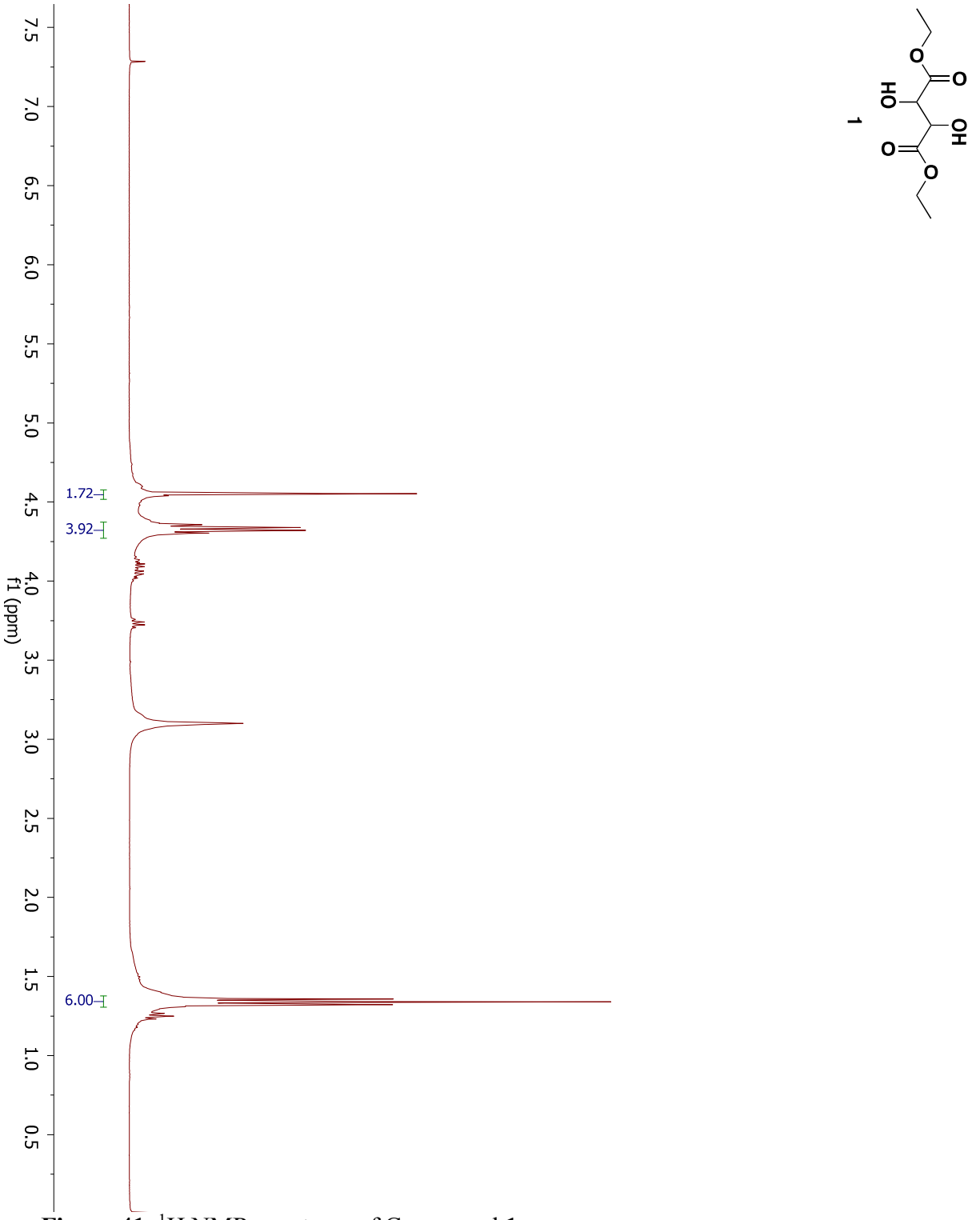

Figure 41. ^{1}H NMR spectrum of Compound **1**.

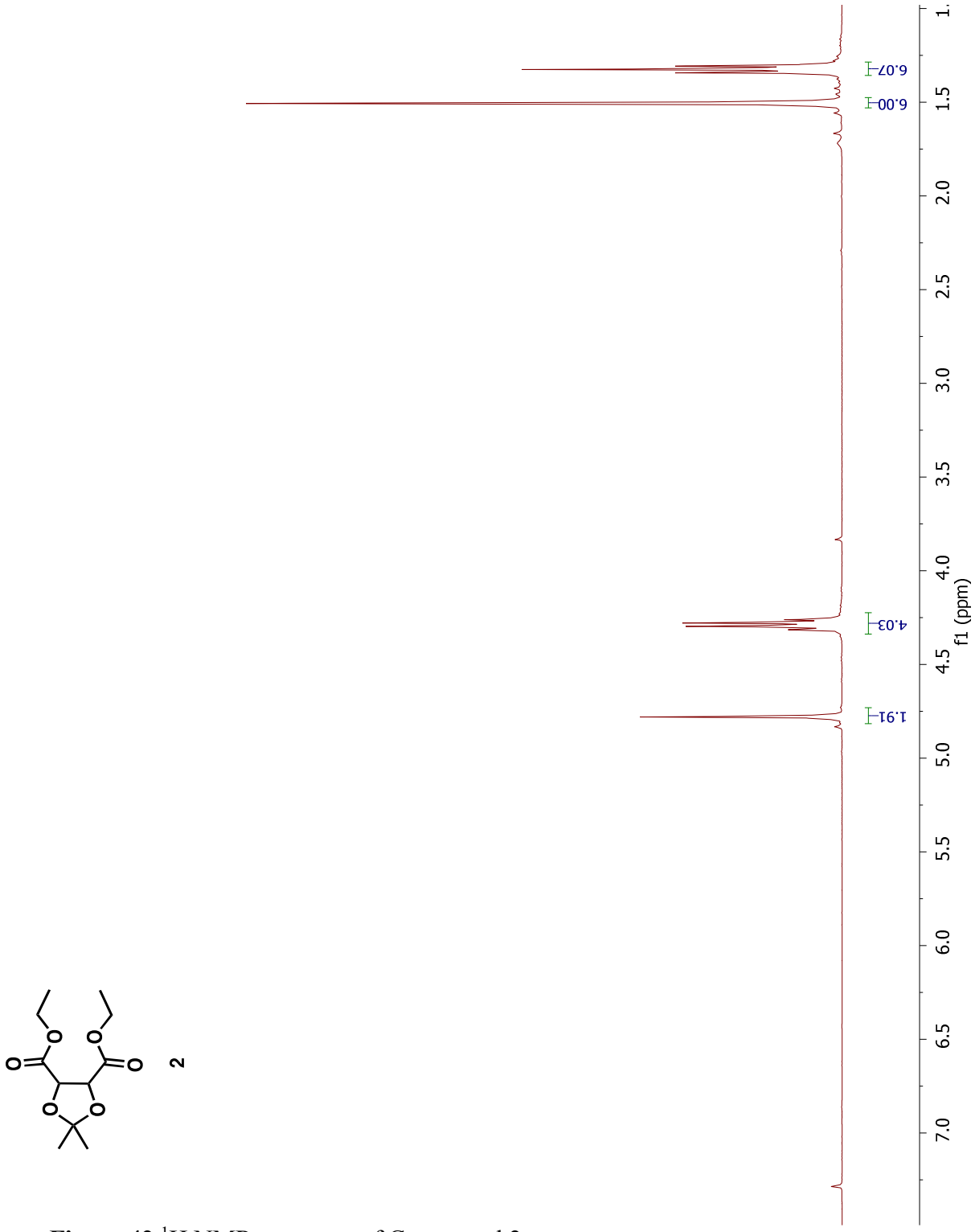

Figure 42. ^{1}H NMR spectrum of Compound **2**.

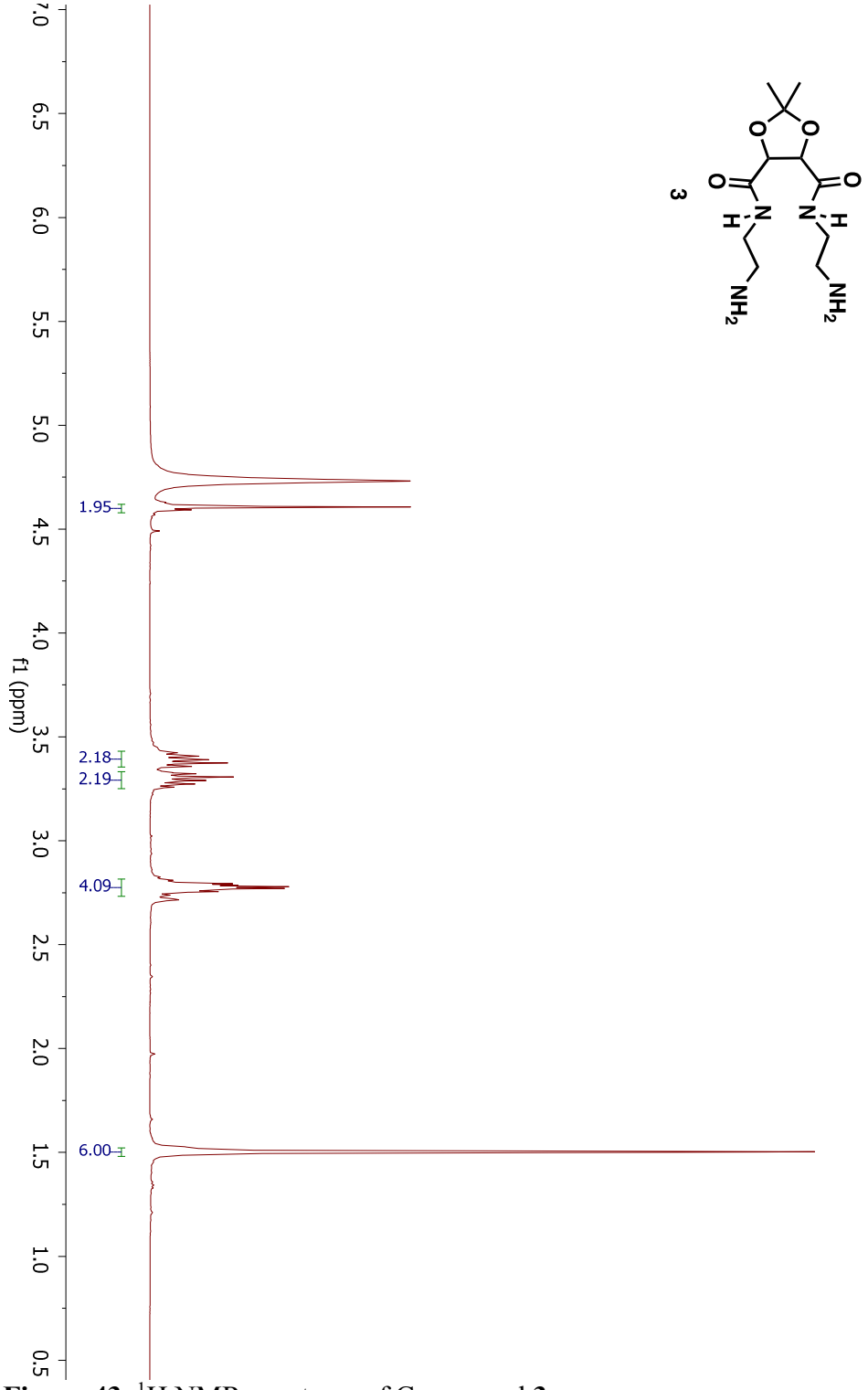

Figure 43. ^{1}H NMR spectrum of Compound **3**.

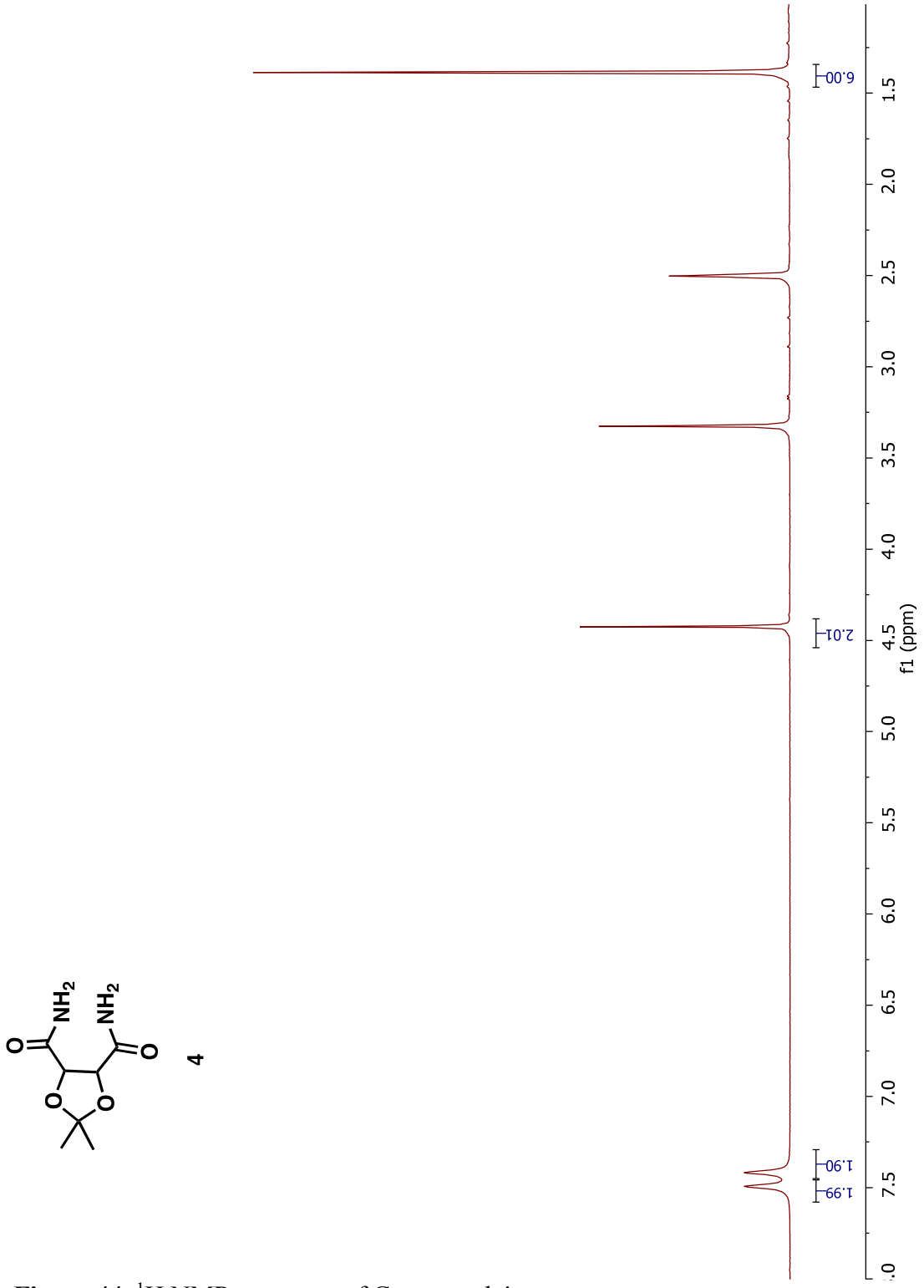

Figure 44. ^{1}H NMR spectrum of Compound **4**.

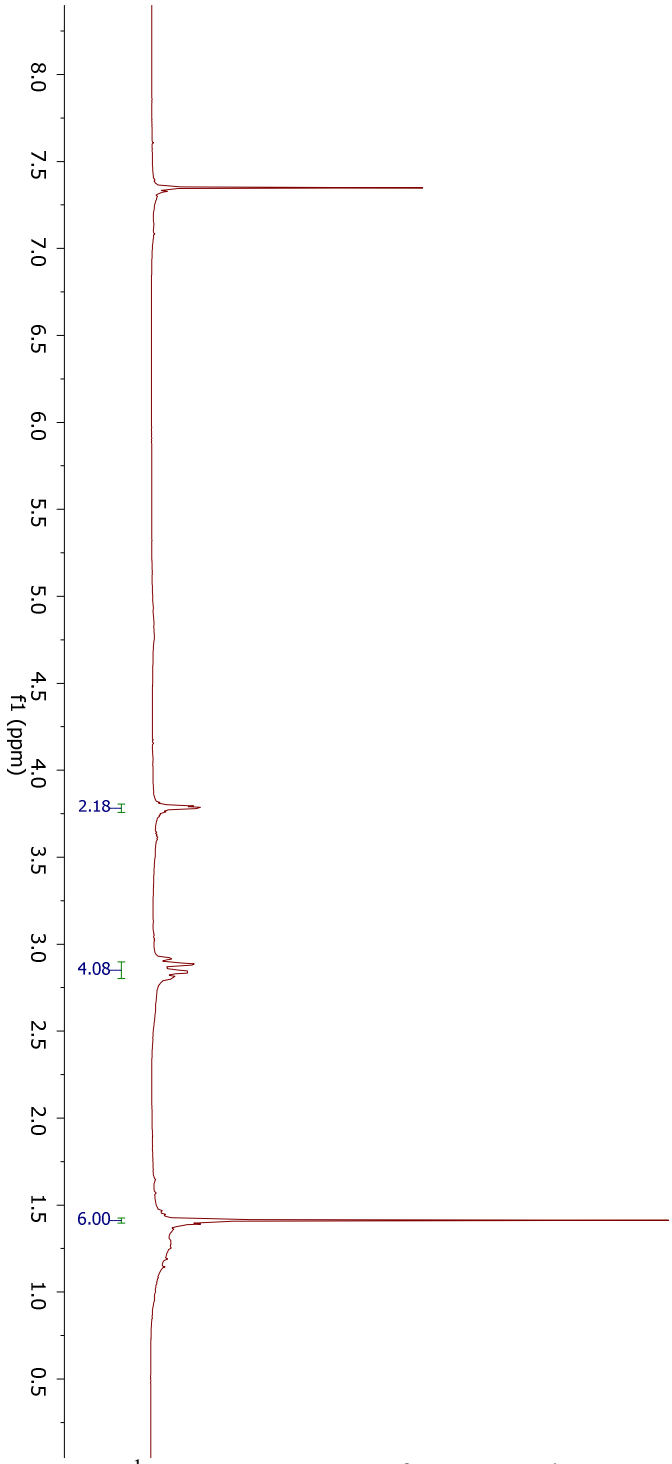

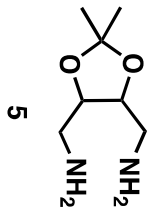

5

Figure 45. ^{1}H NMR spectrum of Compound **5**.

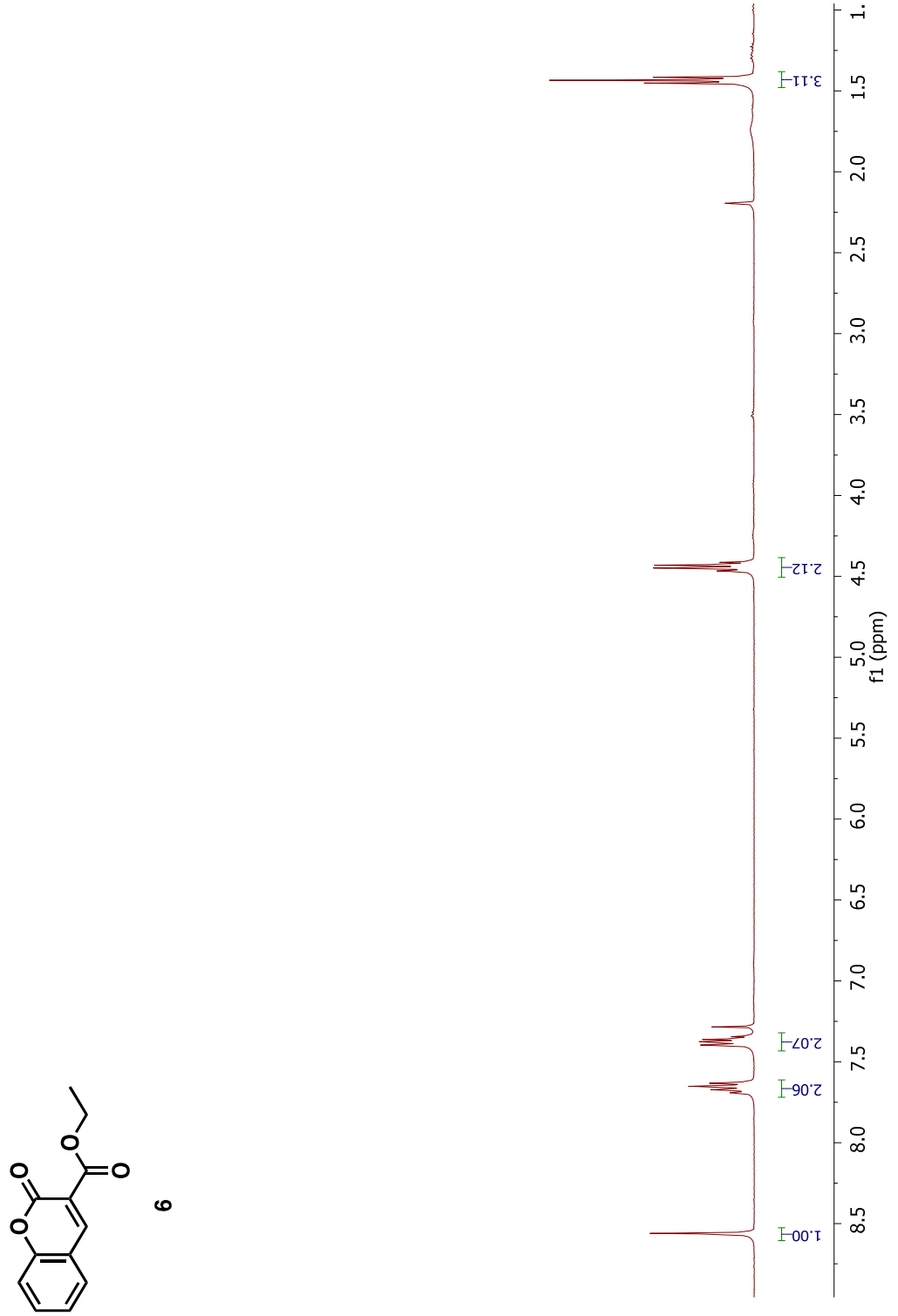

6

Figure 46. ^{1}H NMR spectrum of Compound **6**.

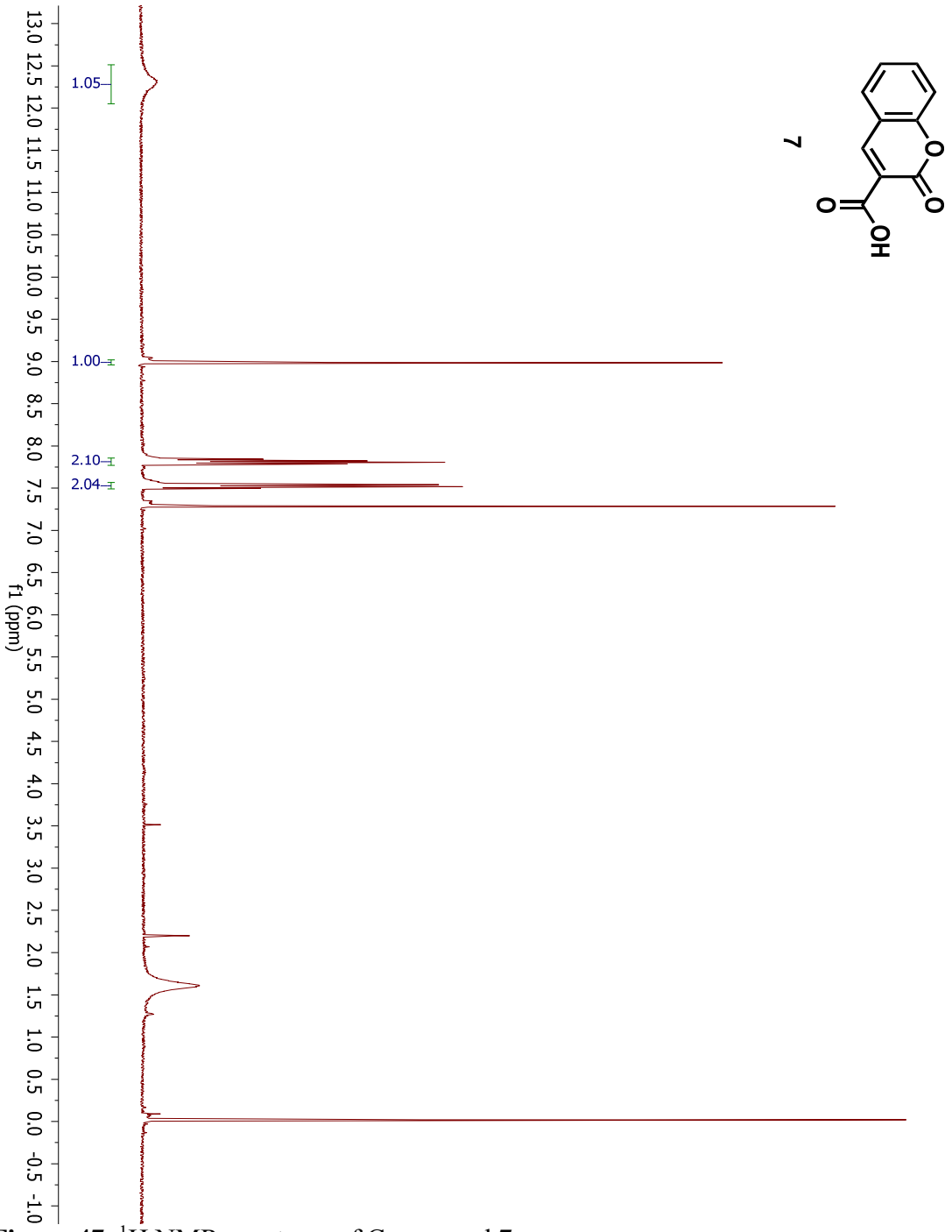

Figure 47. ^{1}H NMR spectrum of Compound **7**.

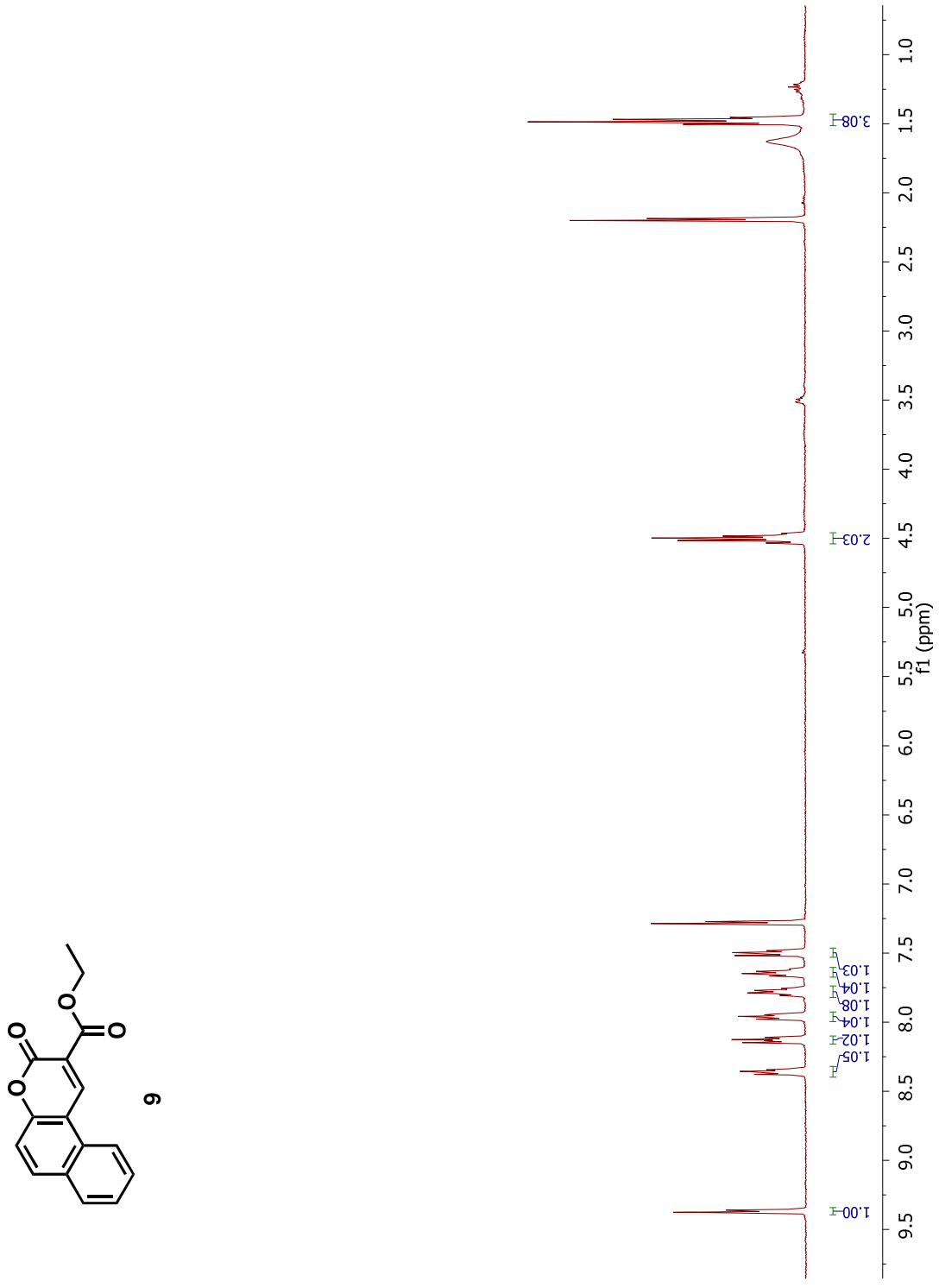

Figure 48. ^{1}H NMR spectrum of Compound **9**

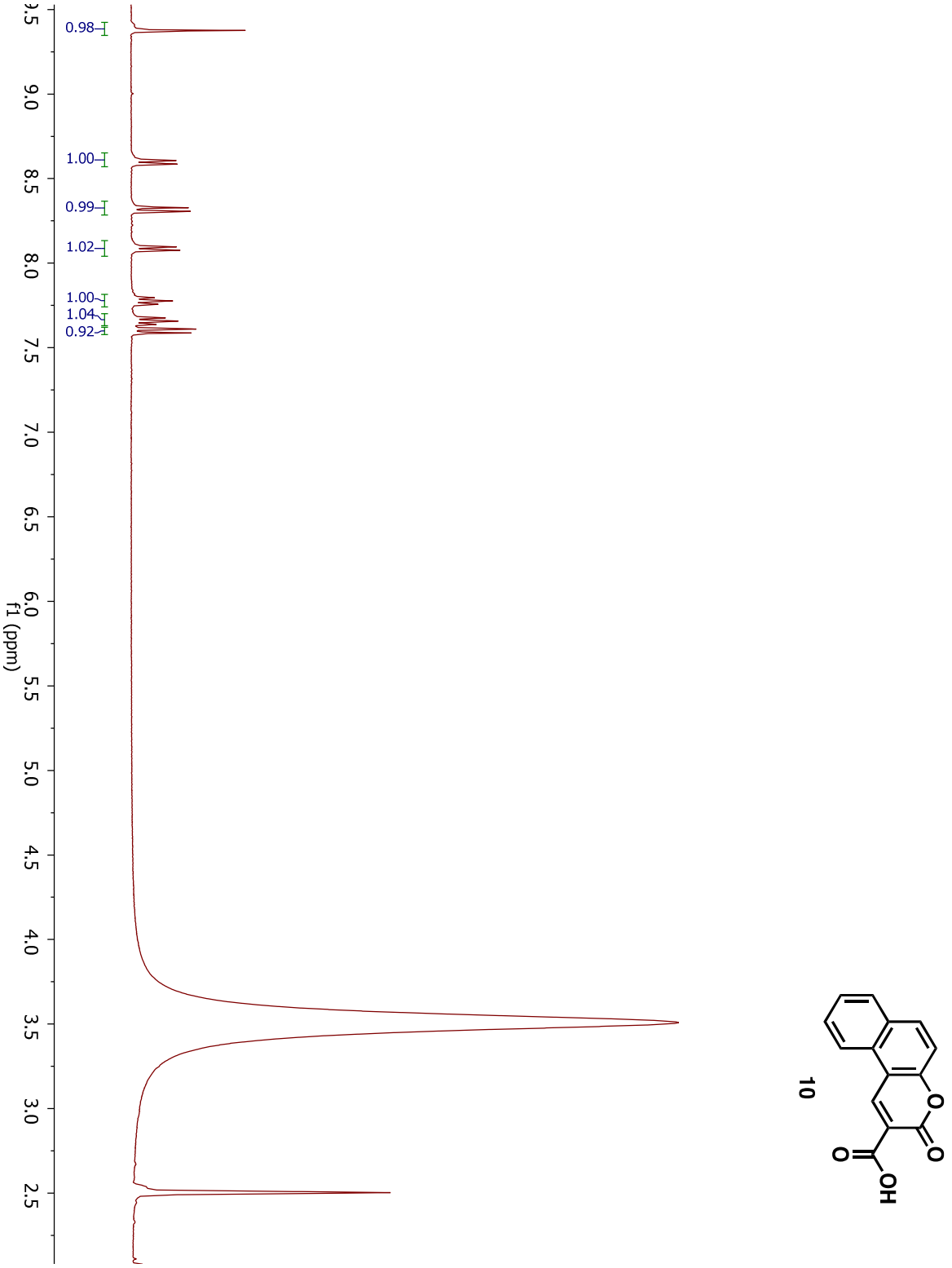

Figure 49. ^{1}H NMR spectrum of Compound **10**.

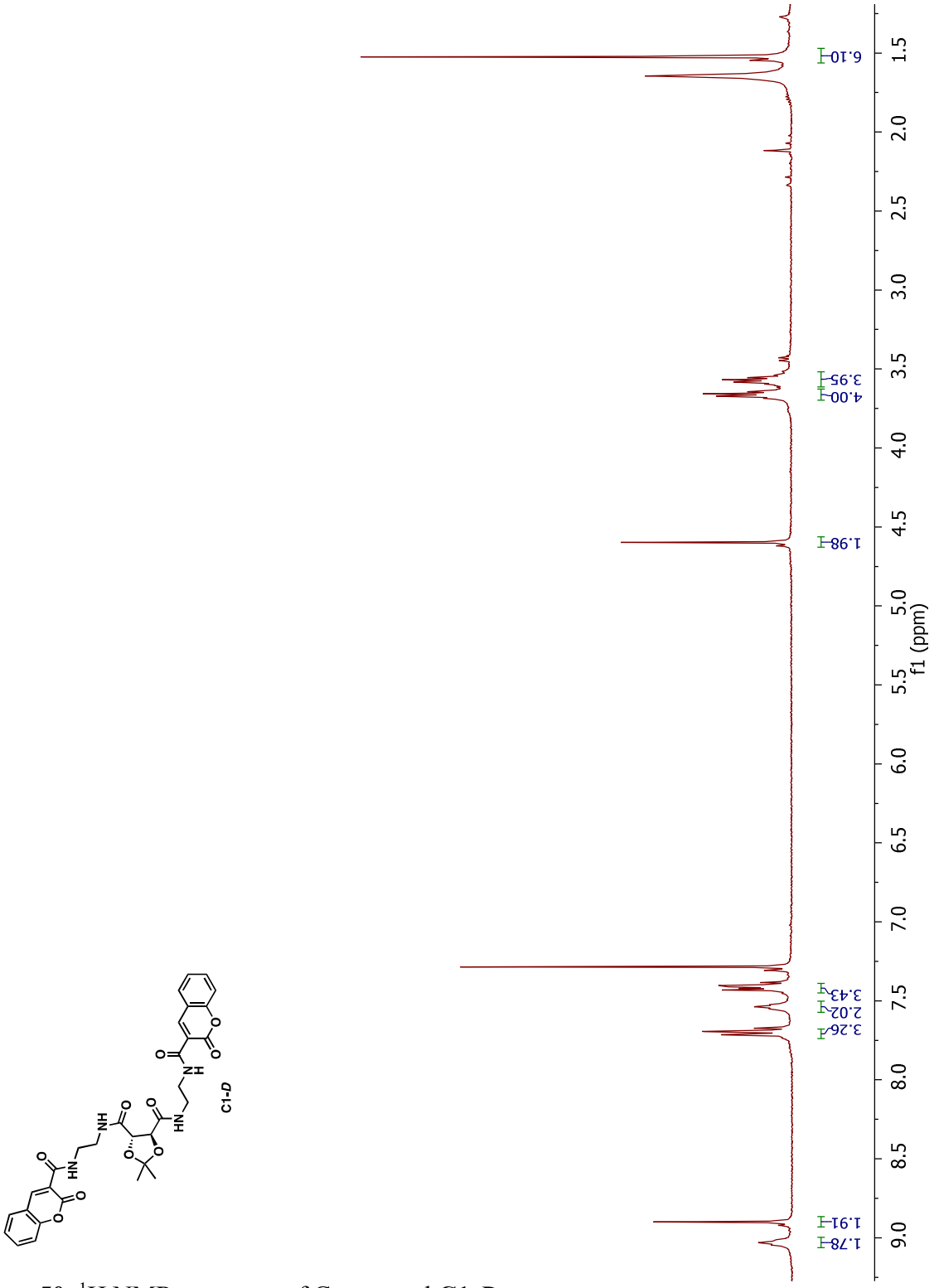

Figure 50. ^{1}H NMR spectrum of Compound **C1-*D***.

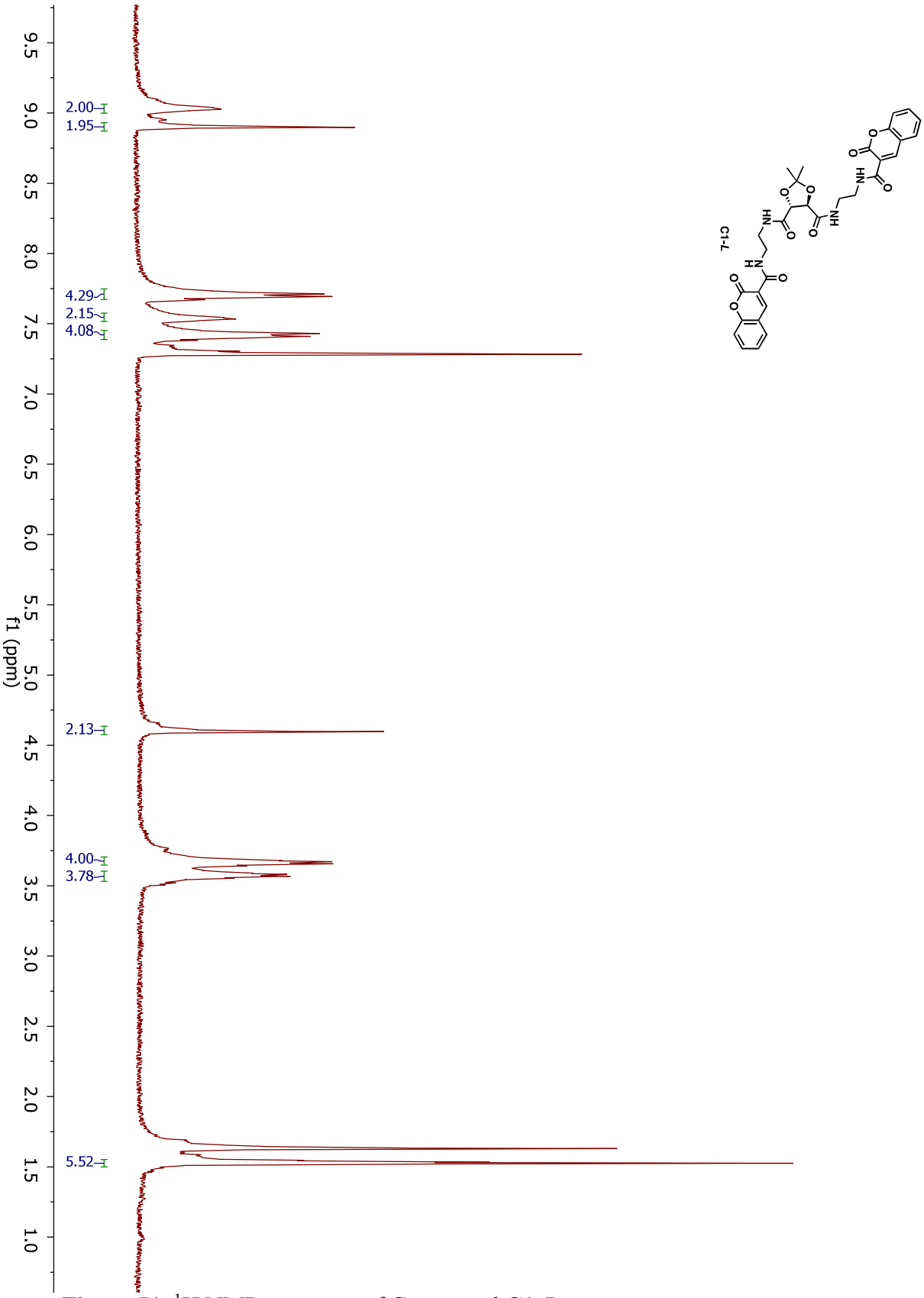

Figure 51. ^{1}H NMR spectrum of Compound **C1-*L***.

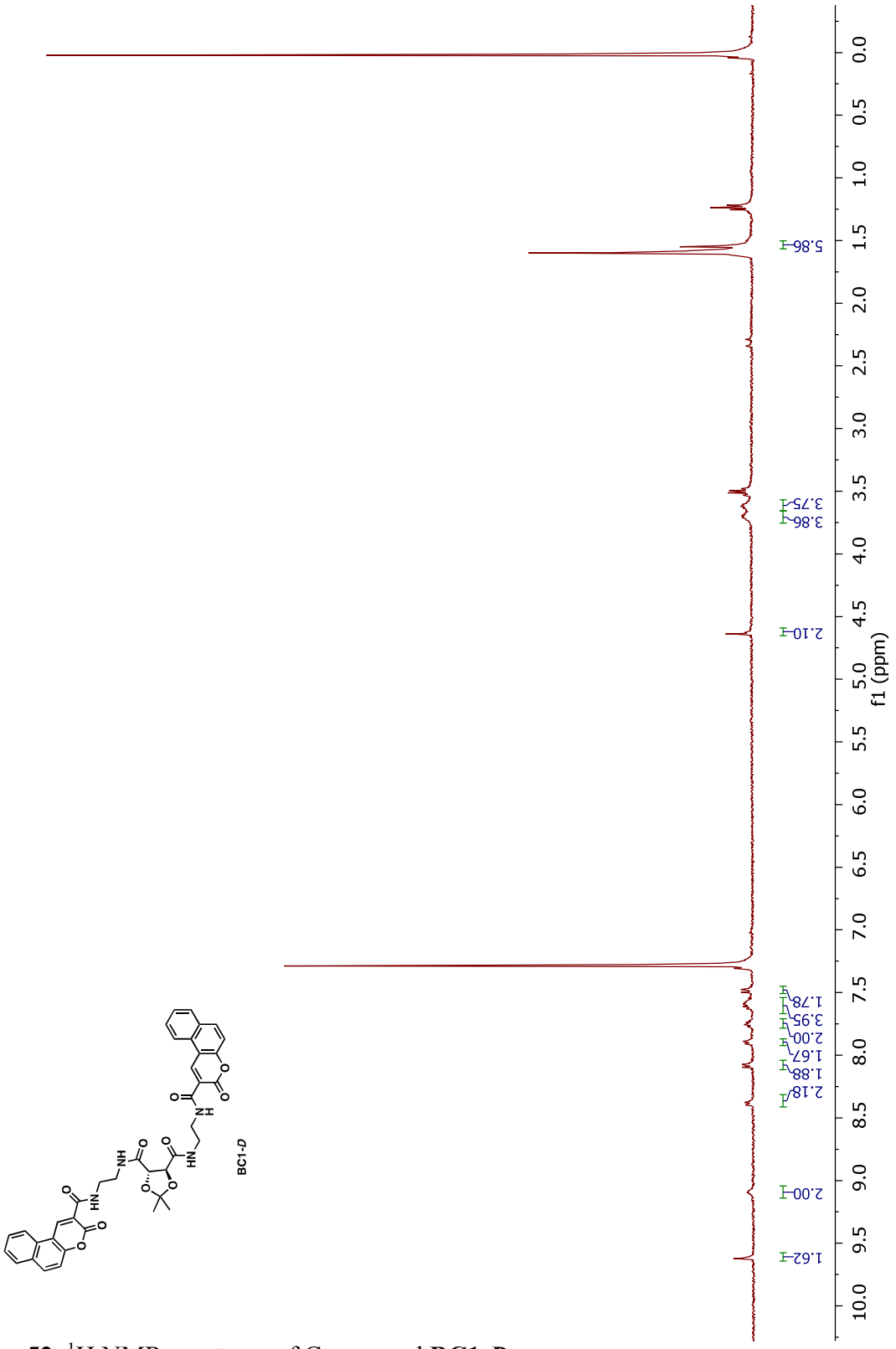

Figure 52. ^{1}H NMR spectrum of Compound **BC1-*D***.

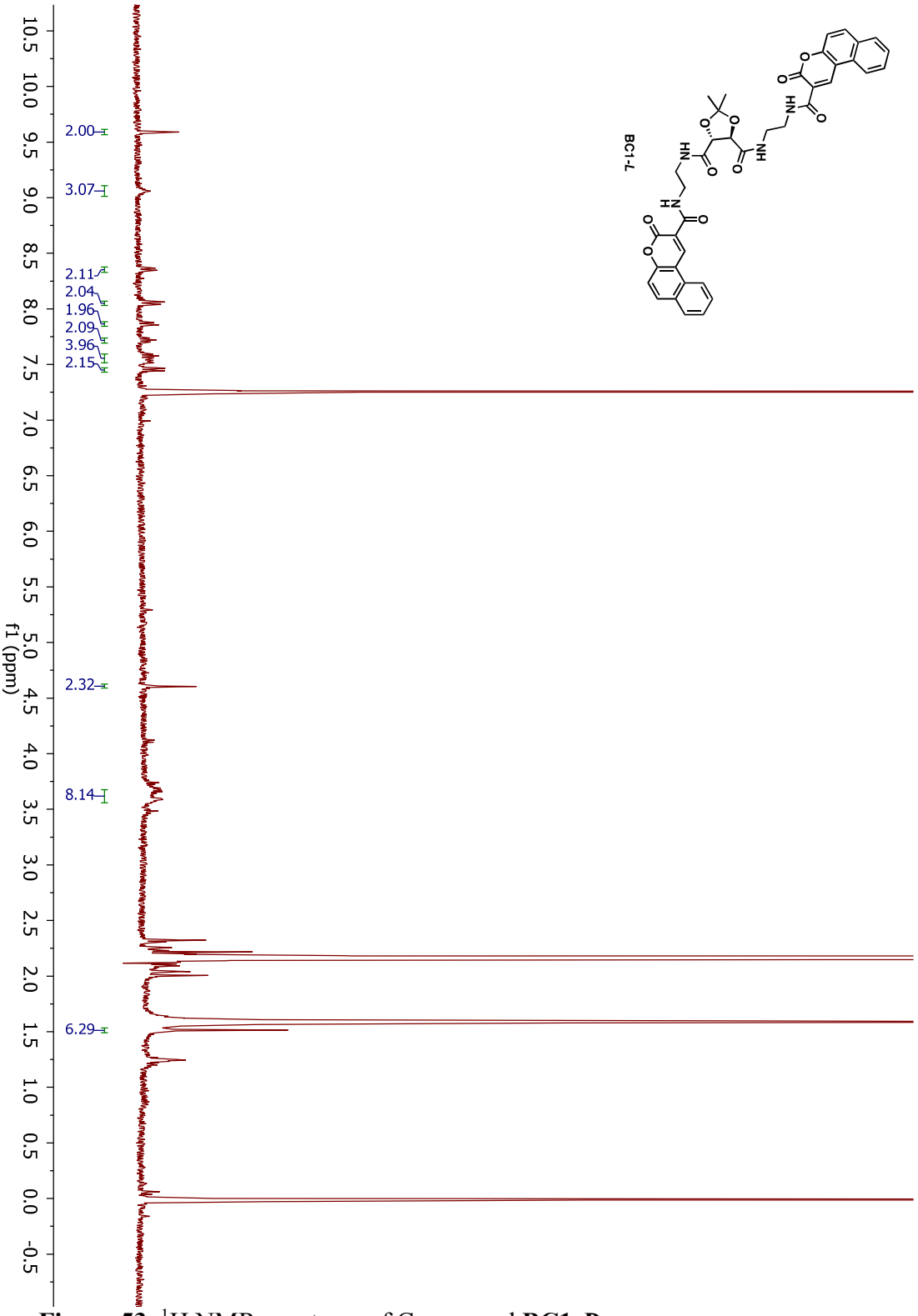

Figure 53. ^{1}H NMR spectrum of Compound **BC1-*D***.

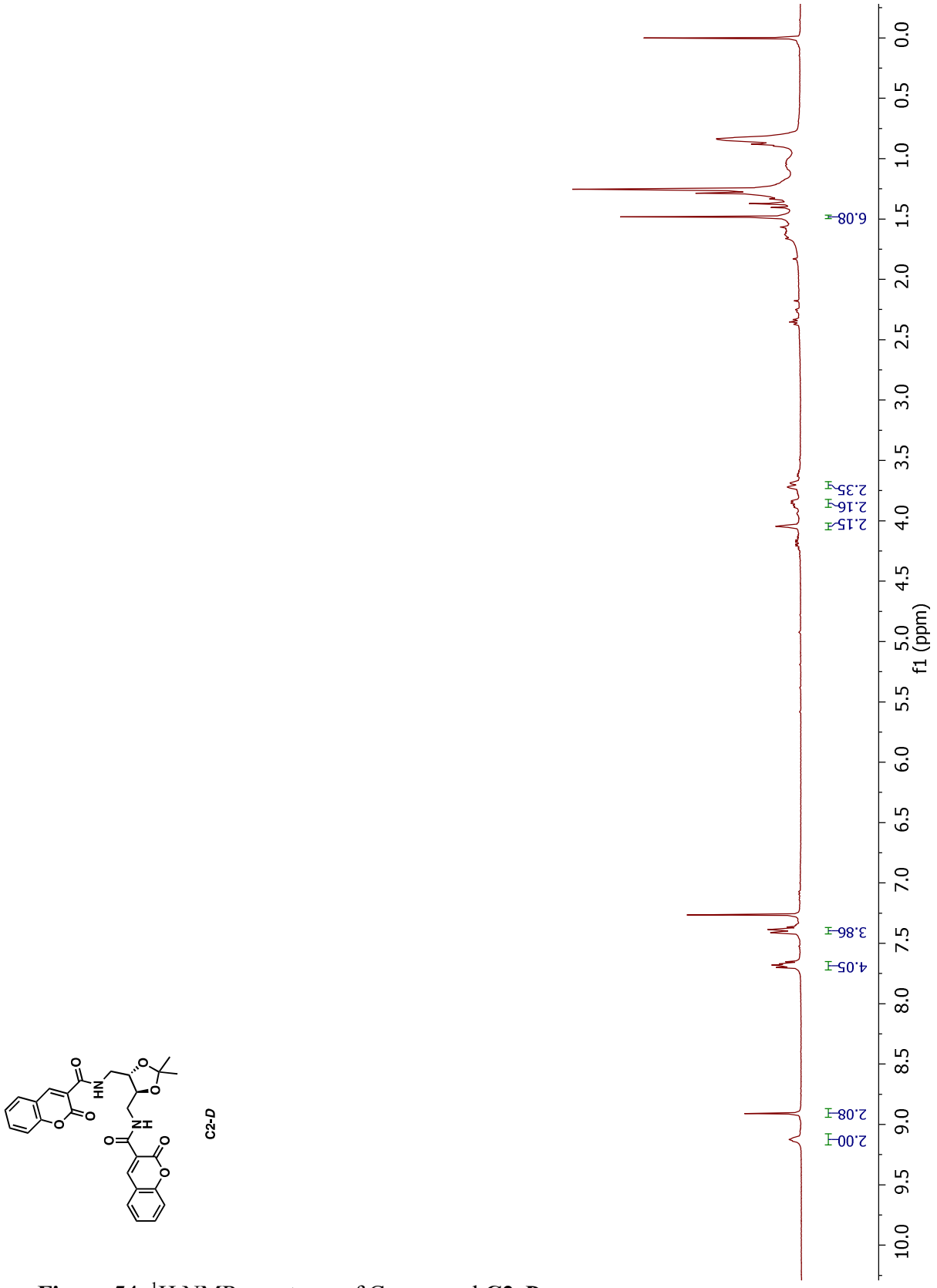

Figure 54. ^{1}H NMR spectrum of Compound **C2-*D***.

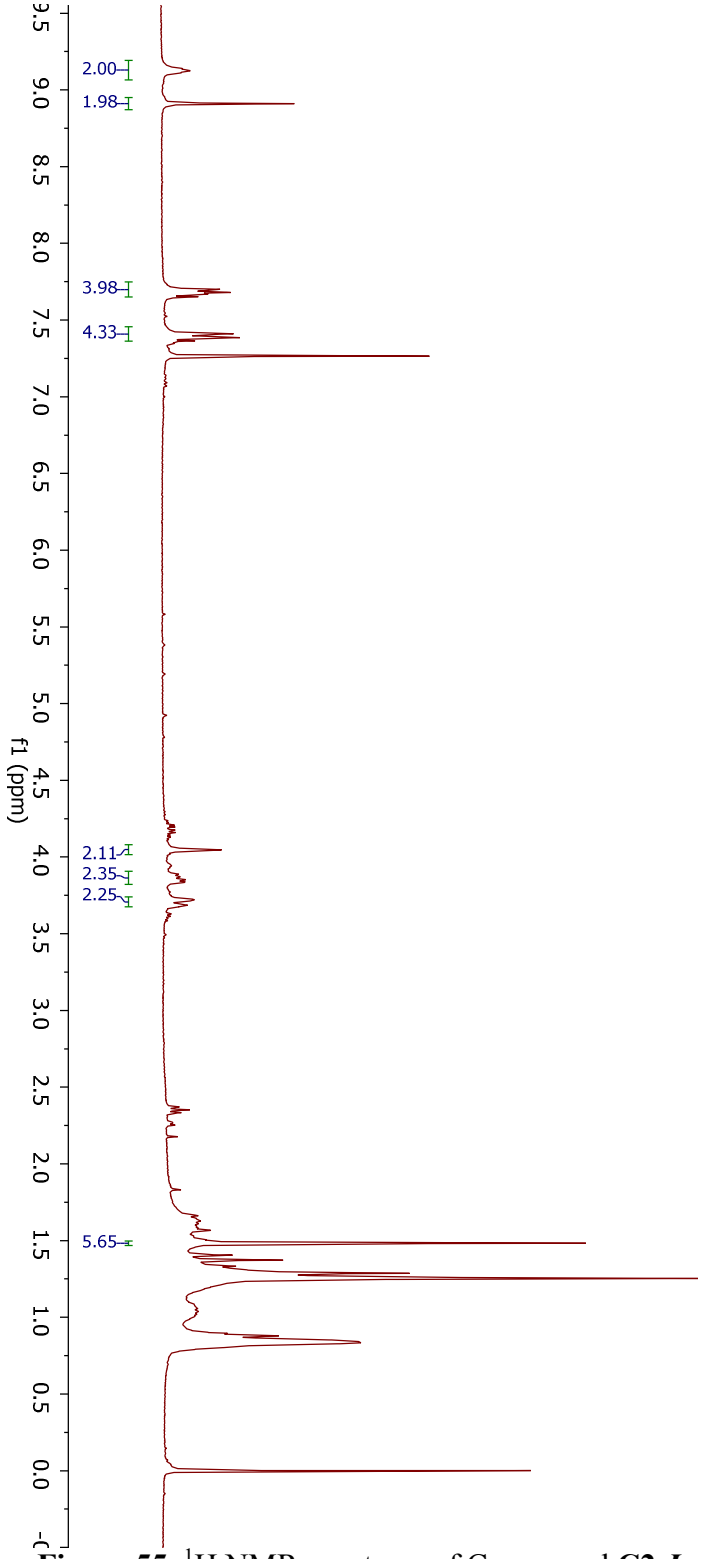

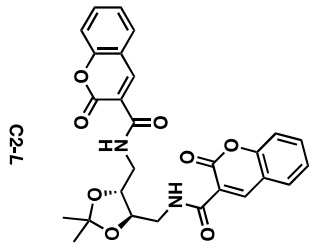

Figure 55. ^{1}H NMR spectrum of Compound **C2-*L***.

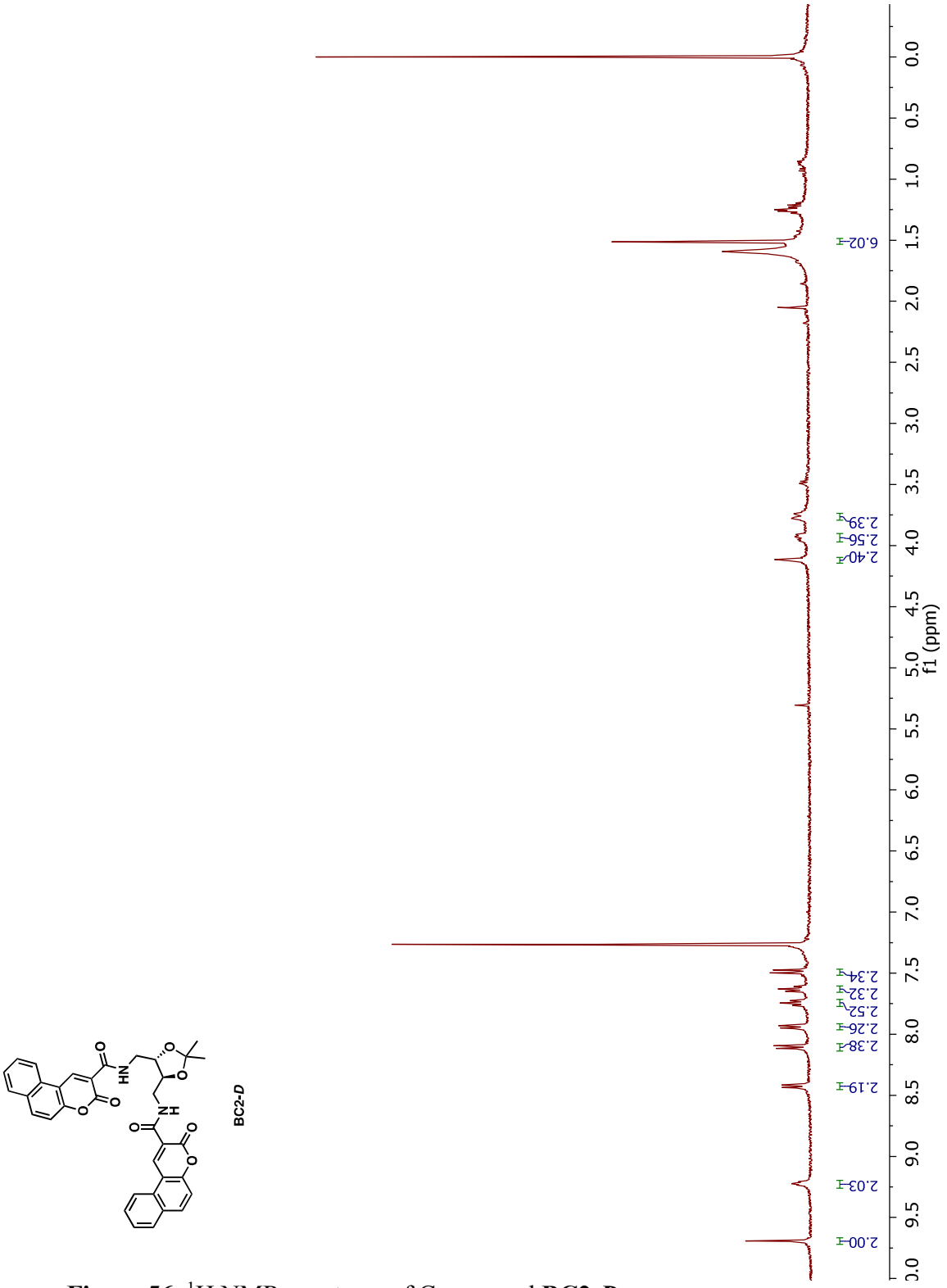

Figure 56. [1]H NMR spectrum of Compound **BC2-*D***.

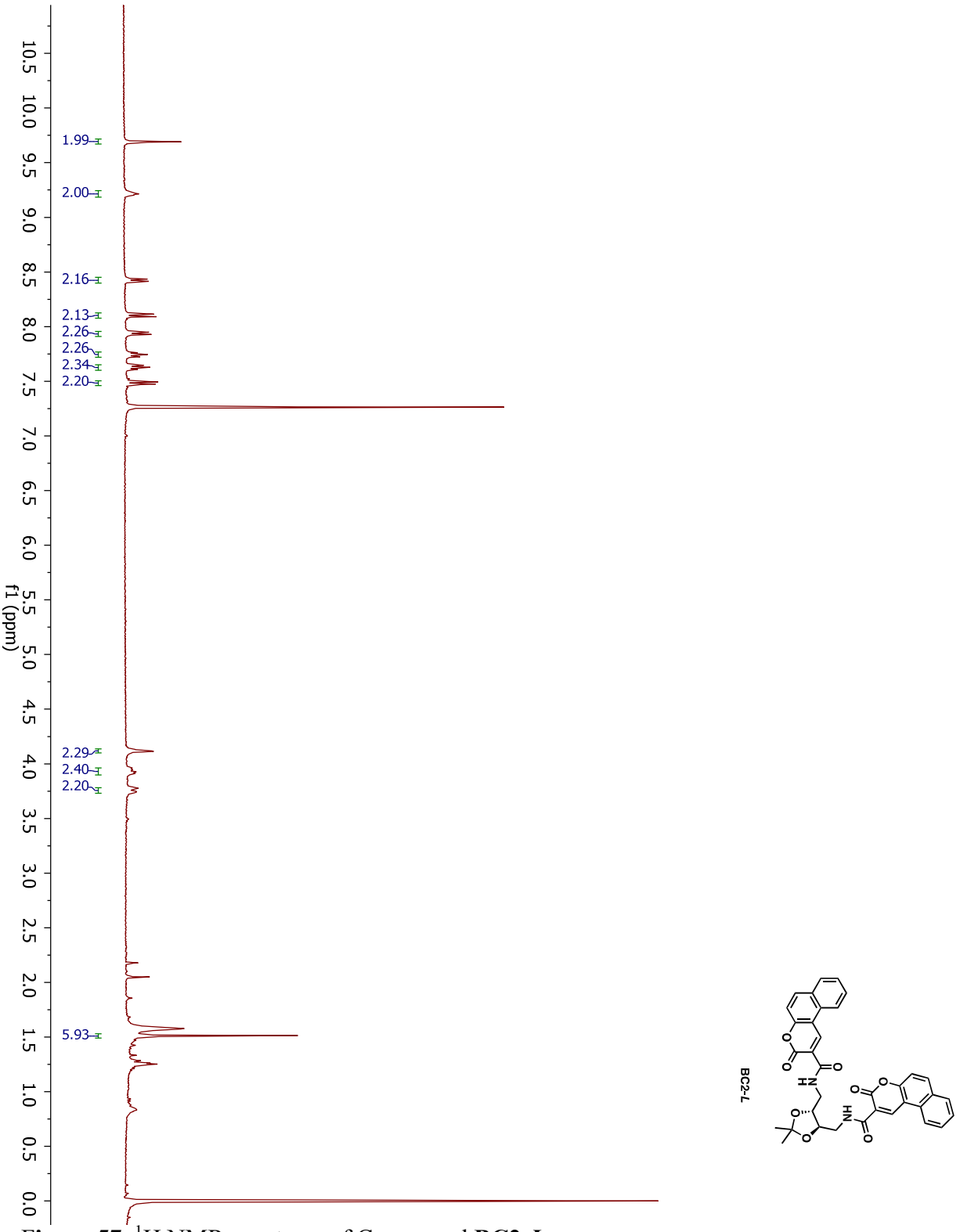

Figure 57. ^{1}H NMR spectrum of Compound **BC2-*L***.

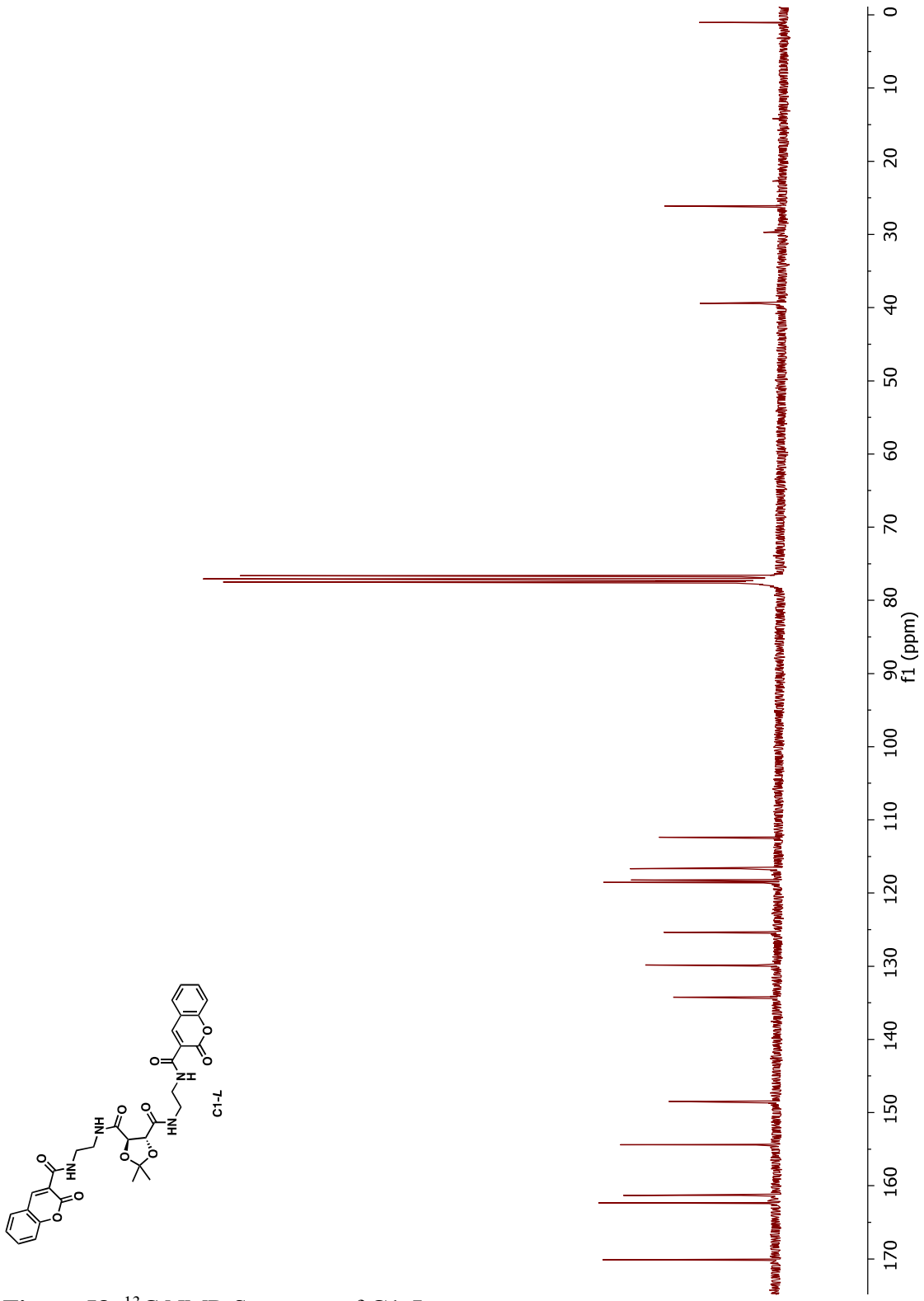

Figure 58. ^{13}C NMR Spectrum of **C1-*L***

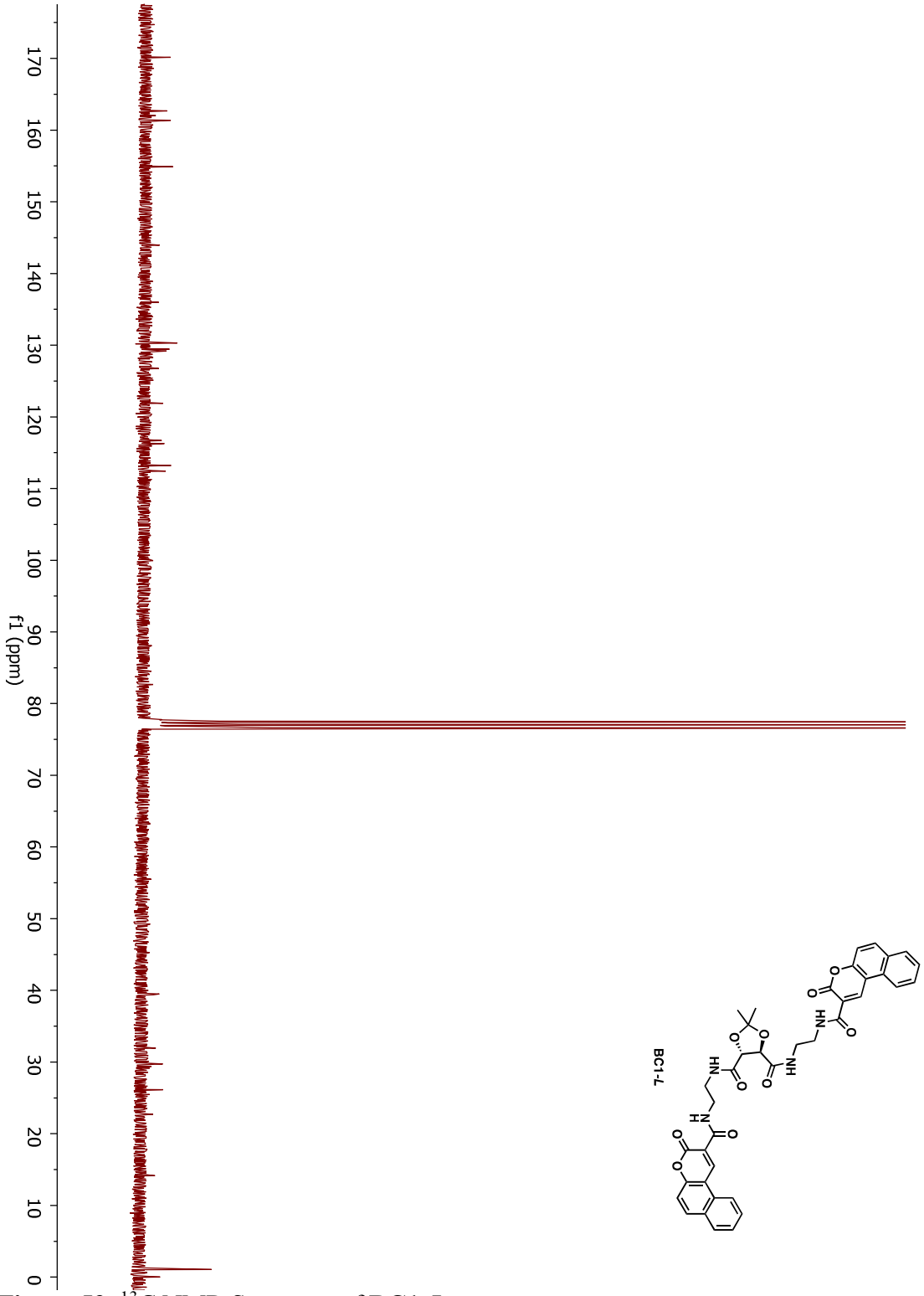

Figure 59. ^{13}C NMR Spectrum of **BC1-*L***

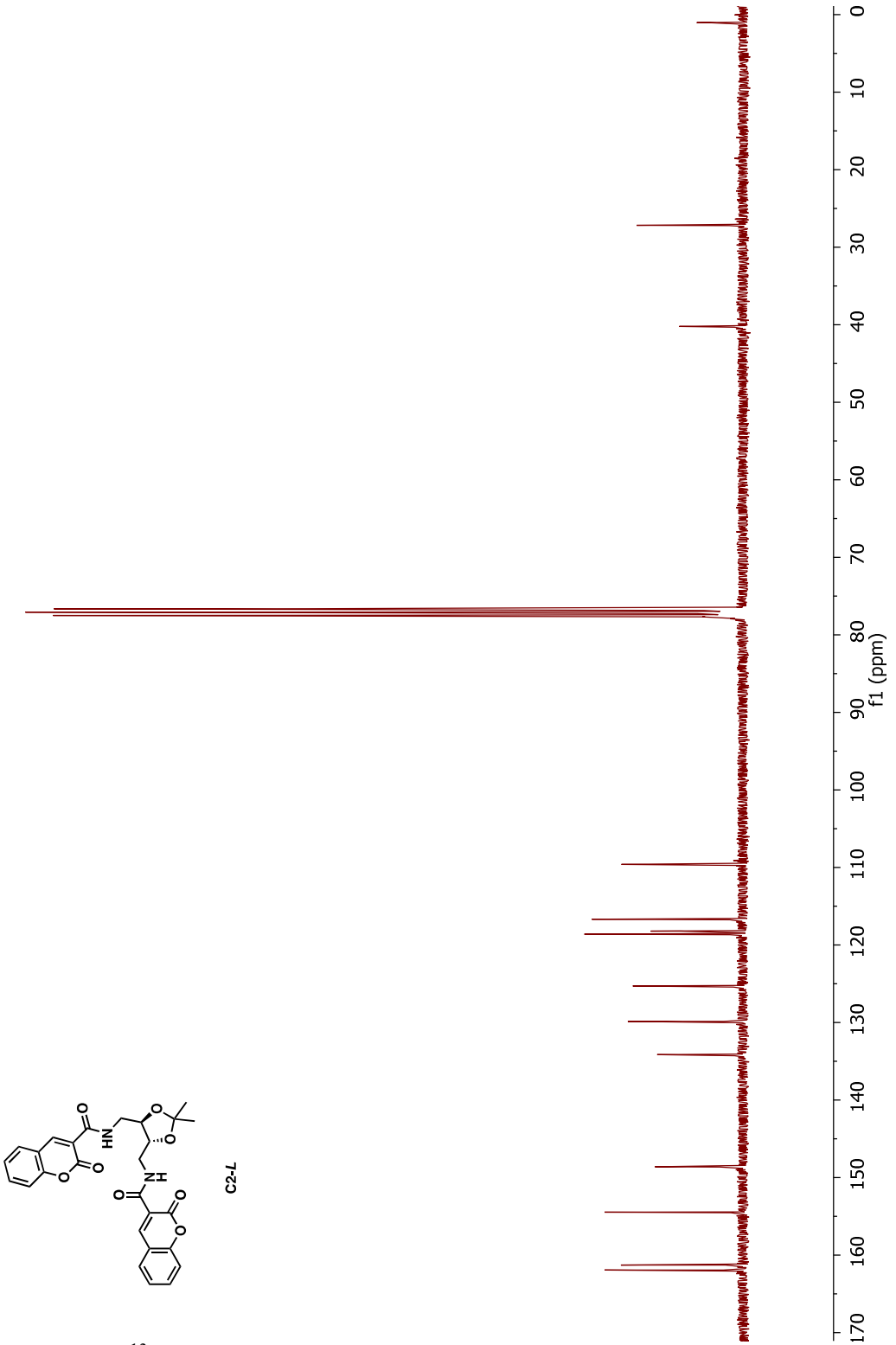

Figure 60. ^{13}C NMR Spectrum of **C2-*L***

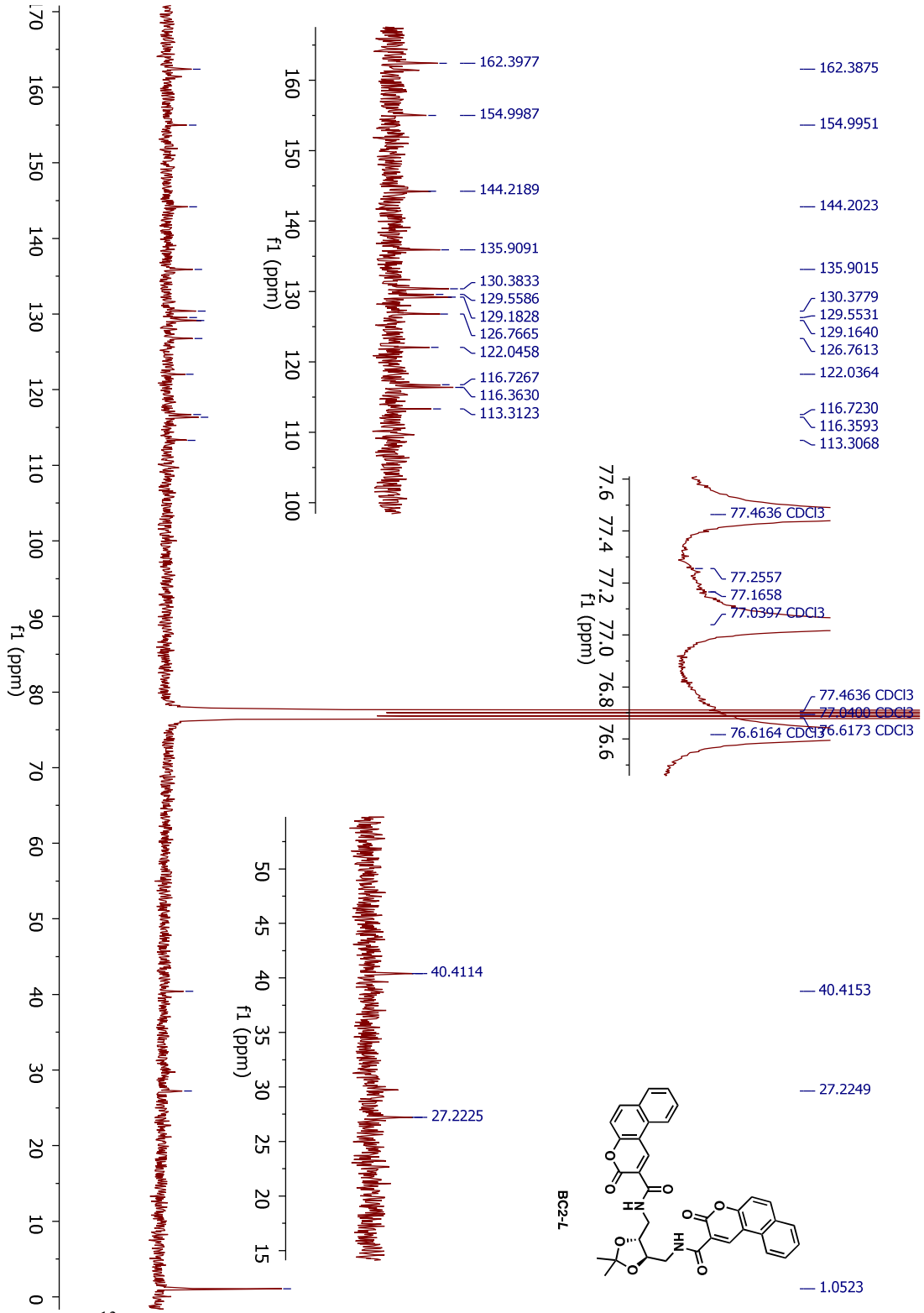

Figure 61. ^{13}C NMR Spectrum of **BC2-*L***

B. IR Spectra

IR spectra were recorded at Thermo Scientific Nicolet iS10 ATR-IR spectrometer.

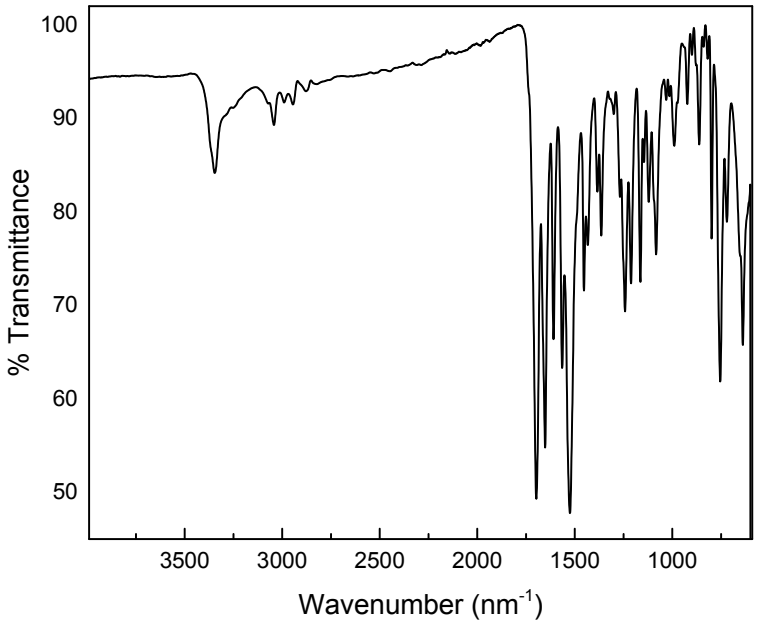

Figure 62. IR spectrum of **C1**.

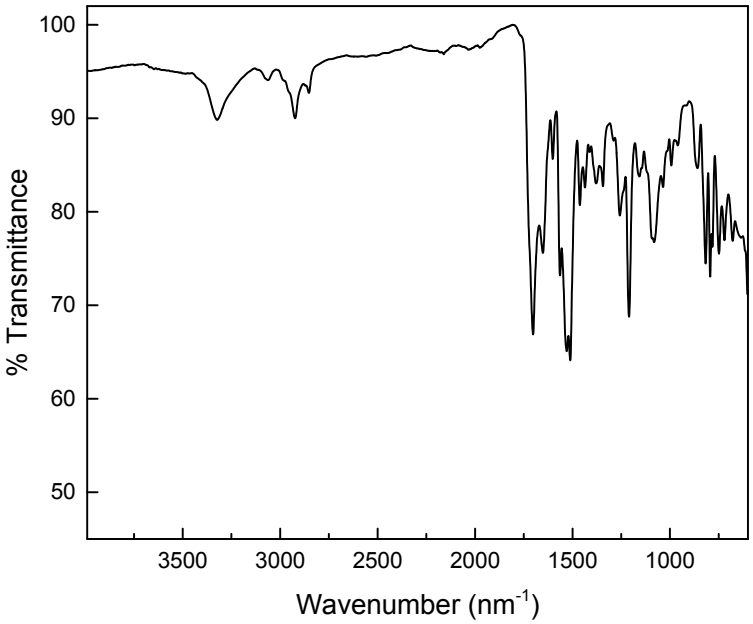

Figure 63. IR spectrum of **BC1**.

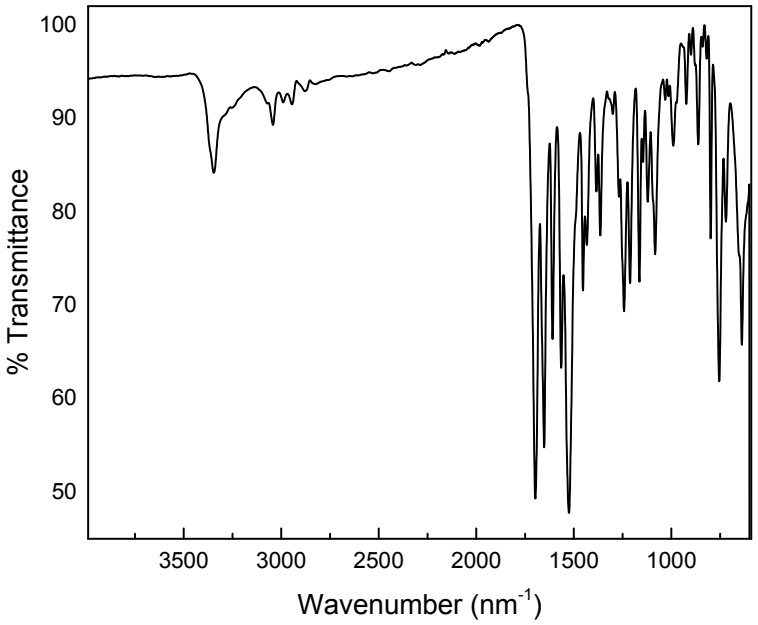

Figure 64. IR Spectrum of **C2**.

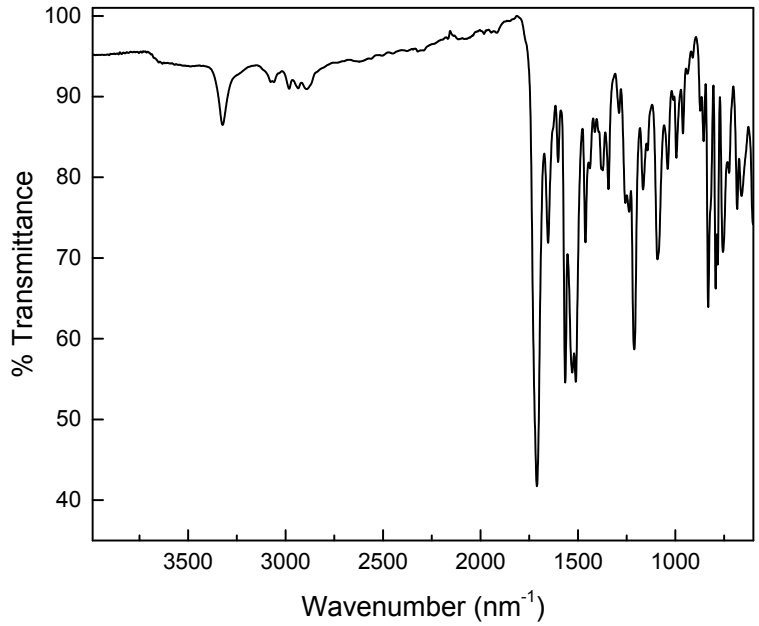

Figure 65. IR spectrum of **BC2**.

C. High Resolution Mass Spectra (HRMS)

High Resolution Mass Spectra (HRMS) Spectra were processed in positive mode on (ES+) using Time of Flight mass analyzer.

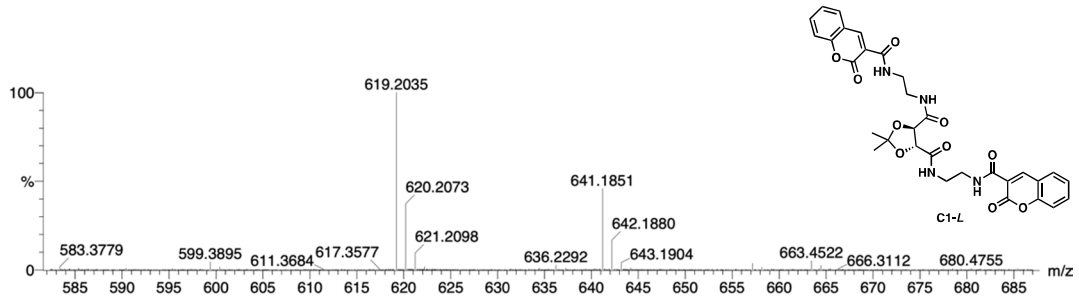

Minimum:				-5.5			
Maximum:		1000.0	1000.0	1000.0			
Mass	Calc. Mass	mDa	PPM	DBE	i-FIT	i-FIT (Norm)	Formula
619.2035	619.2040	-0.5	-0.8	18.5	259.0	0.0	C31 H31 N4 O10

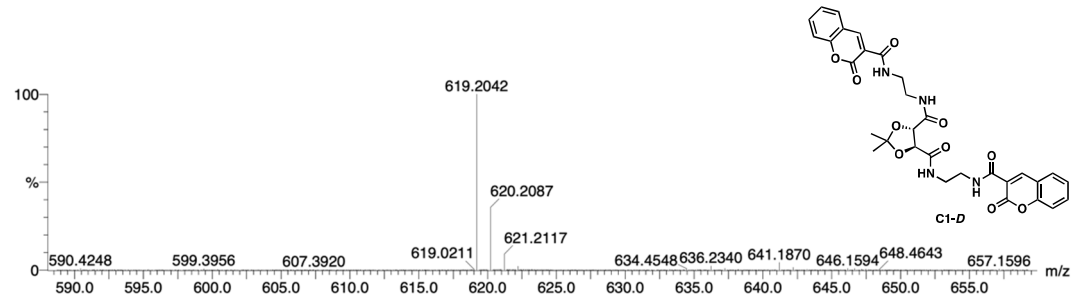

Minimum:				-5.5			
Maximum:		1000.0	1000.0	1000.0			
Mass	Calc. Mass	mDa	PPM	DBE	i-FIT	i-FIT (Norm)	Formula
619.2042	619.2040	0.2	0.3	18.5	318.8	0.0	C31 H31 N4 O10

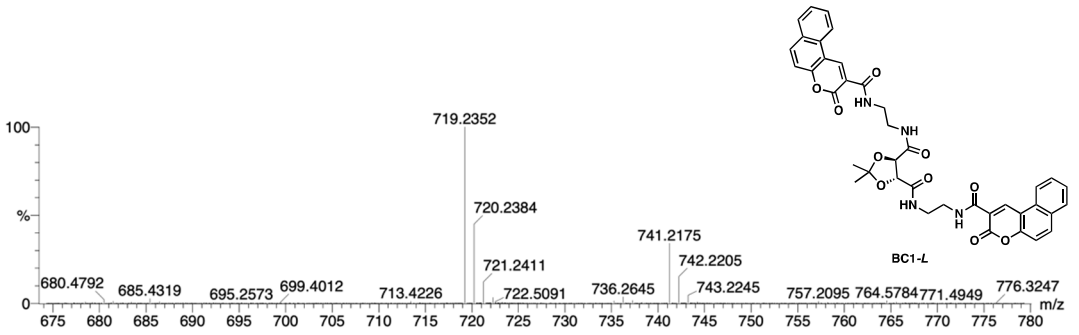

Minimum:				-5.5			
Maximum:		1000.0	1000.0	1000.0			
Mass	Calc. Mass	mDa	PPM	DBE	i-FIT	i-FIT (Norm)	Formula
719.2352	719.2353	-0.1	-0.1	24.5	245.9	0.0	C39 H35 N4 O10

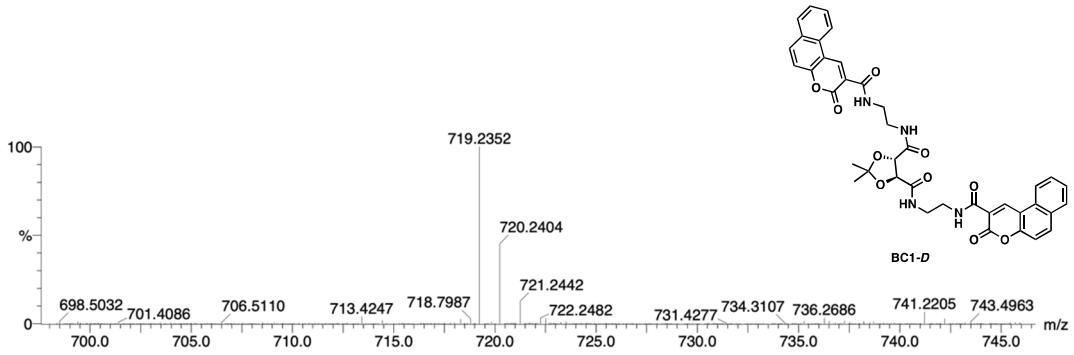

Minimum:				-5.5			
Maximum:		1000.0	1000.0	1000.0			
Mass	Calc. Mass	mDa	PPM	DBE	i-FIT	i-FIT (Norm)	Formula
719.2352	719.2353	-0.1	-0.1	24.5	234.6	0.0	C39 H35 N4 O10

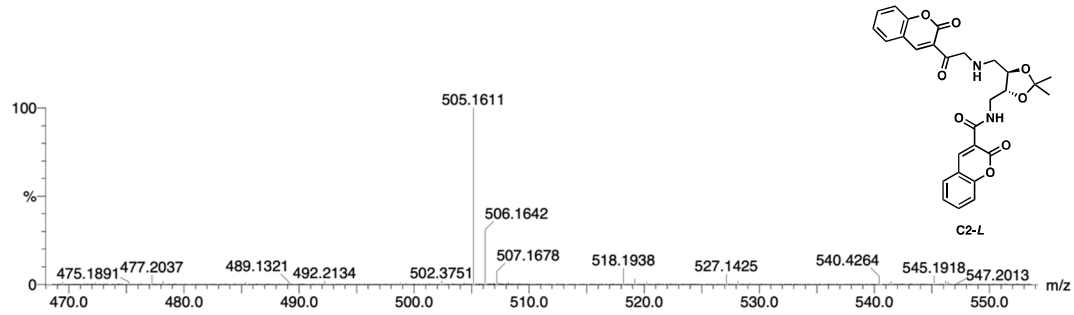

Minimum:				-5.5			
Maximum:		1000.0	1000.0	1000.0			
Mass	Calc. Mass	mDa	PPM	DBE	i-FIT	i-FIT (Norm)	Formula
505.1611	505.1611	0.0	0.0	16.5	376.7	0.0	C27 H25 N2 O8

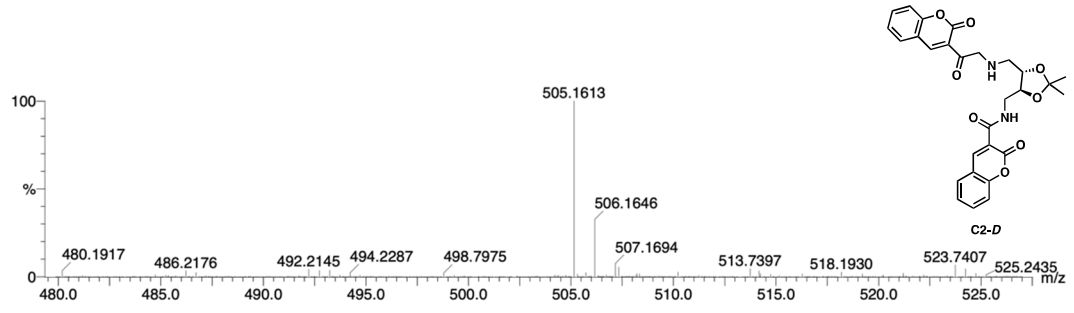

Minimum:				-5.5			
Maximum:		1000.0	1000.0	1000.0			
Mass	Calc. Mass	mDa	PPM	DBE	i-FIT	i-FIT (Norm)	Formula
505.1613	505.1611	0.2	0.4	16.5	315.4	0.0	C27 H25 N2 O8

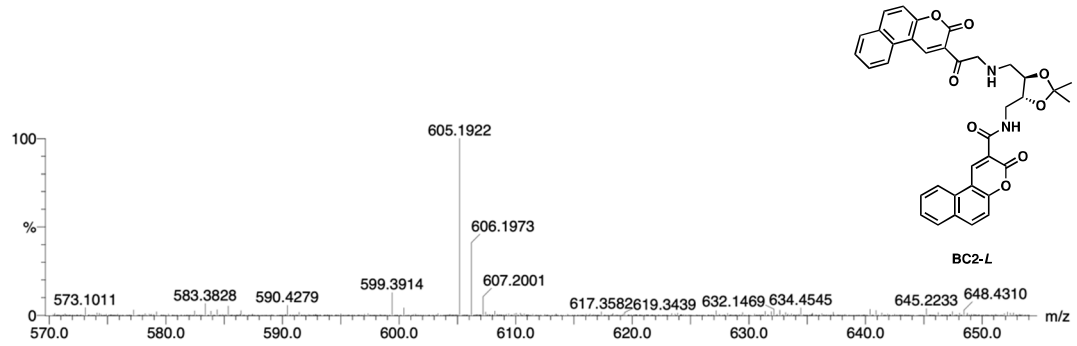

Minimum:				-5.5						
Maximum:		1000.0	1000.0	1000.0						
Mass	Calc. Mass	mDa	PPM	DBE	i-FIT	i-FIT (Norm)	Formula			
605.1922	605.1924	-0.2	-0.3	22.5	238.4	0.0	C35	H29	N2	O8

Figure 66. HRMS spectra of **C1-*L***, **C1-*D***, **BC1-*L***, **BC1-*D***, **C2-*L***, **C2-*D***, and **BC2-*L***.

D. Fluorescence Spectra

Fluorescence spectra were recorded at Perkin Elmer LS55 spectrofluorometer.

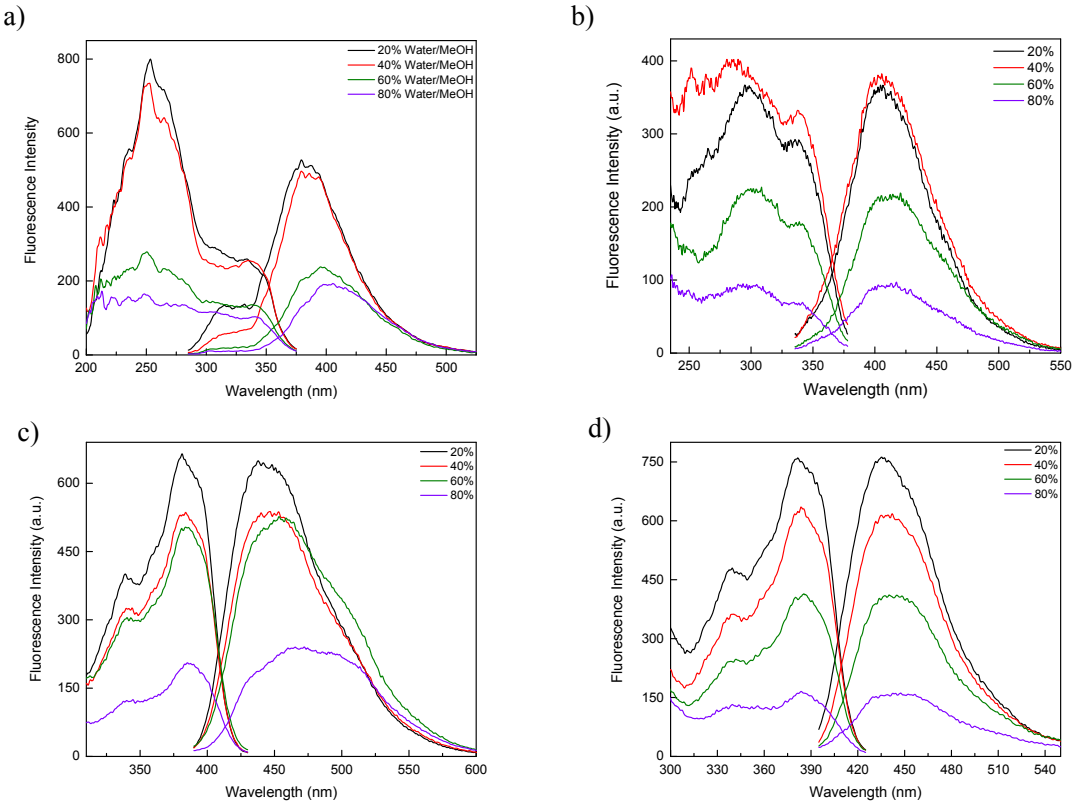

Figure 67. Excitation (left) and Emission (right) spectra of **a) C1-*L*** (10^{-8} M) , **b) C2-*L*** (10^{-8} M) **c) BC1-*L*** (10^{-8} M), **d) BC1-*L*** (10^{-8} M) aggregates at 20% water- 80% MeOH (black), 40% water- 60% MeOH (red), 60% water- 40% MeOH (green), 80% water- 20% MeOH (purple).

E. UV-Vis Spectra

UV-Vis measurements were recorded with Shimadzu UV-2450 spectrophotometer.

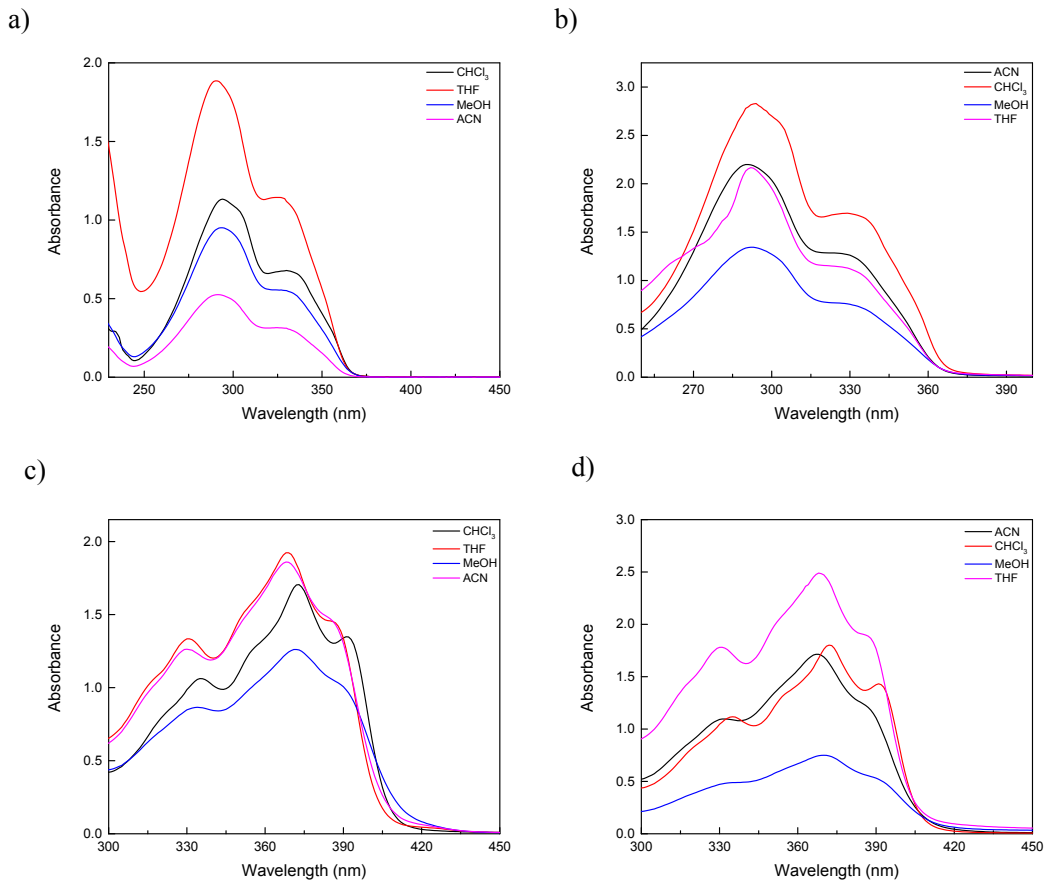

Figure 68. Unnormalized UV-Vis Spectra of **a) C1-*L*** (10^{-5} M) , **b) C2-*L*** (10^{-5} M) **c) BC1-*L*** (10^{-5} M), **d) BC1-*L*** (10^{-5} M) in $CHCl_3$, MeOH, THF and ACN.

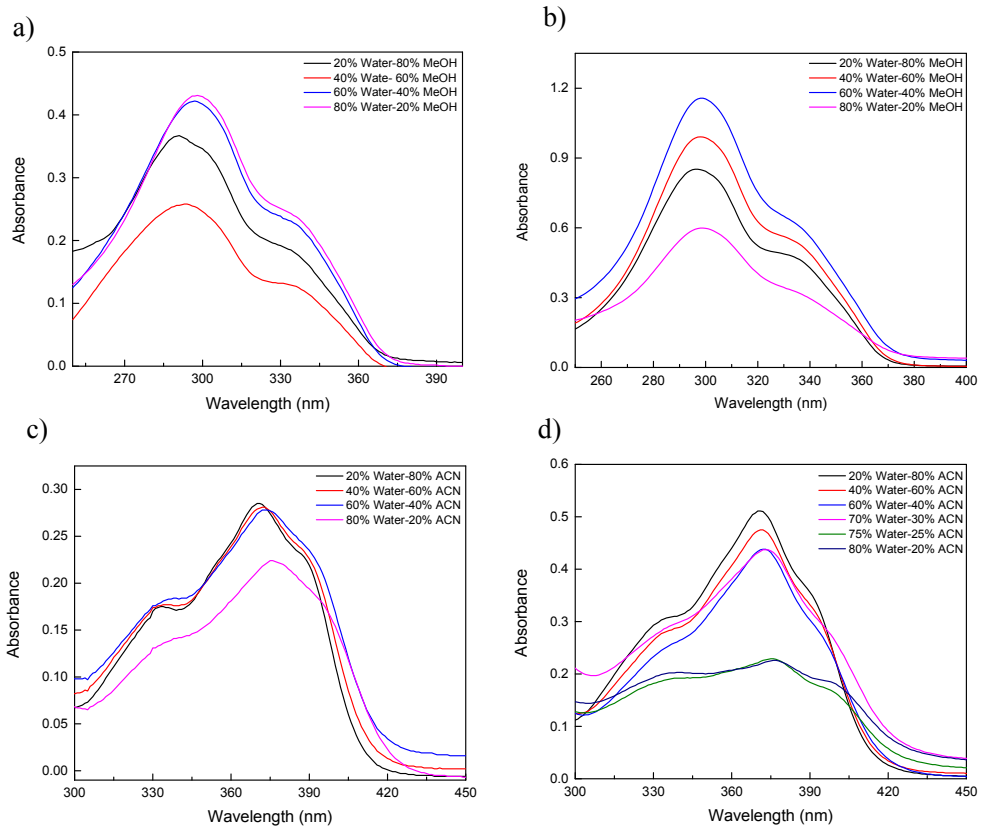

Figure 69. Unnormalized UV-Vis Spectra of aggregates of **a) C1-*L*** (10^{-6} M) , **b) C2-*L*** (10^{-6} M) **c) BC1-*L*** (10^{-6} M), **d) BC1-*L*** (10^{-6} M).

F. CPL Spectra

CPL measurements were recorded with home-made CPL instrument.

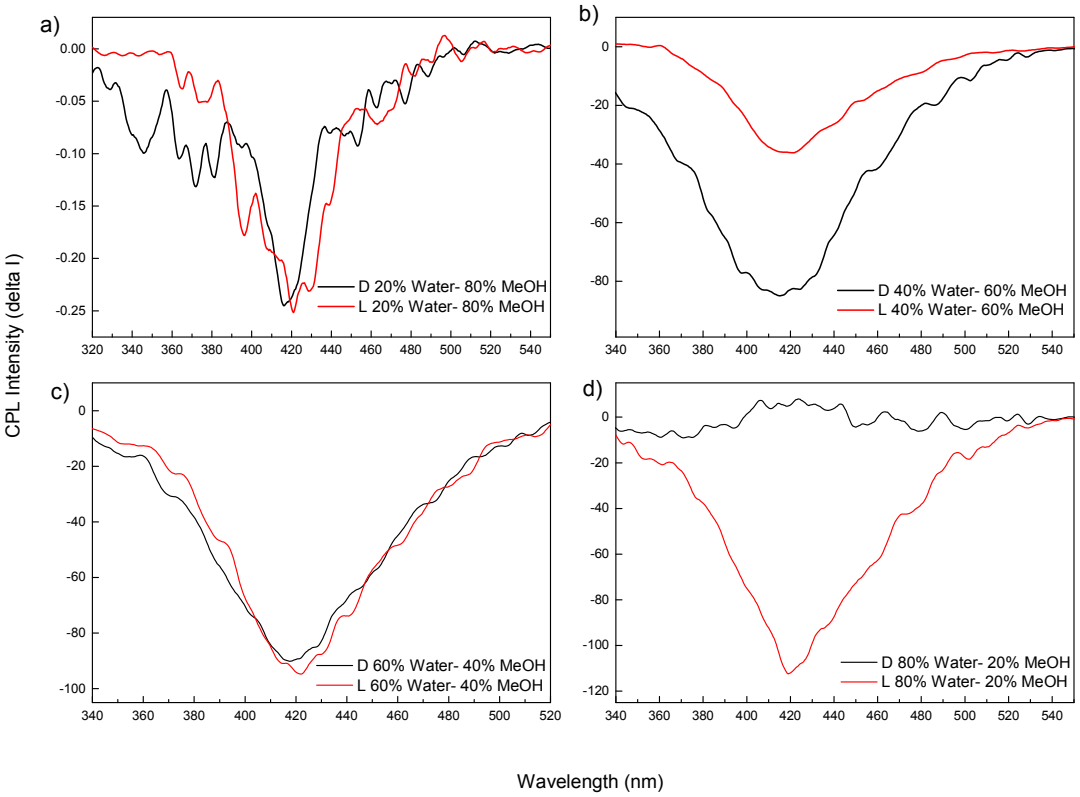

Figure 70. CPL spectra of **C1-*L*** and **C1-*D*** (10^{-6} M) at **a)** 20% water- 80% MeOH, **b)** 40% water- 60% MeOH, **c)** 60% water- 40% MeOH, **d)** 80% water- 20% MeOH.

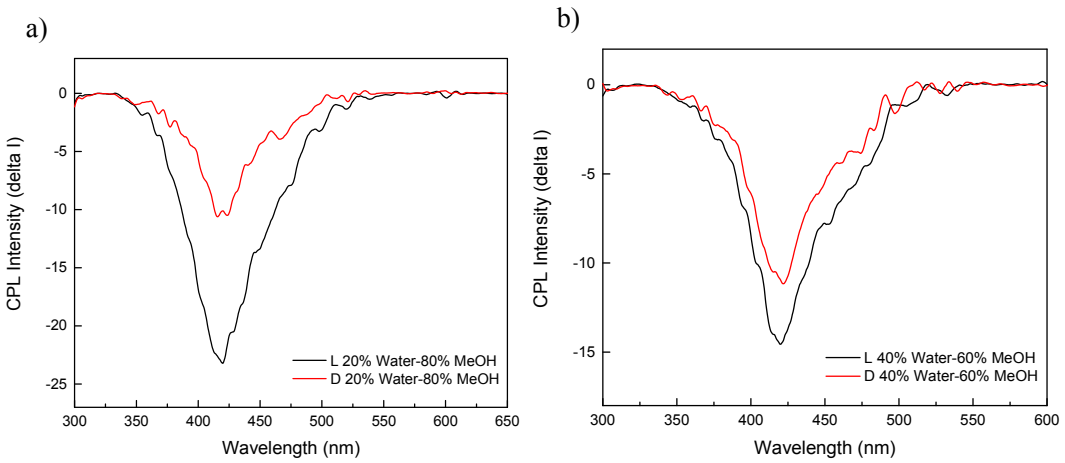

Figure 71. CPL spectra of **C2-*L*** and **C2-*D*** (10^{-6} M) at **a)** 20% water- 80% MeOH, **b)** 40% water- 60% MeOH.

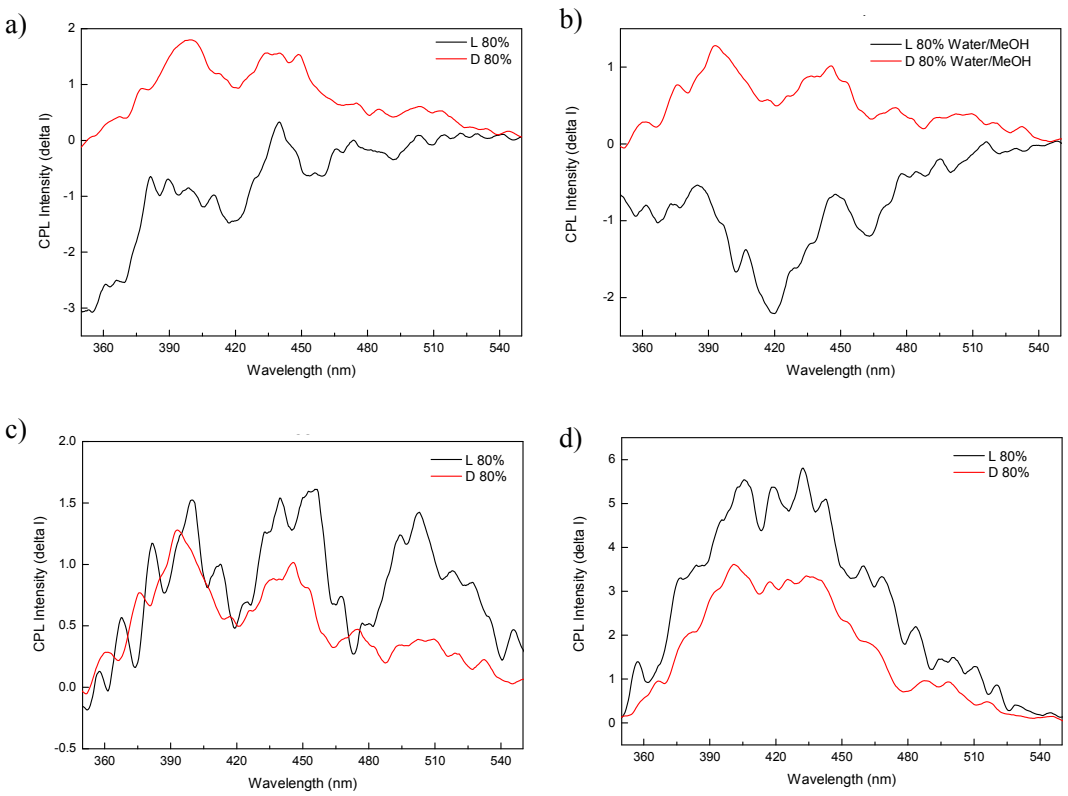

Figure 72. CPL spectra of **C2** at 80% water- 20% MeOH solution (10^{-6}M) **a)** first solution **b)** first solution rested at ambient conditions for 24 hours, **c)** second solution, **d)** second solution rested at ambient conditions for 24 hours.

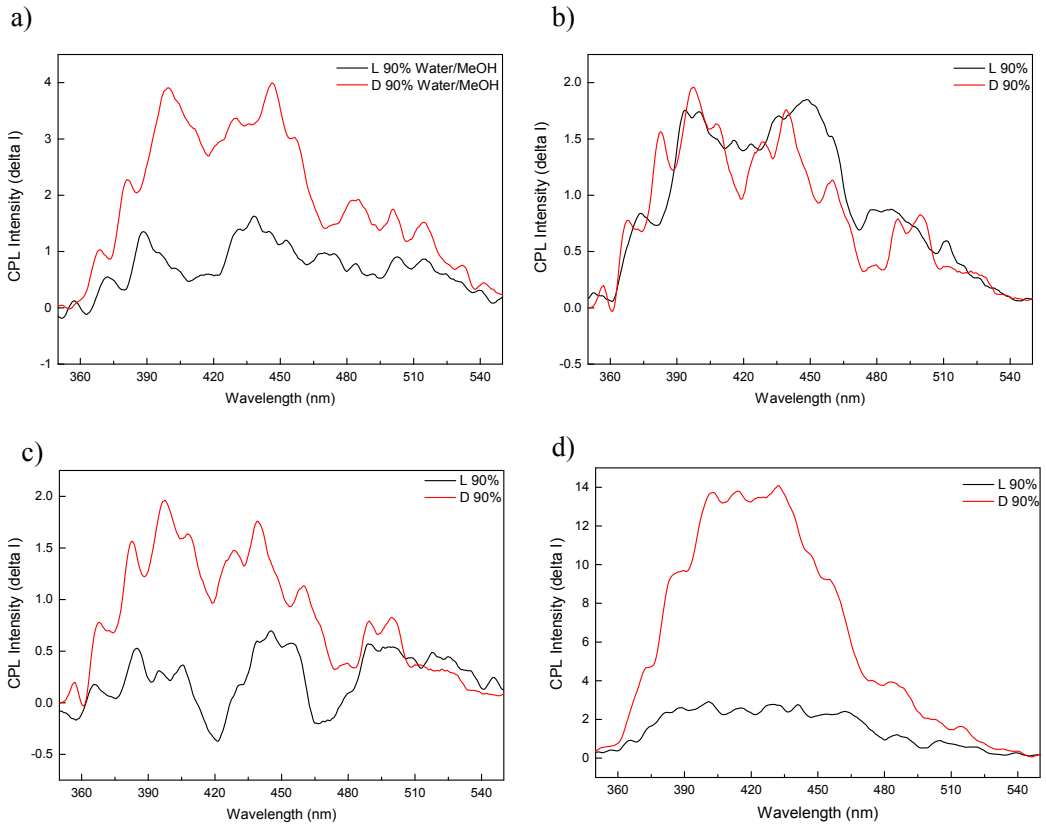

Figure 73. CPL spectra of **C2** at 90% water- 10% MeOH solution (10^{-6}M) **a**) first solution **b)** first solution on the next day, **c)** second solution, **d)** second solution on next day.

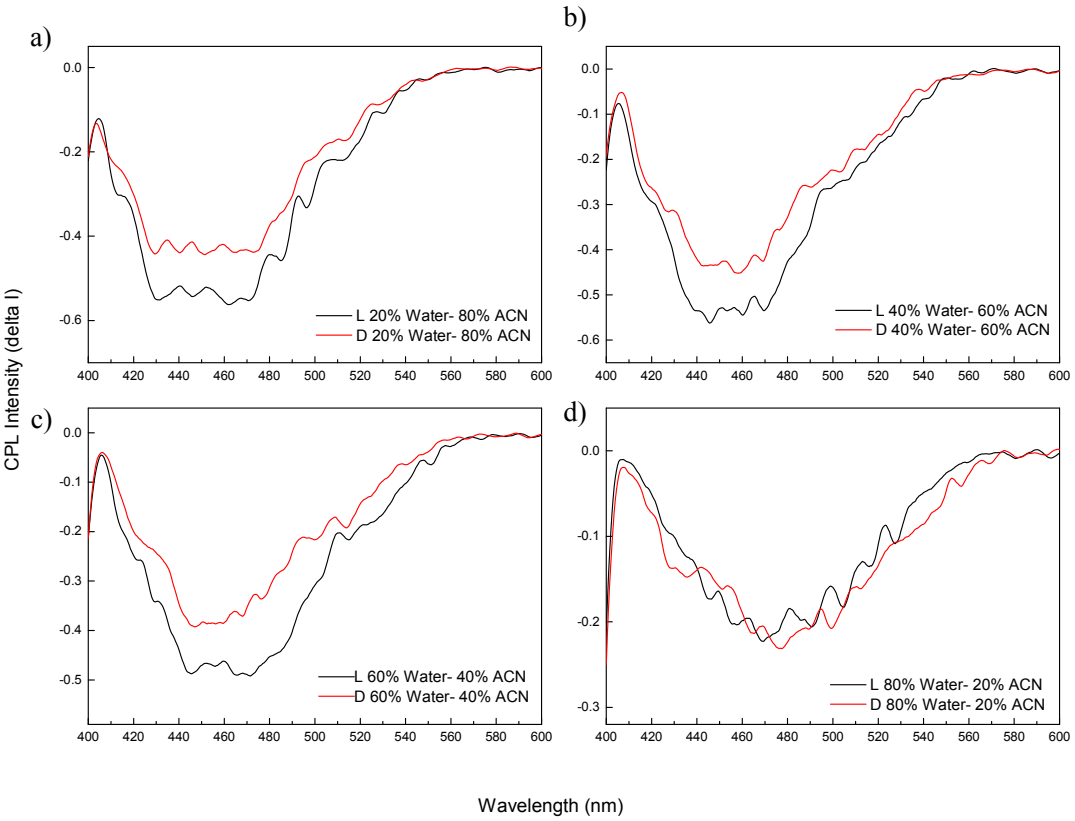

Figure 74. CPL spectra of **BC1-*L*** and **BC1-*D*** (10^{-6} M) at **a)** 20% water- 80% MeOH, **b)** 40% water- 60% MeOH, **c)** 60% water- 40% MeOH, **d)** 80% water- 20% MeOH.

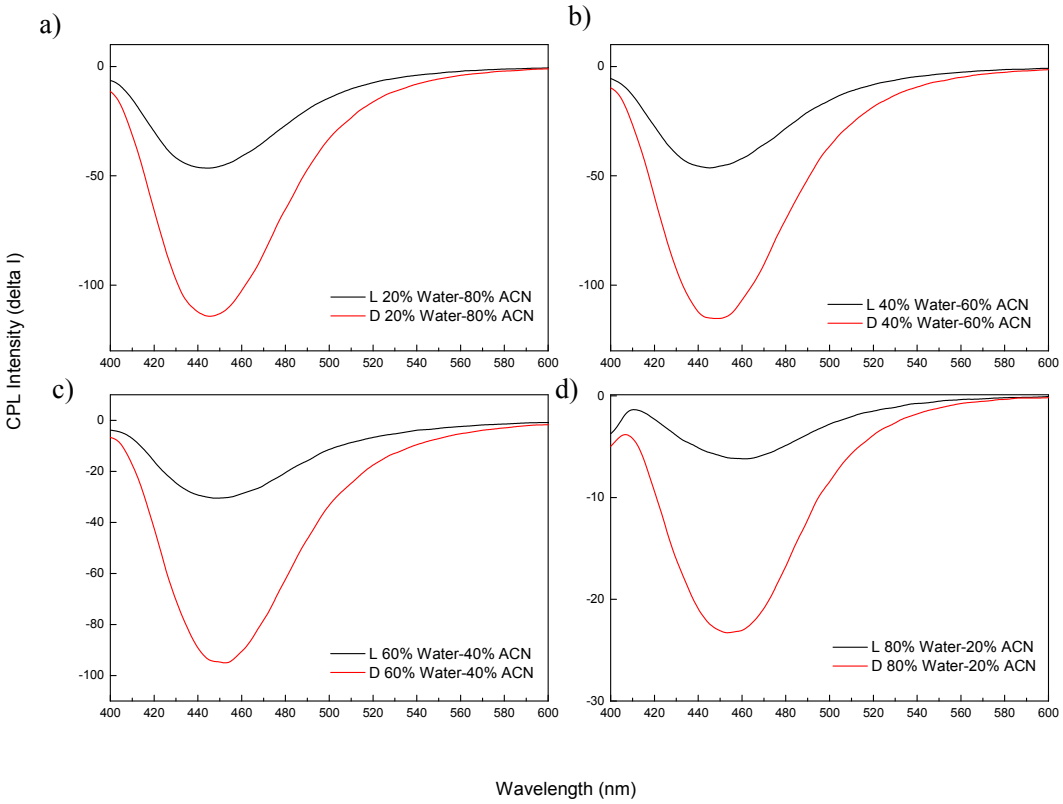

Figure 75. CPL spectra of **BC2-*L*** and **BC2-*D*** (10^{-6} M) at **a)** 20% water- 80% MeOH, **b)** 40% water- 60% MeOH, **c)** 60% water- 40% MeOH, **d)** 80% water- 20% MeOH.

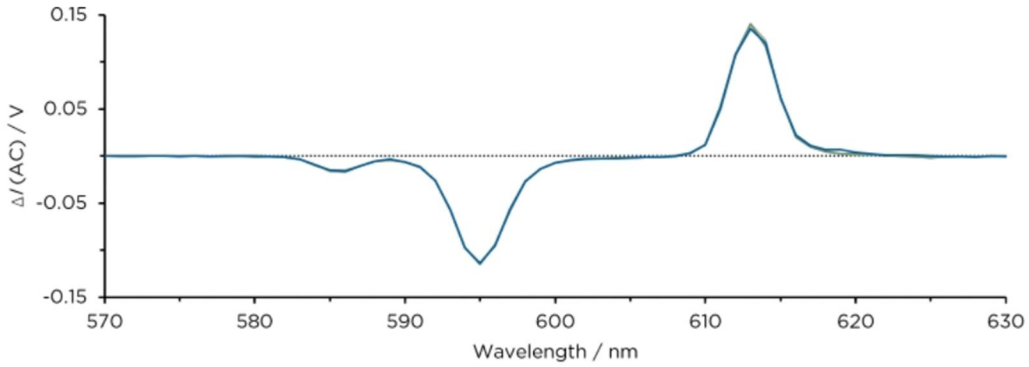

Figure 76. Literature CPL Spectrum of $Eu(facam)_3$ in DMSO (Kondo Y, Suzuki S, Watanabe M, Kaneta A, Albertini P and Nagamori K Temperature-Dependent Circularly Polarized Luminescence Measurement Using KBr Pellet Method *Frontiers in Chemistry* **2020**, *8*, 1-5 DOI: 10.3389/fchem.2020.00527)

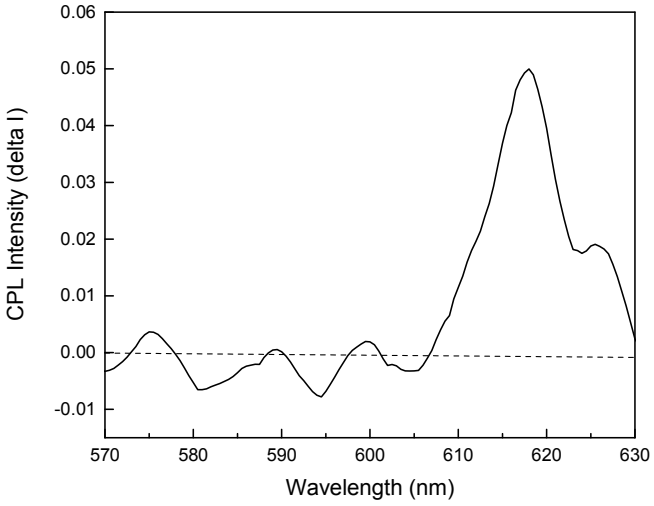

Figure 77. CPL spectrum of $Eu(facam)_3$ in DMSO (10^{-3} M) acquired with our home-made instrument

G. DLS Results

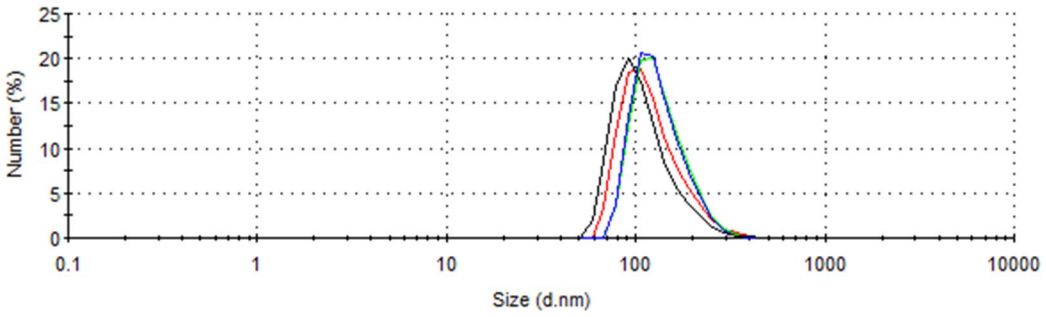
Number (%)
25
20
15
10
5
0
0.1
1
10
100
1000
10000
Size (d.nm)

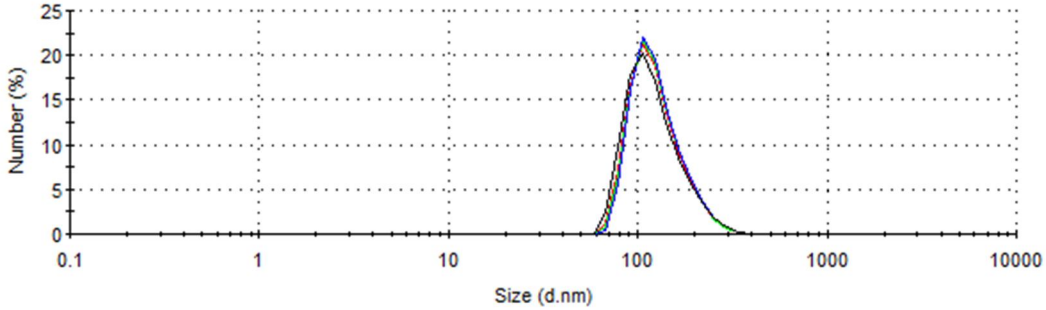
Number (%)
25
20
15
10
5
0
0.1
1
10
100
1000
10000
Size (d.nm)

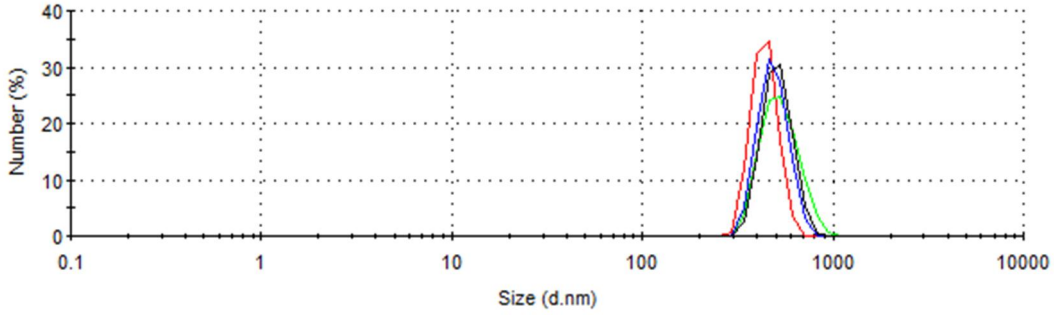
Number (%)
40
30
20
10
0
0.1
1
10
100
1000
10000
Size (d.nm)

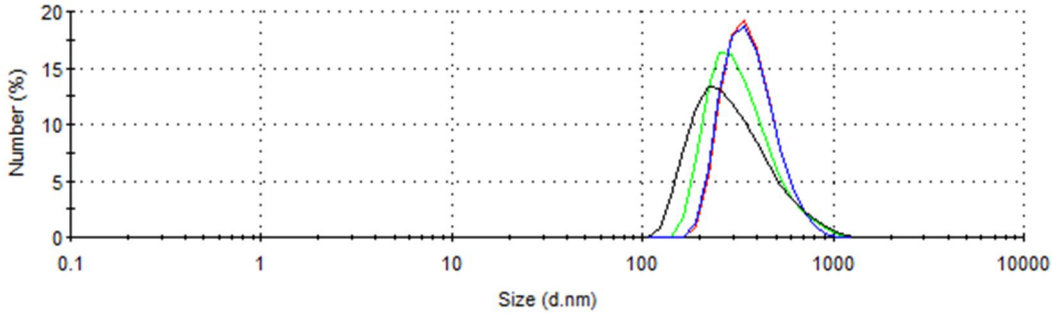
Number (%)
20
15
10
5
0
0.1
1
10
100
1000
10000
Size (d.nm)

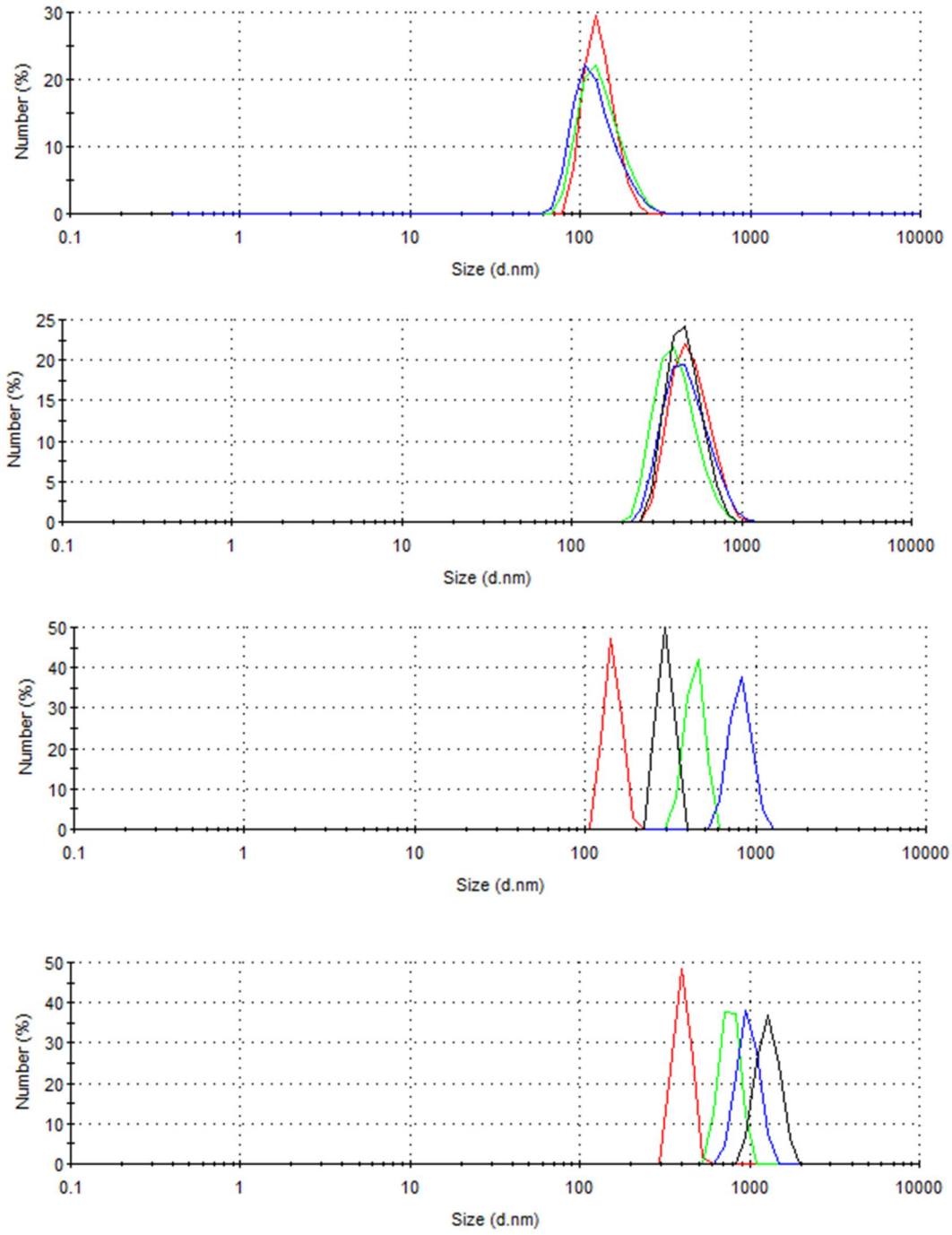

Figure 78. Size distribution curve by number average of **C1-*D***, **C1-*L***, **C2-*L***, **C2-*D***, **BC1-*L***, **BC1-*D***, **BC2-*L*** and **BC2-*D***